Morphology and Mechanical Behavior of Oriented Blends of Styrene - Isoprene - Styrene Triblock Copolymer and Mineral Oil

by Elisabeth Prasman

B.S., Civil Engineering (1995)
Université Libre de Bruxelles

Submitted to the Department of Materials Science and Engineering in Partial Fulfillment of the Requirements for the Degree of Master of Science in Materials Science and Engineering

at the

Massachusetts Institute of Technology
June 1997

© 1997 Massachusetts Institute of Technology
All rights reserved

Signature of Autho.....
Department of Materials Science and Engineering
May 9, 1997

Certified by.....
Edwin L. Thomas
Morris Cohen Professor of Materials Science and Engineering
Thesis Supervisor

Accepted by.....
Linn W. Hobbs
John F. Elliot Professor of Materials
Chairman, Department Committee on Graduate Students

MASSACHUSETTS INSTITUTE OF TECHNOLOGY
JUN 16 1997
LIBRARIES

Science

Morphology and Mechanical Behavior of Oriented Blends of Styrene - Isoprene - Styrene Triblock Copolymer and Mineral Oil

by Elisabeth Prasman

Submitted to the Department of Materials Science and Engineering in Partial Fulfillment of the Requirements for the Degree of Master of Science in Materials Science and Engineering at the Massachusetts Institute of Technology
May 9, 1997

ABSTRACT

Films of blends of styrene - isoprene triblock copolymer and mineral oil have been simple-cast and roll-cast from a toluene solution. Their microstucture has been analyzed by transmission electron microscopy and small-angle x-ray scattering. Samples containing small amounts of mineral oil formed a morphology of cylinders, which are oriented by roll-casting. Samples with high mineral oil content formed polystyrene spheres arranged on a body-centered cubic lattice in a matrix composed of polyisoprene and mineral oil, and the samples display large grain sizes and very long range order. Roll-cast samples of this composition exhibit partial fiber symmetry around the rolling direction, which corresponds to the [111] crystallographic direction of the cubic lattice. A shear-induced sphere to cylinder transition has been observed, since samples processed under high shear exhibit a mixed morphology of bcc spheres and oriented cylinders.

The order-disorder transition temperature of these blends was measured by birefringence and small-angle x-ray scattering, and a thermal roll-casting method has been developed.

The high-strain deformation mechanisms of the oriented sphere-forming blend has been studied by a simultaneous tensile - SAXS experiment, where the sample was stretched up to 300% along the [111] direction. By monitoring the position of the (222) and $(1\bar{1}0)$ reflections, the deformation of the lattice is shown to be affine with the macroscopic deformation of the sample, and the glassy domains remain spherical throughout deformation. Deformation of the microstructure is totally reversible upon unloading. A model is proposed to describe the microstructural changes induced by high-strain deformation.

Thesis Supervisor: Edwin L. Thomas

Title: Morris Cohen Professor of Materials Science and Engineering

Table of Contents

List of Tables 5

List of Figures 6

Acknowledgments 13

1. Introduction 14

1.1 Thermoplastic Elastomers 14

1.2 Morphologies in Block Copolymers 15

1.3 Mineral Oil Extension of Block Copolymers 16

1.4 Orientation Methods and Mechanical Behavior of Block Copolymers 19

1.5 Other Related Studies 21

2. Solvent Casting of Block Copolymer - Mineral Oil Blends 26

2.1 Introduction 26

2.2 Experimental Procedures 26

2.3 Morphological Characterization 27

2.3.1 Cylinder-Forming Blends 29

2.3.1.1 Simple-Cast Samples 29

2.3.1.2 Roll-Cast Samples 32

2.3.2 Sphere-Forming Blends 37

2.3.2.1 Simple-Cast Samples 37

2.3.2.2 Roll-Cast Samples 41

2.3.3 Summary 59

2.4 Mechanical Behavior of Roll-Cast Samples 62

3. Thermal Roll-Casting of Block Copolymer - Mineral Oil Blends 68

3.1 Introduction 68

3.2 Determination of the Order-Disorder Transition of the Blends 69

3.3 Processing and Morphology 77

3.4 Conclusion 81

4. High-Strain Tensile Deformation of a Sphere-Forming Triblock Copolymer / Mineral Oil Blend 83

4.1 Introduction 83

4.2 Experimental Procedure 83

4.3 Results and Discussion 84

4.4 Conclusion 98

Conclusions and Suggestions for Further Work 100

Bibliography 104

List of Tables

Table 1. D-spacings (Å) of cylinders for simple-cast films of V4211-D and mineral oil as measured from SAXS data.

Table 2. D-spacings (Å) of cylinders for roll-cast films of V4211-D and mineral oil as measured from SAXS data.

Table 3. Summary of the morphologies observed in simple-cast and roll-cast blends of styrene - isoprene - styrene triblock copolymer and mineral oil.

Table 4. Mechanical properties of roll-cast samples of triblock copolymer and mineral oil, measured parallel and perpendicularly to the direction of the glassy cylinders. E is Young's modulus, σ_{yield} is the yield stress, σ_{break} and ε_{break} are the stress and strain at break, respectively. The ratio of the modulus parallel to the cylinders by the modulus in the perpendicular direction (E_{par}/E_{perp}) is also reported. The values in this table are the averages of the values measures in 5 experiments.

Table 5. Order-disorder transition temperature measured by birefringence for blends of styrene - isoprene -styrene and mineral oil of various compositions.

Table 6. Change in the d-spacings of the (222) and the $(1\bar{1}0)$ reflections with deformation. These values have been divided by the values of d_{222} and $d_{1\bar{1}0}$ before deformation (designated by $(d_{222})_o$ and $(d_{1\bar{1}0})_o$, respectively). The variable ε_{xx} represents the deformation of the cubic lattice in the [111] direction and is found to be equal to the strain within experimental error. The Poisson ratio for the lattice, ν_{xz}, has been derived for each value of the strain.

List of Figures

Figure 1. **(a)** Cross-sectional view of the roll-casting apparatus and **(b)** definition of the coordinate system. A polymer solution is poured between two parallel counterrotating rollers. The left roller is stainless steel, whereas the right roller is Teflon®-coated. After solvent evaporation, the polymer film adheres to the stainless steel roller. A portion of this film has been magnified in (b) to define the coordinate axes. The $\hat{z}$ axis is parallel to the axes of the rollers, and the $\hat{x}$ axis corresponds to the flow direction in the roll-casting process.

Figure 2. TEM micrograph showing several tilt grain boundaries in a simple-cast SIS sample containing 10wt% mineral oil. The PS microdomains appear light and the OsO_4 stained rubbery matrix appears dark.

Figure 3. Azimuthally averaged intensities scattered by simple-cast, annealed samples of 10, 20 and 30wt% mineral oil content. The curves are vertically shifted by an arbitrary amount. Arrows show the position of the theoretical reflections for a hexagonal lattice of lattice parameter $d_{100} = 311$Å. The numbers above each arrow refer to the relative position of the allowed reflections of a two-dimensional hexagonal lattice.

Figure 4. TEM micrograph of a roll-cast sample containing 10wt% mineral oil. In **(a)** the sample is viewed in the $\hat{x}$ direction; in **(b)** it is viewed in the $\hat{z}$ direction.

Figure 5. Two-dimensional SAXS diffraction pattern of a roll-cast, annealed sample containing 20wt% mineral oil (a) unannealed; (b) annealed. The incident x-ray beam was in the $\hat{y}$ direction.

Figure 6. Azimuthally averaged intensities scattered by roll-cast, annealed samples of 10, 20 and 30wt% mineral oil content. The incident x-ray beam was in the $\hat{y}$ direction.The curves, obtained by averaging the intensities over an azimuthal angle of 40° centered on the main peak, are shifted vertically by an arbitrary amount. Arrows show the position of the theoretical reflections for a hexagonal lattice of lattice parameter d_{100} =300Å. The numbers above each arrow refer to the relative position of the allowed reflections.

Figure 7. TEM micrograph of a simple-cast sample containing 40wt% mineral oil, annealed under vacuum for 6 days at 120°C. This micrograph shows a 4-fold symmetric [100] projection of the body-centered cubic lattice. The unit cell is outlined in the inset.

Figure 8. SAXS plot of simple-cast samples containing 40wt% mineral oil (annealed and unannealed). The two-dimensional intensities were circularly averaged and plotted versus the scattering vector q. The arrows indicate the allowed reflections for a body-centered cubic crystal, based on a unit cell parameter of a=417Å. The numbers above each arrow refer to the relative position of the allowed reflections.

Figure 9. Two-dimensional SAXS pattern of a simple-cast sample containing 40wt% mineral oil, annealed under vacuum for 6 days at 120°C. Note the spotty diffraction rings, indicative of the very large grain size in this sample. The right-hand side of the image has been overexposed in order to reveal the high-q reflections.

Figure 10. TEM micrograph of a roll-cast sample containig 40wt% mineral oil, viewed in the $\hat{x}$ direction. Two grains are evident, and are separated by a clear grain boundary. The tilt angle of this pure tilt boundary is approximately 37.5° on the left side of the image and 29.5° on the right side of the image.

Figure 11 (a). Two-dimensional SAXS patterns of a sample containing 40wt% mineral oil and roll-cast under low shear. The incident x-ray beam was in the $\hat{x}$ direction. The reflections consist of arcs of limited circumferential broadness, indicating a partial fiber symmetry of the microstructure around the [111] axis. The loss of rotational symmetry is due to a slight misalignment of the sample in the beam. The right-hand side of the image has been overexposed in order to reveal the weaker high-q reflections.

Figure 11 (b). Two-dimensional SAXS patterns of a sample containing 40wt% mineral oil and roll-cast under low shear. The incident x-ray beam was in the $\hat{y}$ direction. The right-hand side of the image has been overexposed in order to reveal the weaker high-q reflections.

Figure 11 (c). Two-dimensional SAXS patterns of a sample containing 40wt% mineral oil and roll-cast under low shear. The incident x-ray beam was in the $\hat{z}$ direction. The reflections present in this view are similar to those visible in the $\hat{y}$ view, but their relative intensities are different, suggesting that the fiber symmetry around the [111] axis is only partial. The right-hand side of the image has been overexposed in order to reveal the weaker high-q reflections.

Figure 11 (d). Comparison of the position of the experimental reflections in figures 11 (a), (b), and (c) with the theoretical reflections for a body-centered cubic crystal, presenting a partial fiber symmetry with respect to the [111] direction, which is aligned with the $\hat{x}$-axis. Only the upper right quadrant of each pattern is analyzed. Black dots positions are experimental reflections; white dots represent theoretical reflections, which have been indexed.

Figure 12. Two-dimensional SAXS diffraction pattern of a sample roll-cast under low shear and annealed for 6 days at 120°C. Data was recorded with the incident x-rays in the $\hat{y}$ direction. In addition to the reflections present in Figure 11b, some additional reflections are visible on the $\hat{z}$ axis, which correspond to the cylinders aligned in the $\hat{x}$ direction. (Initial mineral oil content : 40wt%).

Figure 13. TEM micrograph of a sample roll-cast under low shear and annealed for 6 days at 120°C. The sample is viewed in the $\hat{y}$ direction. (Initial mineral oil content : 40wt%). Both spherical and cylindrical domains are evident, and the majority of the cylinders are aligned in the flow direction.

Figure 14 (a). TEM micrograph of an unannealed sample produced by high shear flow, viewed in the $\hat{x}$ direction. (Mineral oil content : 40wt%).

Figure 14 (b). TEM micrograph of an unannealed sample produced by high shear flow, viewed in the $\hat{y}$ direction. (Mineral oil content : 40wt%). The white lines correspond to the glassy cylinders, and the circles correspond to glassy spheres. The cylinders are aligned in the flow direction and at the interface between both phases the cylinders progressively break up into spheres.

Figure 15 (a). TEM micrograph of an annealed sample produced by high shear flow viewed in the $\hat{x}$ direction. (Initial mineral oil content : 40wt%).

Figure 15 (b). TEM micrograph of an annealed sample produced by high shear flow viewed in the $\hat{y}$ direction. (Initial mineral oil content : 40wt%).

Figure 16. Stress-strain curves of roll-cast samples containing 10, 20, and 30wt% mineral oil, measured perpendicular to the glassy cylinders.

Figure 17. Stress-strain curves of roll-cast samples containing 10, 20, and 30wt% mineral oil, measured parallel to the glassy cylinders.

Figure 18. Imposed temperature profile in the first thermal SAXS experiment. The bold lines represent times when SAXS data was recorded.

Figure 19. Azimuthally averaged SAXS intensities recorded at the various temperatures on an annealed, simple-cast sample containing 30wt% mineral oil. The different curves were vertically shifted by an arbitrary constant. The number on each curve refers to the temperature in °C at which data was taken.

Figure 20. Imposed temperature profile in the second thermal SAXS experiment. The bold lines represent times when SAXS data was recorded.

Figure 21. Azimuthally averaged SAXS intensities recorded at the various temperatures on an unannealed, simple-cast sample containing 30wt% mineral oil. The different curves were vertically shifted by an arbitrary constant. The number on each curve refers to the temperature in °C at which data was taken.

Figure 22. TEM micrograph of a thermally roll-cast sample containing 35wt% mineral oil (viewed in the $\hat{z}$ direction).

Figure 23. Two-dimensional SAXS pattern of a thermally roll-cast sample containing 35wt% mineral oil, recorded with the incident x-ray beam in the $\hat{y}$ direction, i.e. perpendicular to the plane of the film.

Figure 24. Applied strain function vs. time for the deformation experiment on the roll-cast sample. The bold lines represent the times of SAXS data acquisition.

Figure 25. Stress - strain curve measured during the deformation experiment on the roll-cast sample. The dots correspond to the points where deformation was interrupted for SAXS data acquisition. Stress relaxation during data acquisition was negligible.

Figure 26. Two-dimensional SAXS patterns of the deformed roll-cast sample. The stretching direction ($\hat{x}$-axis) is vertical. The right-hand side of each image has been overexposed in order to reveal the weaker intensity high-q reflections.

Figure 27. Plot of the extension ratio of the interdomain distance versus the bulk strain of the sample. The line passing through the origin with a slope of 45^{o} represents the perfectly affine deformation.

Figure 28. Circular average of scattered intensities of the various two-dimensional SAXS patterns recorded during deformation of the roll-cast sample.

Figure 29. Comparison of the intensities along the deformation direction and perpendicularly to the deformation direction, at 0% and after 300% deformation.

Figure 30. Model for the deformation mechanism inside a single grain. The (110) plane of a grain with the [111] direction vertical is represented (a) before deformation, (b) after

deformation. After deformation, the grain progressively breaks up into smaller subgrains, due to sliding of the spheres along the new axial subgrain boundaries. A basis unit cell has been drawn in the deformed and in the undeformed lattice.

Figure 31. Schematic of the sliding mechanism along the {110} planes. A is the undeformed configuration. B is the deformed configuration in the absence of sliding. The glassy spheres are very close to eack other and the isoprene chains linking two spheres are 'compressed' in a very small gap. Configuration C, which is obtained by sliding along a (110) plane (dashed line), allows for more freedom in the configuration of the isoprene chains and prevents the collision of two adjacent glassy spheres.

Acknowledgments

This research was financially supported by the Belgian American Educational Foundation, by MasterBuilders Inc., Cleveland, Ohio, by the Air Force (F49620-94-1-0224), and by the National Science Foundation (92-14853). Materials were generously provided by Dexco and Penreco.

I would like to thank the MIT Center for Materials Science and Engineering for the use of its TEM facility, and Dr. M. Capel for his help at the Brookhaven National Laboratories beamline. The hot stage used in the thermal SAXS experiments was kindly provided by Dr. B. Hsiao.The roll-casters used for sample preparation were designed and built by Ramon Albalak.

I am grateful to Professor E.L. Thomas for his guidance during the whole course of my research project. I thank Melody for her help in the sample preparation and the mechanical testing, Christian for supplying the deformation apparatus and training me at Brookhaven, and Beni for her cooperation at the beamline. I also wish to thank John for valuable comments and discussion, and Len for his patience in training me at the microtome.

Chapter 1
Introduction

1.1 Thermoplastic Elastomers

Thermoplastic elastomers represent a class of multiphase polymers of high economic importance. Their molecules are made of a succession of segments or blocks of different nature (generally two or three different monomers). At room temperature these materials usually phase segregate into domains typically 10nm in size. Thermoplastic elastomers consisting of hard blocks (crystalline or glassy) and soft blocks present properties similar to conventional rubbers but are easier to process since the hard blocks, which act as physical crosslinks, can be reversed upon heating or addition of solvent. They can thus be processed with the same equipment used for regular thermoplastics, and can easily be recycled.

The commercial success of thermoplastic elastomers is driven by the possibility of modifying the ratios and lengths of the various blocks, as well as the molecular architecture of the polymer chains, thereby creating materials presenting a very wide range of properties tailored to specific applications. In the past, many studies have focused on understanding the structure - property relationships of these polymers [1-5]. Thermoplastic elastomers based on linear A-B-A triblock copolymers of styrene and isoprene or butadiene have been widely investigated, because their simple structure makes them model copolymers which can serve as a basis for understanding more complicated systems such as segmented multiblock copolymers. They also constitute good model systems for testing theories of polymer physics[6].

The purpose of our work is to study the microstructure and the deformation mechanism in blends of a styrene - isoprene - styrene triblock copolymer with mineral oil. In chaper 2 we study the morphologies of isotropic and oriented samples of various mineral oil contents, as well as the influence of the presence of mineral oil on the mechanical

properties of oriented samples. Chapter 3 deals with our efforts to develop a solvent-free orientation process and the determination of the order-disorder transition of the blends. In chapter 3, we present the results of a SAXS deformation study on a sphere-forming oriented blend.

The goal of the present chapter is to review the various studies which relate to our work. In the first part of this chapter, we review works on morphologies observed in block copolymers, as well the investigations of order-order transitions between the different morphologies. The second part of this introduction reviews the studies of the effect of mineral oil addition on morphology and mechanical behavior of block copolymers. In the last part , we review the existing deformation studies on sphere-forming block copolymer systems, as well as various other studies which present striking similarities with our experimental results.

1.2 Morphologies in ABA Block Copolymers

Linear A-B-A triblock copolymers have long been known to exhibit microstructures of spheres, cylinders, and lamellae, and more recently the double gyroid structure has also been observed in triblocks[7]. Well annealed, near-equilibrium samples with less than 20% minority volume fraction exhibit spheres arranged on a body-centered-cubic lattice[8,9].

Several authors have reported morphology transitions between spheres and cylinders and between cylinders and lamellae. Sakurai *et al.*[10] studied the morphology of a styrene - isoprene diblock copolymer containing 16wt% styrene with TEM and SAXS and observed a thermoreversible order-order transition from bcc spheres at 200°C to hexagonally packed cylinders at 150°C. This work was the first to show that the spherical and cylindrical morphologies can be reversibly changed by changing temperature. The experimental data is successfully described by Leibler's weak segregation limit theory, except for the observation that spatial periodicity increases with decreasing temperature. In a subsequent study[11] the cylinder-sphere transition of solutions of styrene - isoprene

diblock copolymer in dioctyl phthalate was investigated. SAXS data showed that the d-spacing of the (110) peak of the body centered cubic lattice is equal to the d-spacing of the (0001) peak of the hexagonal lattice. This observation can be explained by assuming that neighboring spheres coalesce in the [111] direction of the cubic lattice to form hexagonally packed cylinders aligned along [0001]. If this transition is induced by an interfacial curvature change from a sphere to a spheroid with its long axis oriented in the [111] direction, the radius of the cylinders formed by this mechanism should be smaller than the radius of the spheres. Unfortunately, they do not present evidence of this difference in radius, since they do not provide TEM observations of the cylinder-sphere transition.

A morphology transition from cylindrical to lamellar microdomains was also reported[12] in a styrene - butadiene - styrene block copolymer having a 56% weight fraction of styrene. The metastable polybutadiene cylinders cast from solution were transformed into lamellae upon annealing. TEM and SAXS showed that this transition from quasi-stable to stable morphologies occurs via coalescence of cylinders. As for the sphere-cylinder transition, it is proposed that undulations of the interface might be at the origin of the coalescence mechanism. A more detailed study of the transition mechanism was given by Hadjuk *et al.*[13]. They examined the intermediate structures which form during the transition from lamellae to cylinders in a polystyrene-poly(ethene-co-butene) diblock copolymer. In the first step, fluctuations along the interface grow in amplitude and the lamellae transform into sheets of cylinders; in the second step this structure anneals into hexagonally packed cylinders.

1.3 Mineral Oil Extension

In order to modify the properties or improve the processability of block copolymers, they are often blended with additives such as homopolymers, resins or extender oils. These mineral oils contain known quantities of paraffinic-naphtenic and aromatic molecules, which are preferentially absorbed by the rubbery and glassy phases,

respectively. These oils affect the copolymer microdomain structure and chain dynamics, thereby changing the rheological and mechanical properties of these materials. Several authors have studied the influence of mineral oil blending on the morphology and mechanical properties of block copolymers[14-23].

Ceausescu *et al.*[14] investigated the effect of mineral oil extension on the mechanical properties of linear and star-shaped butadiene-styrene block copolymers. Tensile strength and large strain tensile modulus were found to decrease with mineral oil content, whereas elongation at break and stress at break increase with increasing mineral oil content. The hardness dependence on oil concentration presents two branches separated by a clear transition. This transition, occurring at an effective styrene volume fraction of 20%, is attributed to a morphological transition (most likely from cylinders to spheres) occurring at a critical oil level[15]. Canevarolo *et al.*[16] studied the effect on the melt viscosity of systems composed of a SBS triblock copolymer and various types of extender oils, and investigated the change in the 'melt rheological transition' temperature upon addition of such oils. At temperatures lower than the rheological transition temperature, the addition of aromatic oil weakens and gradually dissolves the polystyrene domains, whereas addition of paraffinic oil induces a better segregation between the polystyrene domains and the butadiene domains.

The first study of the changes in microstructure upon mineral oil extension was reported by Polizzi *et al.*[17] SAXS was used to investigate the influence of different oils on the structure of a cylindrical microdomain forming styrene - butadiene - styrene block copolymer. The d-spacings of the cylinders were observed to increase with paraffinic mineral oil content, and the decrease of the long-period after addition of a critical amount of mineral oil was interpreted in terms of a transition from polystyrene cylindrical domains to spherical domains. In the case of aromatic oils, the broadness of the diffraction peaks are attributed to a 'smearing out of the superstructure'. Flosenzier and Torkelson[20] used TEM to investigate the change in the morphology of a commercial grade of styrene - butadiene -

styrene block copolymer containing mineral oil upon removal of the mineral oil. A spheres to cylinders transition was also observed, and the morphology resulting from mineral oil blending was found to be dictated by the total styrene content of the system.

Some authors have studied the morphology and structure of thermoplastic elastomer gels, i.e. oil-rich blends of a thermoplastic elastomer and a mineral oil which acts as a selective solvent for one of the blocks. Mischenko *et al.*[21] used SAXS and SANS to investigate the structure of gels composed of triblock copolymers (Shell Kraton G) with a paraffinic oil, as well as the influence of temperature and deformation on these systems. The system is thought to form a liquid-like arrangement of polystyrene micelles in the rubbery matrix. The deformation experiments indicate an affine deformation of the gels up to an elongation of λ=2.5, and deformation is fully reversible. The interdomain distance was found to increase with increasing oil content. The width of the first peak decreases with increasing copolymer concentration up to a threshold value, beyond which the width of the peak increases with increasing polymer content. The results are interpreted in terms of a hard-sphere interaction potential between glassy domains, and various types of coordination models between neighboring polystyrene domains are discussed. Laurer *et al.*[22] examined gels containing SEBS triblock copolymer and at least 70wt% of a midblock-selective oil. The morphology of samples prepared by solution casting and by mechanical mixing are compared. TEM micrographs of samples containing 70 wt% mineral oil showed a mixed morphology of spherical and cylindrical domains. The gel produced by mechanical mixing formed regions where the spherical domains are ordered on a body centered cubic lattice. For a mineral oil concentration of 90wt%, the morphology was found to consist of spherical styrene micelles uniformly dispersed in the rubber/oil matrix. TEM micrographs also show that some oil (a saturated aliphatic oil) is imbibed within the polystyrene micelles.

The possibility of mineral oil penetrating the polystyrene domains raises the issue of the effects of mineral oil on the glass transition and the mechanical properties of

polystyrene. Anderson *et al.*[23] investigated the effect of mineral oil blending on the properties of polystyrene homopolymer, and in particular the antiplasticization phenomenon. Antiplasticization has been observed in many polymer - diluent systems. Although the glass transition temperature of the glassy polymer is lowered upon addition of the plasticizer, its modulus and tensile strength can increase significantly when it is blended with a small quantities of plasticizer. In Anderson's study, polystyrene was blended with Penreco Drakeol 500, which is the mineral oil we use in our experiments. The glass transition of the polystyrene was found to decrease monotonously with increasing mineral oil concentration. However, for low molecular weight polystyrene, mechanical properties such as flexural modulus and flexural strength increase dramatically at small mineral oil concentrations ('antiplasticization'), then decrease at higher concentrations ('plasticization'). Spectroscopy was used to determine the free volume in samples of various mineral oil concentrations, and the mobility of the polymer chains was studied by NMR. The antiplasticization effect of mineral oil on polystyrene was attributed to a decrease in fractional free volume at the chain ends. The diluent is thought to fill the small regions of free volume at the chain ends at low concentrations of oil, which restricts the mobility of the chain ends and results in higher moduli and strength.

The studies on blends of block copolymers with mineral oil show that addition of mineral oil induces important changes in morphology and mechanical properties. The morphology of cylinder-forming block copolymers can change into a morphology of spheres upon addition of a sufficient amount of a rubber-selective mineral oil. Aromatic oils penetrate both the glassy and the rubbery domains, whereas paraffinic oils preferentially swell the rubber phase. However, in some cases paraffinic oils have been found to penetrate the glassy domains.

1.4 Orientation Methods and Mechanical Behavior of Block Copolymers

In order to fully understand the mechanical behavior of block copolymers in relation to their microstructure, it is of paramount importance to perform experiments on samples presenting an oriented single-crystal-like structure, in order to minimize the effects of grain orientation, grain boundaries and defects. A review of the different orientation techniques and deformation studies has been published recently [24]. An orientation technique which has proved very effective in producing single-crystal-like samples of cylinders and lamellae is roll-casting [25-27]. In this method, a solution of the block copolymer is poured between two counter rotating cylinders. The flow field between the two rollers is a combination of a shear flow and an elongational flow and has been analyzed in detail elsewhere[25,28]. As the solvent evaporates, the material goes through its order - disorder transition while it is submitted to the flow, thereby forming a macroscopically oriented film. In situ scattering techniques as well as electron microscopy can then be used to study the changes in microstructure during subsequent deformation of these oriented samples.

Deformation studies on block copolymers have mainly focused on block copolymers forming cylindrical or lamellar morphologies. Samples with the body-centered-cubic spheres morphology have not received as much attention. In addition to the above-mentioned deformation study on thermoplastic elastomer gels[21], we have found only three other deformation studies[29-31] of sphere-forming block copolymers. In 1971, Inoue *et al.*[29] used light scattering, x-ray scattering, and electron microscopy to investigate the deformation mechanism of glassy polystyrene spheres in a rubbery matrix in both styrene-isoprene block copolymers and in blends of these copolymers with the corresponding homopolymers. The SAXS data on the deformed diblock indicate that the change in interdomain spacings becomes nonaffine at strains above 20%. Changes in light scattering patterns are attributed to the appearance of density fluctuations at lower strains and void formation at higher strains. TEM micrographs of the stretched specimens also show regions of low concentrations of spherical domains, suggesting a nonuniform block

copolymer composition. Deformation of the spherical domains into spheroidal shapes was also observed, but this deformation correlated with the microtoming direction rather than with the stretching direction. In this early study, the PS spheres were not on an ordered lattice before the deformation experiment (the samples were not annealed), and a one-dimensional detector was used for light scattering.

Richards and Thomason[30] reported a deformation study on a polycrystalline triblock copolymer of styrene and isoprene during extension. Before deformation, the styrene spheres were proposed to be arranged on a face-centered cubic lattice, and SANS data on the deformed sample suggests that extension induces a deformation texture into the specimen, due to the slip and rotation of grains. The [111] direction of the cubic lattice is found to orient parallel to the direction of stress and also constitutes a fiber axis. The deformation of the lattice was not affine with the macroscopic deformation of the sample. Although the SANS patterns of the deformed sample present some interest, the authors do not provide any clear discussion of the undeformed morphology, which is thought to be spherical although the styrene content is 41wt%. This composition usually gives rise to a lamellar morphology, raising the possibility that the sample before deformation was in a non-equilibrium spherical morphology. The sample was prepared by simple-casting from a toluene solution, and a vacuum was used to remove the solvent. This fast evaporation process can induce non-equilibrium morphologies. TEM micrographs of the sample would have been very useful in verifying the morphology before deformation.

Richards and Welsch[31] measured molecular deformation of the diene matrix by small-angle neutron scattering experiments in a styrene - isoprene - styrene triblock copolymer containing 16wt% of styrene. Changes in the component of the radius of gyration were found to be greater than affine parallel to the stretching direction, whereas the chain dimensions hardly changed perpendicular to the stretching direction. The experimental data was fitted to a model for the molecular deformation. The authors attribute the observations to 'local shear stress fields being caused by the movement of the large

polystyrene domains when bulk strain is applied'. These movements are thought to cause considerable disturbance of the polyisoprene blocks in the stretching direction, whereas perpendicularly to the extension direction the isoprene chains can move to regions where disturbance due to movements of the glassy domains is minimal. Although the finite size of the physical crosslinks of finite size is likely to influence the degree of deformation of the rubber chains, the authors' explanation does not seem very compelling. One would rather expect that perpendicular to the stretching direction the isoprene chains are considerably 'compressed' between the glassy spheres which come close together. The small change in the perpendicular radius of gyration may be due to the tendency of the spheres to move in such a way to allow more space to the rubber chains which tend to relax back to their initial size. Parallel to the deformation, the polyisoprene chains support most of the tensile deformation, since the glassy spheres are unlikely to deform. This effect can explain an greater than affine increase of the radius of gyration parallel to the stretching direction.

1.5 Other Related Studies

Other works, although not directly related to the study of block copolymer morphology upon tensile deformation, present some interest to the work that will be discussed in chapter 4. These studies include the investigation of block copolymer microstructure under shear[32-35], sheared colloidal suspensions[36-38], rheology of triblock copolymer solutions[39-41], and deformation of cellular polymer films[42-44]. Theses works present striking similarities with some aspects of our experimental results.

Almdal *et al.*[32] submitted a poly(ethylenepropylene)-poly(ethylethylene) diblock copolymer melt to a reciprocating shear deformation. SANS measurements performed with an *in situ* shearing device demonstrated a twinned body centered cubic crystal structure. The shear direction corresponds to the family of <111> directions, and the shear gradient direction is coincident with the $<1\bar{1}0>$ directions. The roles of shear rate and temperature on this ordering was investigated in a more detailed study[33] by SANS and rheological

measurements. At low temperature the material forms hexagonally packed cylinders, which orient in the shear direction. After shear orienting such a sample using a 100% shear strain, the sample was then heated under relaxed conditions and epitaxial growth of a twinned body centered cubic phase of spheres was observed, with the [111] direction of the bcc lattice coincident with the [0001] direction of the hexagonal lattice. Experimental data thus indicate an order-order transition from hexagonally packed cylinders to body centered cubic spheres. This hexagonal to bcc order-order transition was also observed in a quenched, unoriented sample. It was found to be completely thermally reversible, and the d-spacing of the (110) planes of the cubic lattice was equal (within 1% error) to the d-spacings of the (0001) planes of the hexagonal lattice.

A similar study was conducted by Okamoto *et al.*[34] on a polystyrene-poly(ethylene-propylene) diblock copolymer at a very low temperature and a high frequency. Under the oscillatory shear deformation, the body centered cubic polystyrene spheres orient with the (110) plane parallel to the shearing plane. No twinning is reported in this study, and the conclusions are related to the rheological behavior of those systems.

Those studies on block copolymer melts present a striking resemblance with the structures previously observed in sheared colloidal suspensions. Ackerson and Clark[36] analyzed the structure of a colloidal crystal composed of aqueous suspensions of highly charged polystyrene latex spheres submitted to shear flow. In such a low concentration suspension, a body centered cubic crystal structure is observed at equilibrium. The shearing process orients the body centered cubic crystal with the [111] direction parallel to the velocity of the flow, and with the (110) plane perpendicular to the shear. The low shear rate structure is a 'flowing crystal' which exhibits a transition from three- to two-dimensional order with increasing shear. The shear flow causes the crystal to oscillate between two twin structures. For larger shear rates this structure transforms into a sliding-layer structure with two-dimensional order. As the shear rate is further increased, the sliding-layer structure becomes unstable, producing a one-dimensionally ordered system of

strings of particles extending in the flow direction. Finally at the largest shear rate, the strings disorder and an amorphous structure results. A more concentrated charge stabilized suspension was analyzed later by Ackerson *et al.*[37]. SANS was used to analyze the effect of a shear Couette flow on the structure of the system. At equilibrium it exhibits a close packed face centered cubic structure (not a body centered cubic crystal). Shearing orients the structure such that a close packed direction is parallel to the flow direction and close packed planes are perpendicular to the shear gradient. At small shear stress the three-dimensional structure distorts by sliding of layers in a zig-zag fashion. At larger shear rates the structure is a 'flowing crystal'. Finally at the largest shear rates the system exhibits an amorphous order, with a tendency to form strings of particles parallel to the flow direction.

Rheological studies conducted on solutions of triblock copolymer in a selective solvent can also provide us with further insight on the deformation mechanisms of the systems investigated in our work. Watanabe *et al.*[39] studied the effect of concentration and temperature on gels of a SBS triblock copolymer in tetradecane. Rheological measurements performed with a concentric cylinder type rheometer show that such gels exhibit rubberlike linear viscoelasticity under small-amplitude oscillation. When temperature is raised, the rubbery gel changes to a plastic fluid, and further to a viscoelastic liquid. These transitions can be interpreted in terms of stability of the microstructure of the system. At low temperatures, the styrene domains act as permanent physical crosslinks. At intermediate temperatures, they become softer, and stress can cause the pullout of styrene blocks from the styrene domains into the rubbery matrix. These blocks can then migrate to other styrene domains or return to the same styrene domain. At high temperatures, the transfer of styrene blocks from one domain to another takes place spontaneously by thermal motion of the rubber blocks, even when no strain is applied to the system. In a more detailed study[40], these transitions were examined by rheological and dielectric measurements. The results suggested that the mechanism of the plastic to viscous transition is not only due to the pullout of the styrene blocks, but is also influenced by the type of configuration of the

rubber blocks (loops vs. bridges). In a bridge configuration, an applied strain can effectively stretch the rubber block and pull out the styrene block, whereas a loop is not significantly stretched by an applied deformation. The contribution of bridges and loops to elasticity and plasticity has been investigated in a subsequent work[41]. The arrangement of the glassy domains and the deformation behavior of block copolymer micellar systems are also thought to be influenced by osmotic constraints[42]. For diblock copolymer solutions in selective solvents, the arrangement of the spherical micelles (with glassy cores) on cubic lattices is attributed to the osmotic constraint induced by the presence of solvated corona blocks of the micelles. This osmotic constraint is also thought to be responsible for the viscoelastic relaxation processes during shear deformation.

Deformation studies[43-45] on cellular polymeric films also present features similar to the ones observed in our system. The system is made of a dispersed phase of latex particles surrounded by a continuous hydrophilic membrane. The addition of a selective solvent was used to vary the relative strength of the matrix and the spherical cores. SANS was used to measure the relative displacements of the cells during deformation under various wetting conditions. The systems present long range order with face centered cubic symmetry. In the cases where the membranes were softer than the spheres, the films can be described as dispersions of hard spheres in a viscoelastic matrix. The SANS patterns of the deformed state of such films exhibit stripes that are elongated in the direction perpendicular to the stretching direction. This effect can be associated with a loss of correlation of the structure in the direction perpendicular to stretching, whereas the correlation is preserved in the stretching direction. The diffraction patterns also indicate that the deformation of the structure is non affine.

Chapter 2

Solvent Casting of Block Copolymer - Mineral Oil Blends

2.1 Introduction

In practical applications of block copolymers, mineral oil is often used in order to improve their processing behavior. Since a considerable proportion of the present consumption of thermoplastic elastomers is in the form of oil-extended grades, it is important to understand how the addition of mineral oil affects the morphology and the mechanical properties of these materials.

In this chapter we investigate the effect of blending white mineral oil on the morphology and mechanical behavior of a styrene - isoprene - styrene triblock copolymer. Morphology of both simple-cast samples and films oriented by roll-casting are studied by small-angle x-ray scattering and transmission electron microscopy in section 2.3. The mechanical properties of roll-cast films is investigated in section 2.4.

2.2 Experimental Procedures

Sample Preparation

The material used in the present study was a poly(styrene-b-isoprene-b-styrene) triblock copolymer, containing 30wt% polystyrene, with block molecular weights of 14K-66K-14K, commercialized by Dexco under the name Vector 4211-D. This polymer, which originally exhibits a cylindrical morphology, was blended with Penreco Drakeol 500 mineral oil, containing 67.5% carbons as paraffins, 32.5% carbons as naphtenes, and 0% carbons as aromatics, as stated by the manufacturer. Both simple-cast and roll-cast samples were prepared from toluene solutions made of 100g of polymer in 150 mL of toluene, and a variable amount of mineral oil depending on the desired final oil content. Samples containing 10, 20, 30, 35, and 40wt% mineral oil were simple-cast and roll-cast.

Films were simple-cast in petri dishes for approximately one week. Roll-casting was performed using rollers of 2 inches in diameter and 5 inches in length. Both rollers were rotating in opposite directions at an angular speed of 40 rpm. The polymer solution was poured between the rotating rollers in three batches, and the gap between the cylinders was progressively increased each time a new volume of solution was added. The final film thickness was typically on the order of 1mm. Annealing was performed under vacuum for 6 days at 120°C. The coordinate system for roll-cast samples is shown in Figure 1.

Characterization

Thin sections for electron microscopy were prepared using a Reichtert-Jung FC 4E Ultracut microtome at -110°C, and subsequently stained for 2 hours with OsO_4 on 600 mesh Cu grids. Bright field transmission electron microscopy was then performed with a JEOL 200CX microscope operated at 200kV. Synchrotron SAXS experiments were performed on the X12B beamline at Brookhaven National Laboratories, using $\lambda = 1.54$Å wavelength x-rays. Scattering patterns were recorded on a two-dimensional position-sensitive gas-proportional detector. Sample thickness in the direction of the x-ray beam was approximately 1mm. For most samples, the sample to detector distance was 153 cm and exposure time was 60 seconds. For samples containing 40wt% mineral oil, the sample to detector distance was 260 cm and exposure time was 10 minutes. SAXS data are reported in arbitrary intensity units.

2.3 Morphological Characterization

The morphology of blends containing 10, 20 30, and 40wt% mineral oil was investigated by TEM and SAXS. Since the samples containing 40wt% mineral oil were found to exhibit a very different morphology than the samples of lower mineral oil content, they are studied separately in section 2.3.2. Most samples, containing up to 35wt% mineral oil, exhibit a cylindrical morphology and are discussed in section 2.3.1.

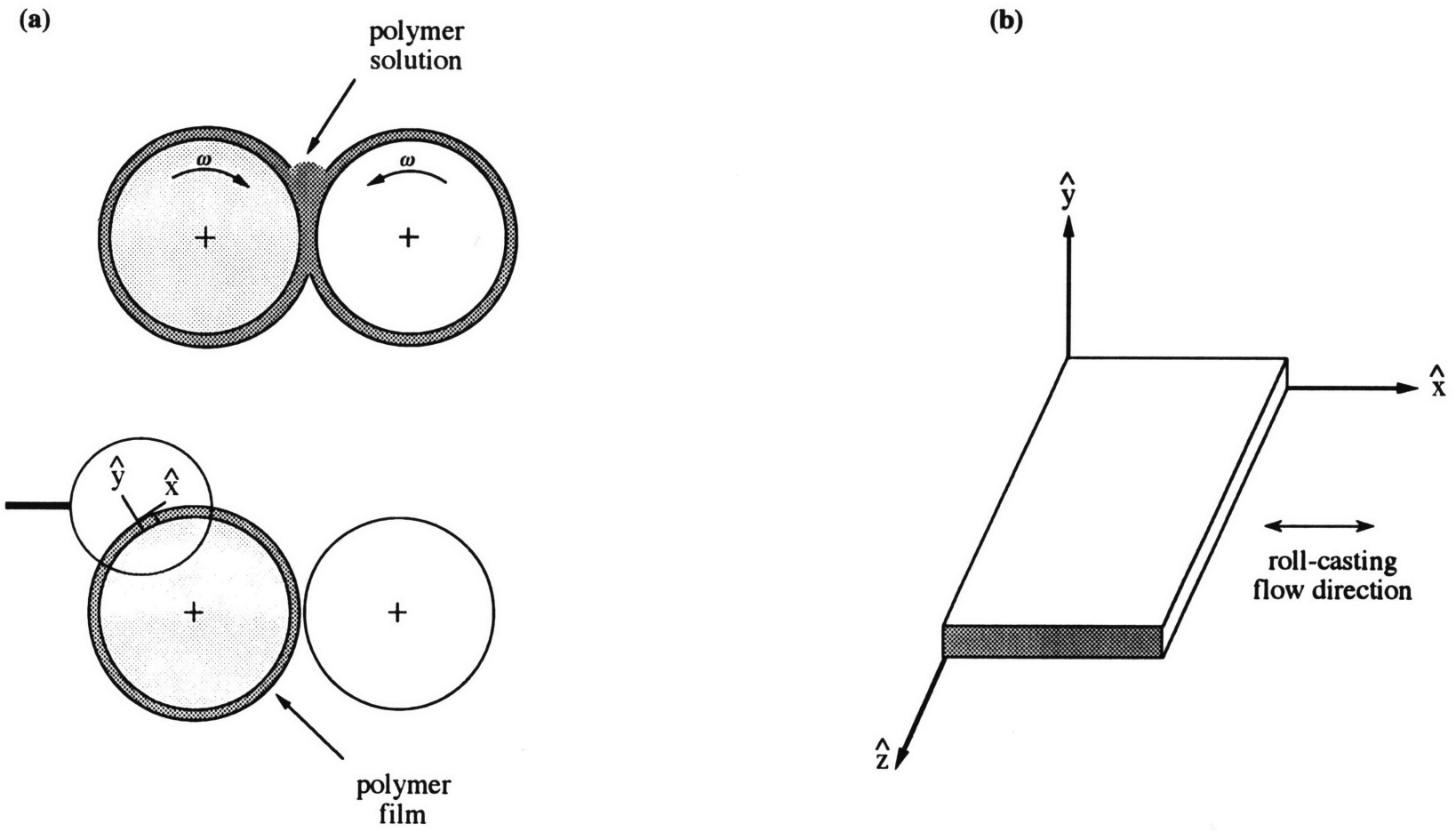

Figure 1. (**a**) Cross-sectional view of the roll-casting apparatus and (**b**) definition of the coordinate system. A polymer solution is poured between two parallel rollers. The left roller is stainless steel, whereas the right roller is Teflon-coated. After solvent evaporation, the polymer film adheres to the stainless steel roller. A portion of this film has been magnified in (b) to define the coordinate axes. The z-axis is parallel to the axes of the rollers, and the x-axis corresponds to the flow direction in the roll-casting process.

2.3.1 Cylinder-Forming Blends

2.3.1.1 Simple-Cast Samples

Figure 2 shows a TEM micrograph of a simple-cast sample containing 10wt% mineral oil. This micrograph is typical for all samples containing 35wt% mineral oil or less. The polystyrene domains form cylinders arranged on a hexagonal lattice in a matrix composed of polyisoprene and mineral oil, and the grains are randomly oriented. The d-spacings of the (100) planes of the hexagonal lattice in simple-cast films of the various compositions have been measured from SAXS and are reported in Table 1.

mineral oil content	unannealed	annealed
10%	300	294
20%	306	299
30%	318	311

Table 1. D-spacings (Å) of cylinders for simple-cast films of V4211-D and mineral oil as measured from SAXS data.

Data shows that the d-spacings between the cylinders increase with mineral oil content. Since the mineral oil contains no aromatics, it mainly swells the rubber phase, thereby increasing the lattice parameter. Annealing under vacuum causes some fraction of the mineral oil to leave the sample, inducing a decrease in the d-spacings. The azimuthally averaged two-dimensional SAXS pattern for the annealed simple-cast samples, shown in Figure 3, confirms this observation. The circularly averaged scattered intensity is plotted as the natural logarithm of the number of x-ray counts vs. the magnitude of the scattering vector $q= (4\pi(\sin\theta)/\lambda)$, where 2θ is the scattering angle. The q values of the lattice peaks are in excellent agreement with the allowed reflections for a hexagonal lattice. As the

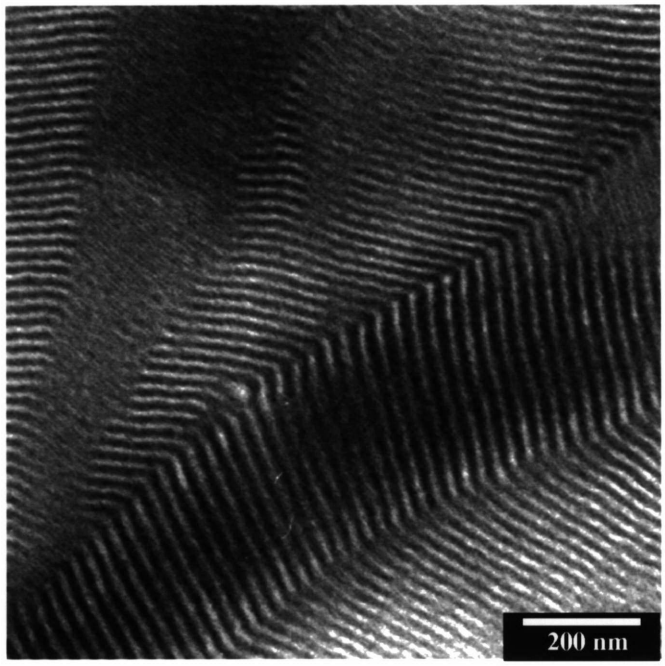

Figure 2. TEM micrograph showing several tilt grain boundaries in a simple–cast SIS sample containing 10wt% mineral oil. The PS microdomains appear light and the OsO_4 stained rubbery matrix appears dark.

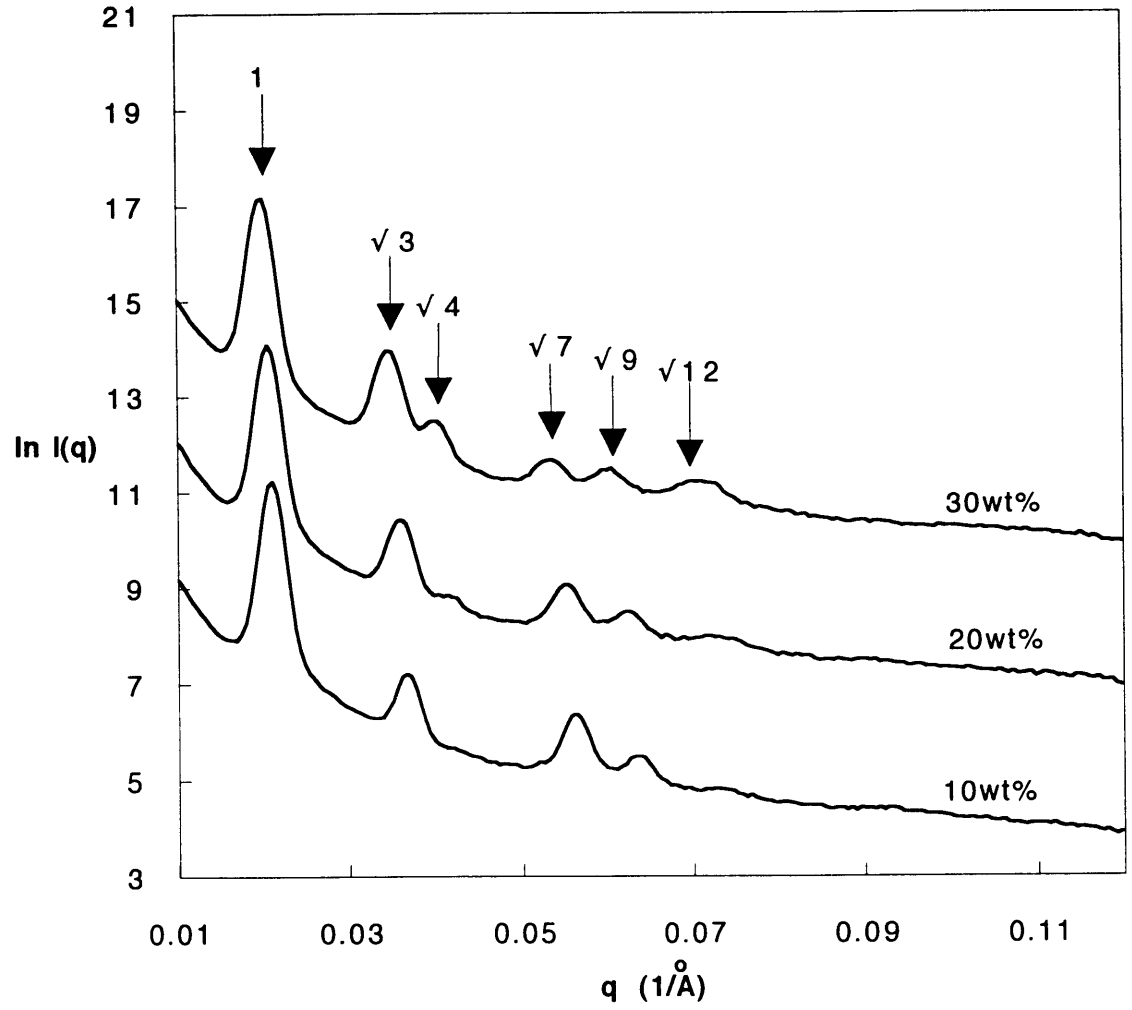

Figure 3. Azimuthally averaged intensities scattered by simple-cast, annealed samples of 10, 20 and 30wt% mineral oil content. The curves are vertically shifted by an arbitrary amount. Arrows show the position of the theoretical reflections for a hexagonal lattice of lattice parameter d_{100} = 311Å. The numbers above each arrow refer to the relative position of the allowed reflections of a two-dimensional hexagonal lattice.

mineral oil content increases, the reflections become sharper, indicating that ordering of the hexagonal lattice improves with mineral oil content. The third and sixth peaks in particular (corresponding to the (200) and (220) reflections, respectively), are increasingly visible after addition of mineral oil. The increasing order of triblock copolymer / mineral oil blends with mineral oil content can be attributed to several factors. Firstly, the presence of the mineral oil in the rubber matrix facilitates the isoprene chain motions, allowing for better ordering of the styrene domains. Secondly, since the mineral oil lowers the glass transition temperature of the polystyrene and the order - disorder transition temperature of the block copolymer, its presence is also likely to decrease the dependence of the order - disorder transition temperature with solvent concentration. Therefore when the solvent evaporates at a given rate, the transition from the homogeneous state to the phase-segregated state occurs over a longer time, resulting in larger grain sizes than is commonly observed in block copolymer systems.

2.3.1.2 Roll-Cast Samples

Figure 4 shows TEM micrographs of a roll-cast annealed sample containing 10wt% mineral oil. The polystyrene domains still form cylinders arranged on a hexagonal lattice in the matrix composed of polyisoprene and mineral oil, but in all grains the glassy cylinders are aligned in the shear direction. The d-spacings of the (100) planes of the hexagonal lattice for these samples are reported in Table 2.

These d-spacings are smaller than those observed in the simple-cast samples. This effect is due to the elongational component of the roll-casting flow, which is known to induce a distorsion in the hexagonal lattice. The increase in d-spacings upon annealing is explained by the relaxation of the distorsion introduced by roll-casting. Some fraction of mineral oil is expected to leave the samples during annealing under vacuum (as for the simple-cast samples), but the decrease in d-spacings due to mineral oil loss is more than compensated by the increase in d-spacings caused by the relaxation of the distortion.

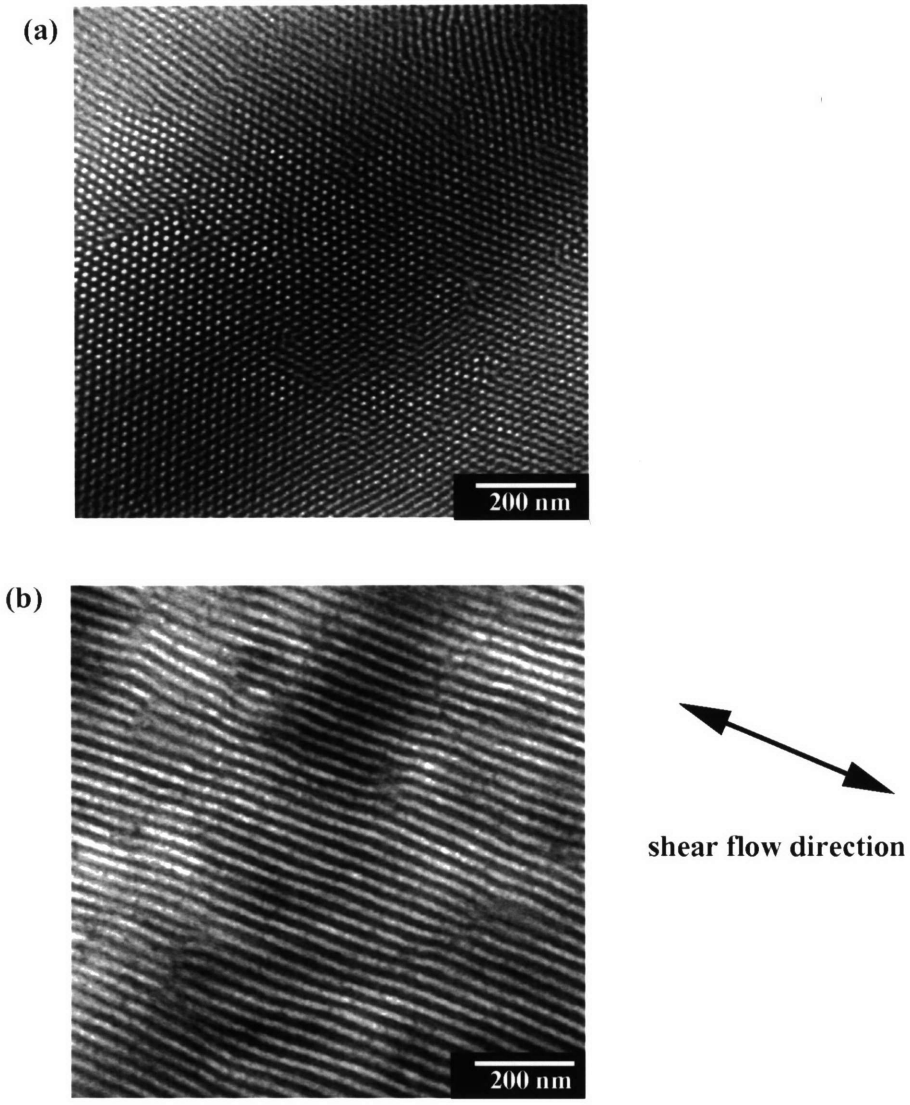

Figure 4. TEM micrographs of a roll–cast sample containing 10wt% mineral oil. In **(a)** the sample is viewed in the $\hat{x}$ direction; in **(b)** it is viewed in the $\hat{z}$ direction.

mineral oil content	unannealed	annealed
10%	255	286
20%	262	292
30%	272	300

Table 2. D-spacings (Å) of cylinders for roll-cast films of V4211-D and mineral oil as measured from SAXS data.

Figure 5 shows two-dimensional SAXS diffraction patterns of a roll-cast sample containing 20wt% mineral oil before and after annealing. They confirm our observation that the cylinders are aligned in the $\hat{x}$ direction. In the unannealed sample, the reflections present a smaller circumferential broadness than in the annealed sample, indicating that annealing reduces the degree of orientation of the glassy cylinders. The radial sharpness of the peaks is increased upon annealing, since annealing improves the overall ordering of the microstructure.

The azimuthally averaged two-dimensional SAXS pattern for the annealed roll-cast samples of various compositions is shown in Figure 6. The q values of the lattice peaks are in excellent agreement with the allowed reflections for a hexagonal lattice. As for the simple-cast samples, the reflections become sharper as mineral oil content increases, indicating that ordering of the hexagonal lattice is facilitated by the presence of mineral oil.

The mechanical properties of these roll-cast blends of triblock copolymer and mineral oil are investigated in section 2.3.

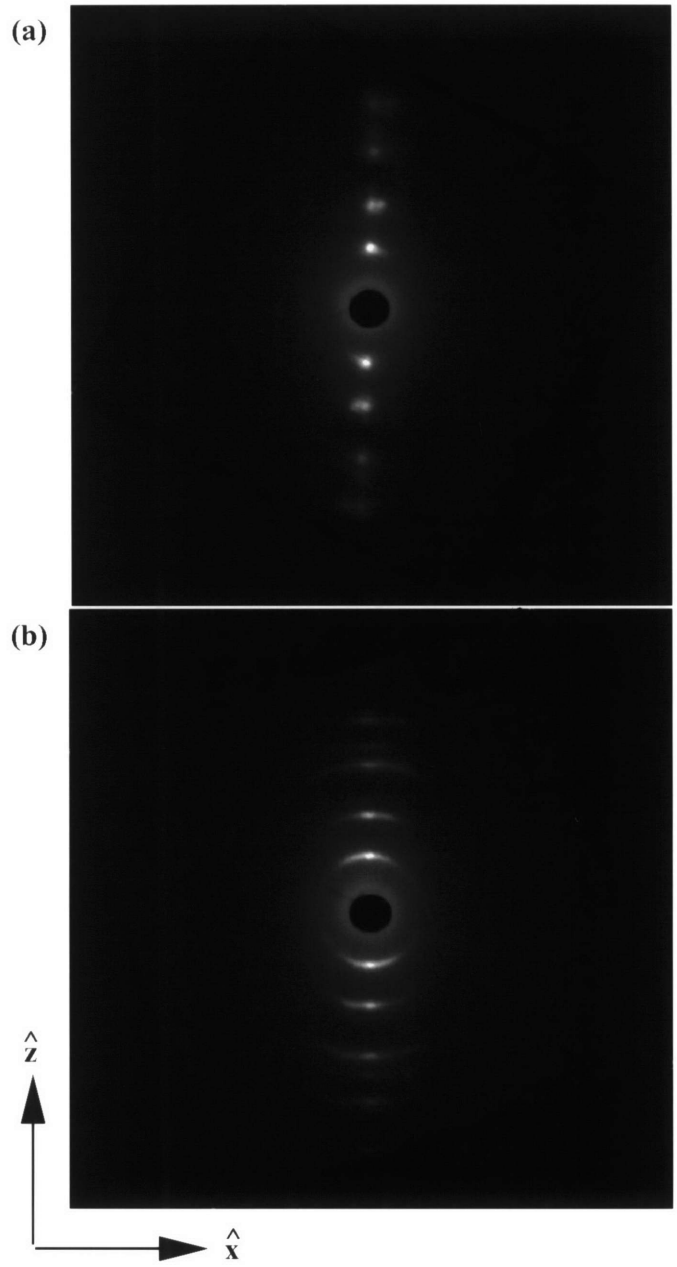

Figure 5. Two–dimensional SAXS diffraction pattern of a roll–cas sample containing 20wt% mineral oil **(a)** unannealed; **(b)** annealed.The incident x–ray beam was in the $\hat{y}$ direction.

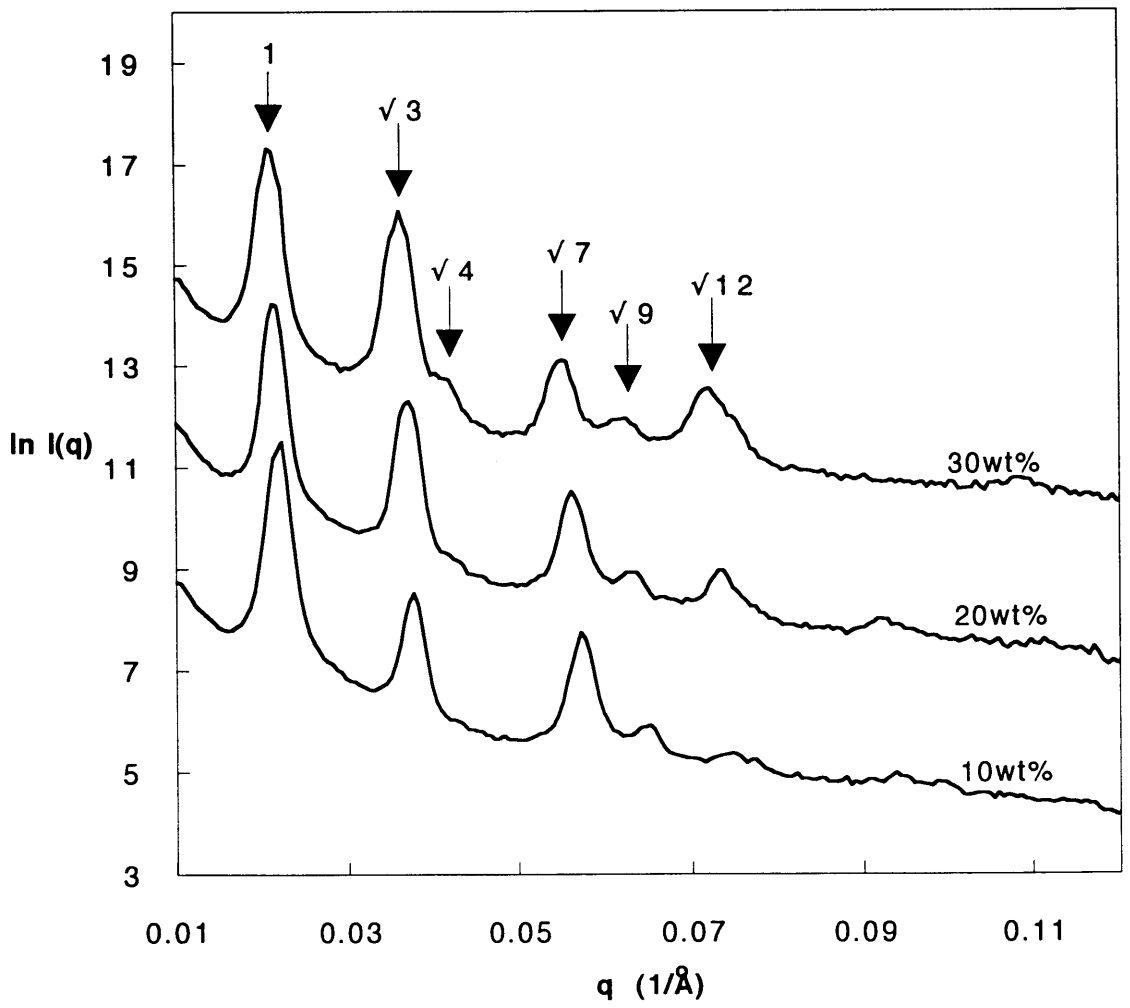

Figure 6. Azimuthally averaged intensities scattered by roll-cast, annealed samples of 10, 20 and 30wt% mineral oil content. The incident x-ray beam was in the $\hat{y}$ direction.The curves, obtained by averaging the intensities over an azimuthal angle of 40° centered on the main peak, are shifted vertically by an arbitrary amount. Arrows show the position of the theoretical reflections for a hexagonal lattice of lattice parameter d_{100} =300Å. The numbers above each arrow refer to the relative position of the allowed reflections.

2.3.2 Sphere-Forming Blends

All the morphologies discussed in this section relate to samples whose initial mineral oil content (before annealing) is 40wt%. Some of these samples present a mixed morphology of spheres and cylinders and thus are not strictly speaking 'sphere-forming' blends, but will still be discussed in this section.

2.3.2.1 Simple-Cast Samples

Figure 7 shows a TEM micrograph of a simple-cast film containing 40wt% mineral oil, annealed under vacuum for 6 days at 120°C. The morphology is clearly one of glassy polystyrene spheres embedded in a rubbery matrix. Since the mineral oil contains no aromatics, it mainly swells the isoprene phase of the block copolymer, and therefore causes the actual styrene content to decrease from 30wt% to 18wt%. The 18wt% PS composition is known to give rise to a spherical morphology for triblock copolymers. The azimuthally averaged two-dimensional SAXS pattern for a simple-cast specimen, shown in Figure 8, confirms this observation. The q values of the lattice peaks are in excellent agreement with the allowed reflections for a body-centered-cubic lattice, and peaks are resolved up to the ninth, which suggests that samples are well-ordered. The unit cell parameter a is found to be 412Å for the unannealed sample, and 417Å for the annealed sample. The TEM micrograph, as well as the two-dimensional SAXS pattern shown in Figure 9 reveal large grain sizes and very long range order. The large grain sizes observed in these samples can be explained by the same factors discussed in section 2.3.1.1.

In a work that is not reported here, a lamellar-forming styrene - isoprene - styrene triblock copolymer has been blended in a similar way with mineral oil, and depending on their composition, those blends were found to exhibit a morphology of lamellae (at low mineral oil contents), double gyroid (at intermediate mineral oil contents), and cylinders (at

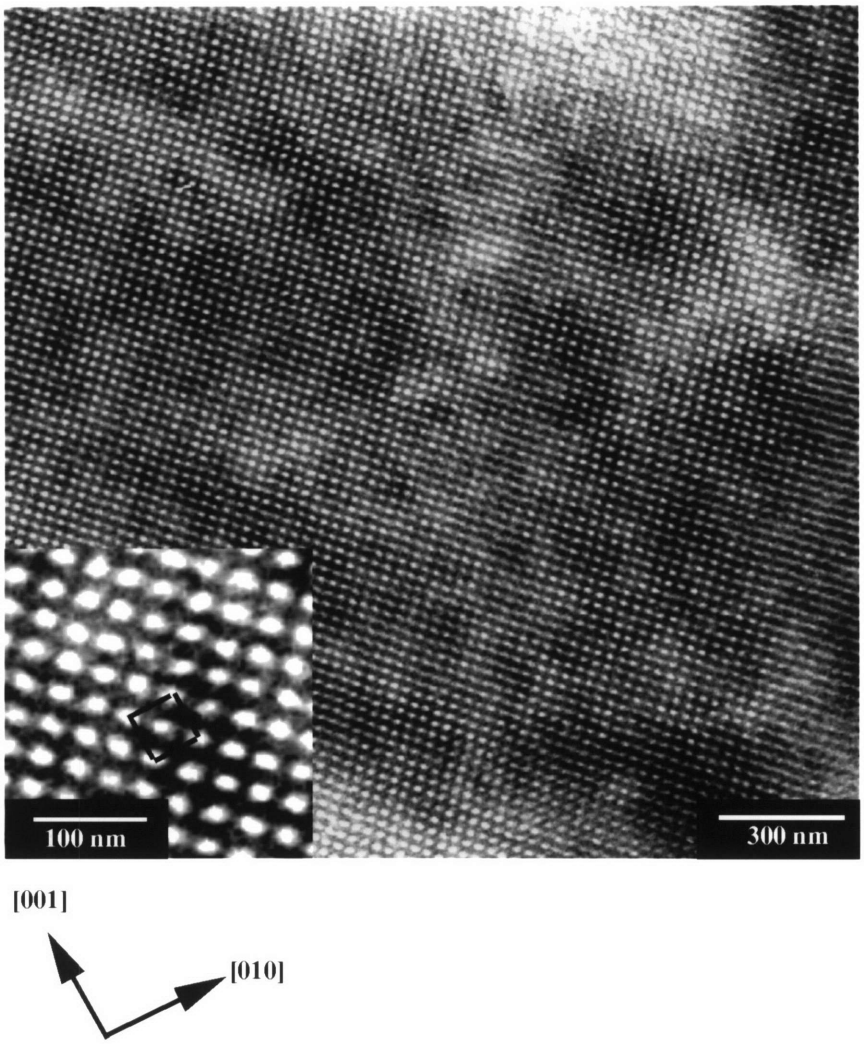

Figure 7. TEM micrograph of a simple–cast sample containing 40wt% mineral oil, annealed under vacuum for 6 days at 120C. This micrograph shows a 4–fold symmetric [100] projection of the body–centered cubic lattice. The unit cell is outlined in the inset.

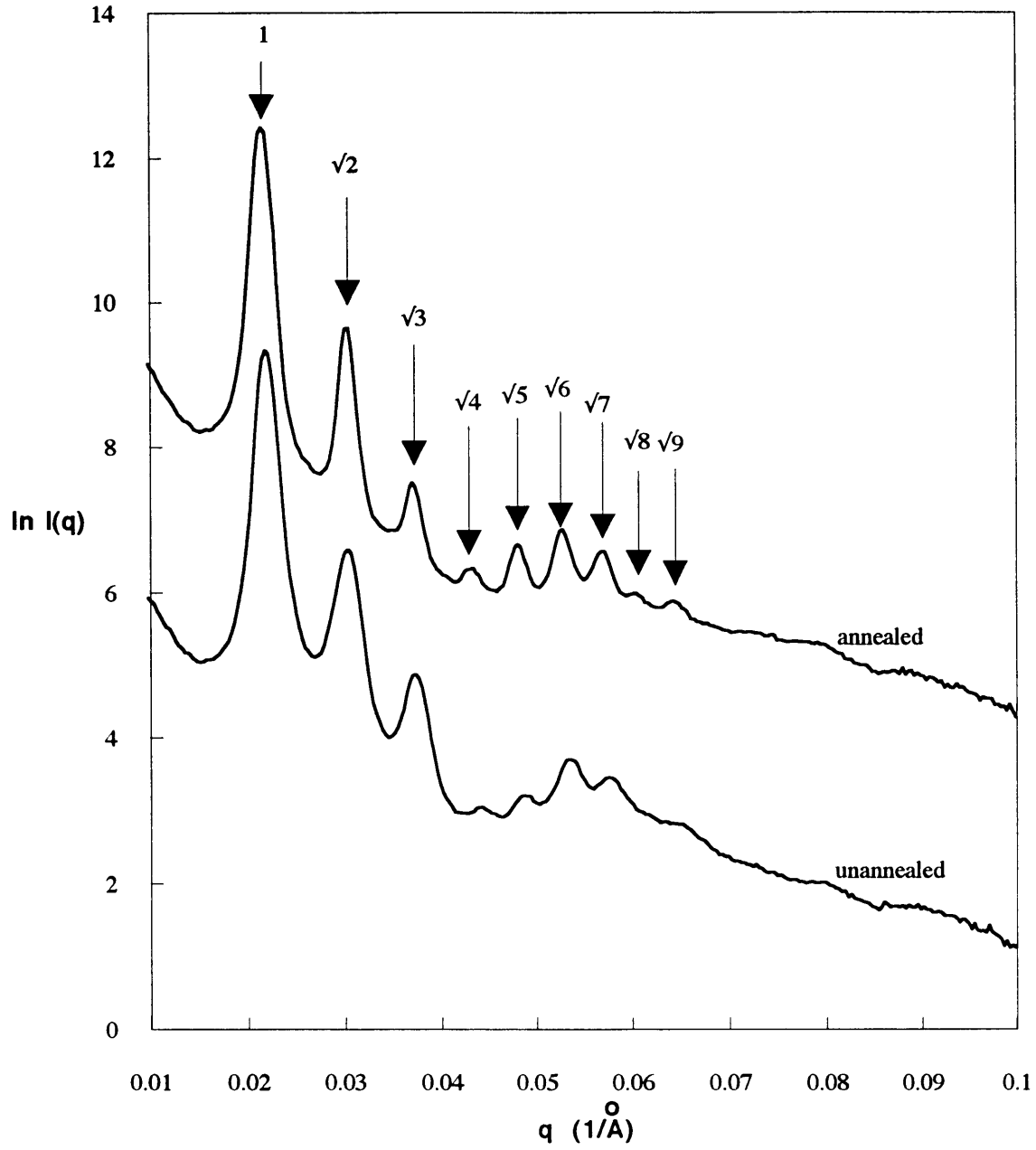

Figure 8. SAXS plot of simple-cast samples containing 40wt% mineral oil (annealed and unannealed). The two-dimensional intensities were circularly averaged and plotted versus the scattering vector q. The arrows indicate the allowed reflections for a body-centered cubic crystal, based on a unit cell parameter of a=417Å. The numbers above each arrow refer to the relative position of the allowed reflections.

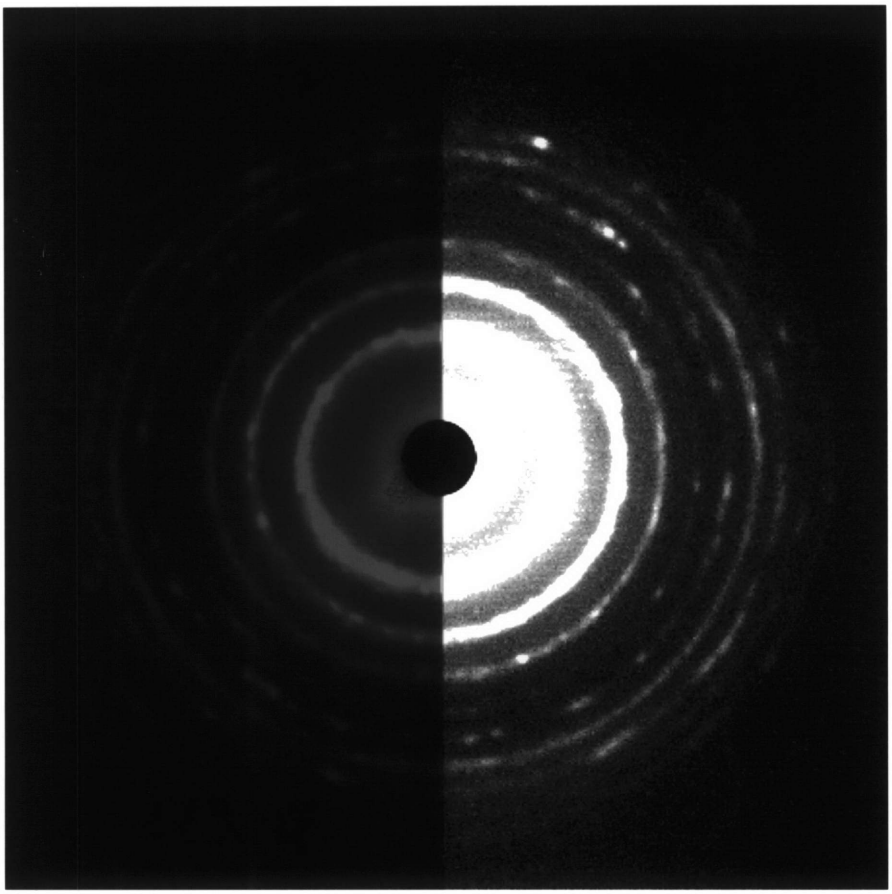

Figure 9. Two–dimensional SAXS pattern of a simple–cast sample containing 40wt% mineral oil, annealed under vacuum for 6 days at 120C. Note the spotty diffraction rings, indicative of the very large grain size in this sample. The right–hand side of the image has been overexposed in order to reveal the high–q reflections.

high mineral oil contents). The addition of mineral oil to a block copolymer can thus be used as a way to conveniently alter its morphology.

2.3.2.2 Roll-Cast Samples

The morphologies of roll-cast samples containing 40wt% mineral oil strongly depend on the experimental parameters. Whereas most samples exhibit no birefringence when observed through crossed polarizers, some samples, submitted to higher shear flow during roll-casting (due to a smaller gap between the rollers) exhibit a strong birefringence, similar to what is observed for roll-cast films presenting a cylindrical morphology. Moreover, such films also present a strong mechanical anisotropy.

Annealing also strongly affects the microstructure. As explained earlier, annealing under vacuum causes a fraction of the mineral oil to leave, which changes the composition of the sample and the effective styrene content. Samples containing 40wt% mineral oil have an effective styrene content of 18wt%. This composition is known to give rise to a spherical morphology for triblock copolymers, but it is very close to the phase transition between cylinders and spheres. It is thus to be expected that annealing under vacuum can affect the morphology of samples of this composition.

Samples produced under low shear flow - unannealed

A TEM micrograph of the roll-cast film viewed along the $\hat{x}$ direction is shown in Figure 10. This region exhibits two different grain orientations. To our knowledge this is the first time that clear grain boudaries are observed in sphere-forming block copolymer systems. A detailed investigation of all the types of grain boundaries present in our samples would constitute an interesting study, but lies beyond the scope of the present work.

TEM is not the most useful tool for studying the long-range order of a sample because of poor sampling statistics and problems with maintaining sample orientation, section orientation, and projection direction. Figure 11 shows SAXS diffraction patterns of

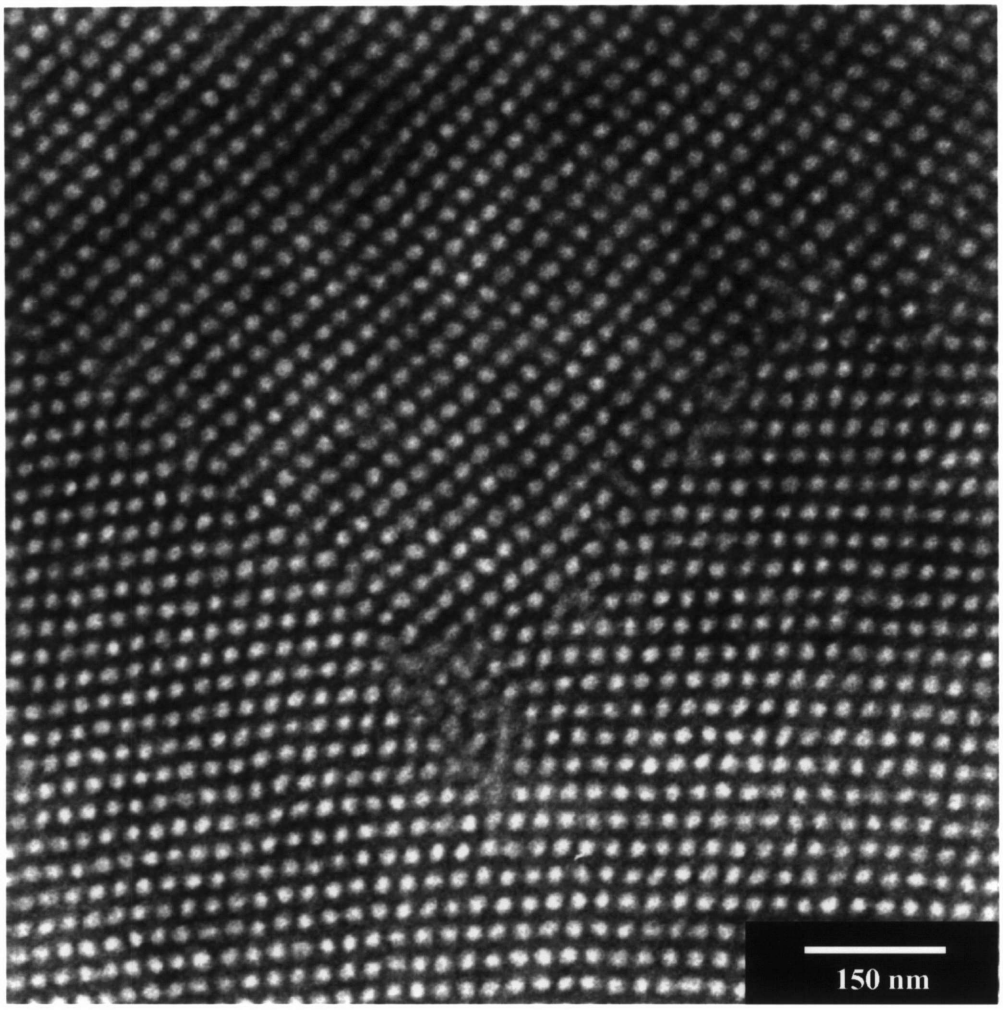

Figure 10. TEM micrograph of a roll–cast sample containing 40wt% mineral oil, viewed in the $\hat{x}$ direction. Two grains are evident, and are separated by a clear grain boundary. The tilt angle of this pure tilt boundary is approximately 37.5^{o} on the left side of the image and 29.5^{o} on the right side of the image.

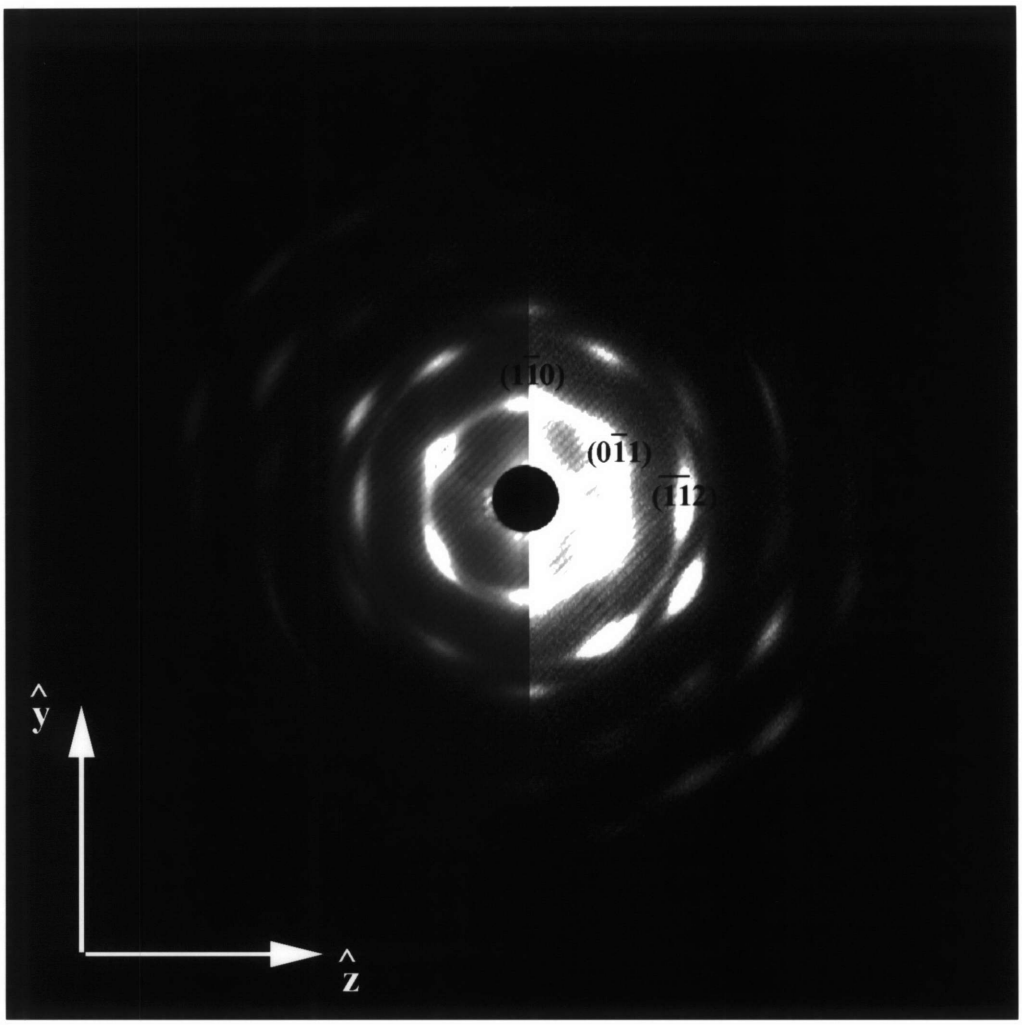

Figure 11a. Two-dimensioanl SAXS pattern of a sample containing 40wt% mineral oil and roll-cast under low shear. The incident x-ray beam is in the $\hat{x}$ direction. The reflections consist of arcs of limited circumferential broadness, indicating a partial fiber symmetry of the microstructure around the [111] axis. The loss of rotational symmetry in this pattern is due to a slight misalignment of the sample in the beam. The right-hand side of the image has been overexposed in order to reveal the weaker high-q reflections.

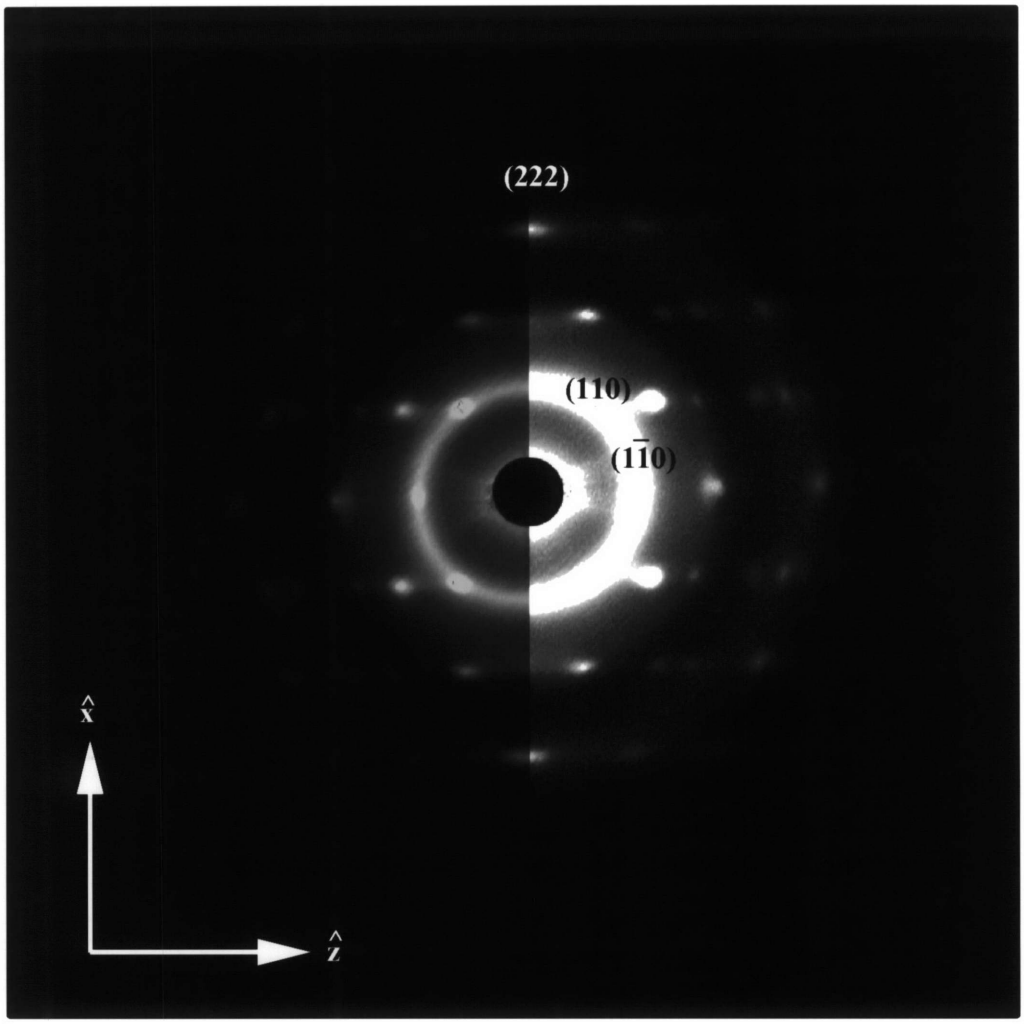

Figure 11b. Two–dimensional SAXS pattern of a sample containing 40wt% mineral oil and roll–cast under low shear. The indcident x–ray beam was in the $\hat{y}$ direction. The right–hand side of the image has been overexposed in order to reveal the weaker high–q reflections.

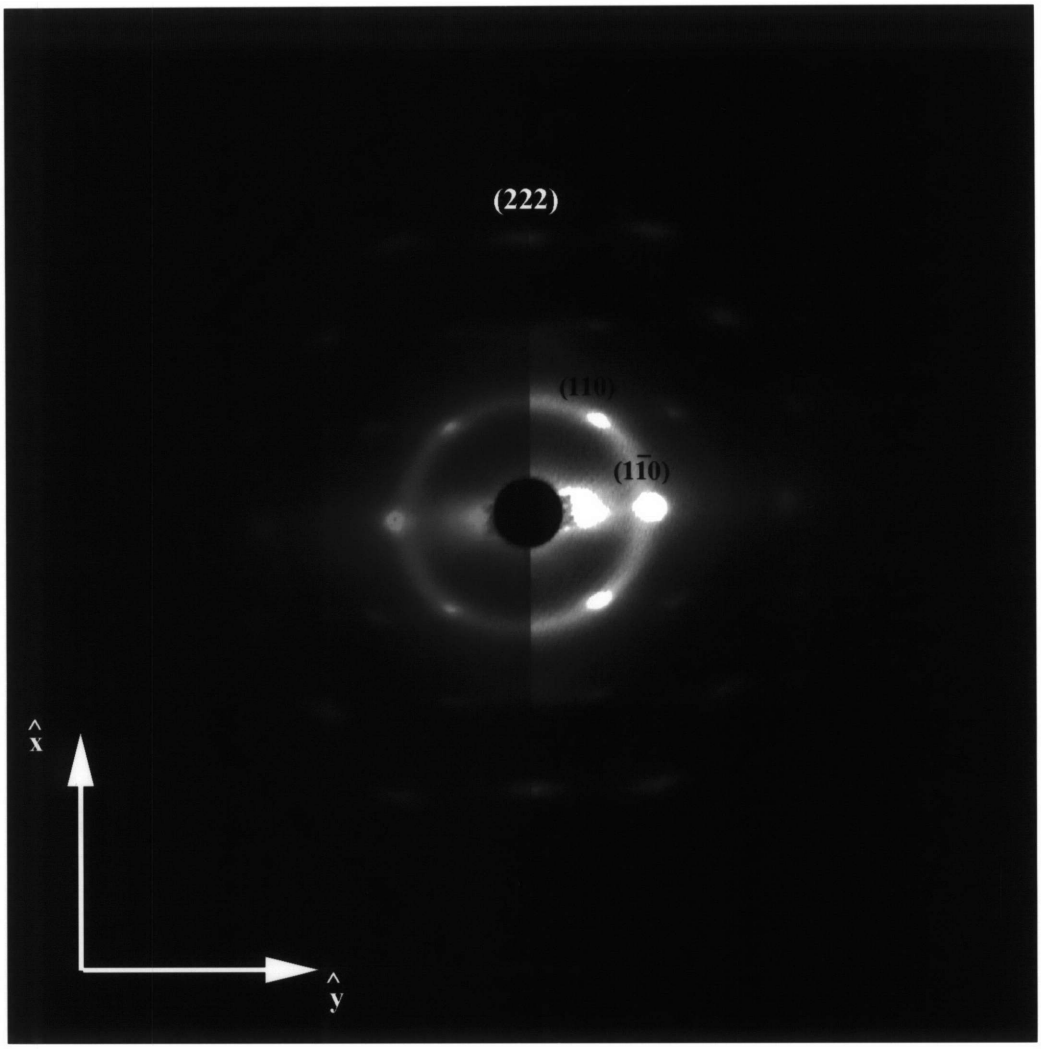

Figure 11c. Two–dimensioanl SAXS pattern of a sample containing 40wt% mineral oil and roll–cast under low shear. The incident x–ray beam was in the $\hat{z}$ direction. The reflections present in this view are similar to those visible in Figure 11b, but their relative intensities are different, suggesting that the fiber symmetry around the [111] axis is only partial. The right–hand side of the image has been overexposed in order to reveal the weaker high–q reflections.

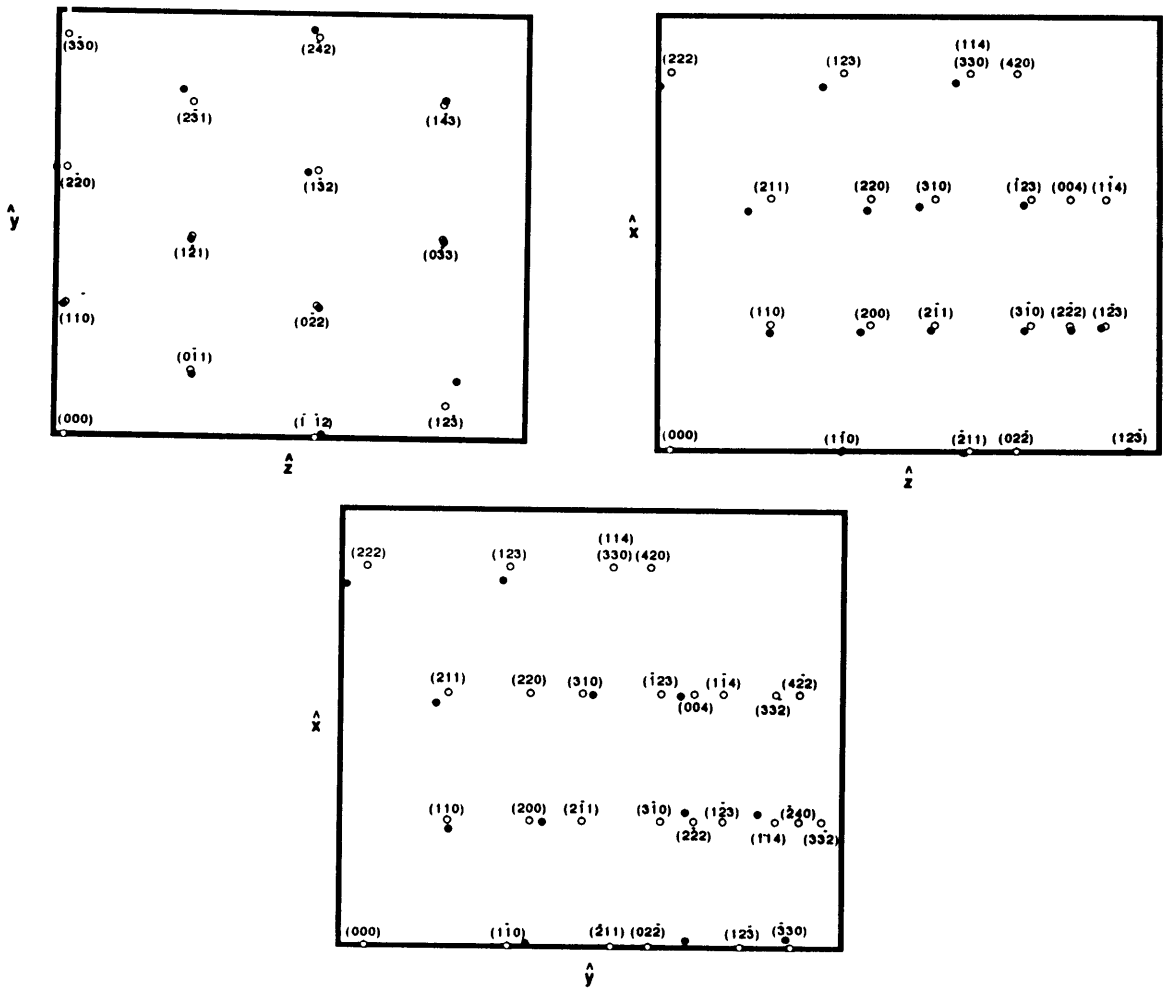

Figure 11 (d). Comparison of the position of the experimental reflections in figures 11 (a), (b), and (c) with the theoretical reflections for a body-centered cubic crystal, presenting a partial fiber symmetry with respect to the [111] direction, which is aligned with the $\hat{x}$-axis. Only the upper right quadrant of each pattern is analyzed. Black dots positions are experimental reflections; white dots represent theoretical reflections, which have been indexed.

the roll-cast film, respectively, the sample being viewed along the $\hat{x}$, $\hat{y}$, and $\hat{z}$ directions defined in Figure 1. In Figure 11d, one quadrant of each SAXS pattern is indexed assuming that the glassy polystyrene spheres are arranged on a body-centered cubic lattice in the rubbery matrix, with the [111] direction of the lattice aligned with the $\hat{x}$ axis. The allowed reflections for this structure are in good agreement with the experimental SAXS pattern. A partial fiber symmetry around the [111] direction of the cubic lattice (which corresponds to the direction of the roll-casting), is necessary to account for all the reflections observed in the $\hat{y}$ and $\hat{z}$ patterns. However, some observations suggest that this fiber symmetry is only partial: (i) reflections in the $\hat{x}$ view are not circular, but present a finite circumferential arc (full width at half maximum is 18° for the (110) reflections); (ii) the $\hat{y}$ and $\hat{z}$ patterns, although similar, differ in the relative intensities of the various peaks.

Comparison of the theoretical position of the peaks with the observed patterns shows that the lattice exhibits significant distortion. This effect is especially visible in Figures 11a and 11c (patterns taken in the $\hat{x}$ and $\hat{z}$ directions, respectively). This distortion can be explained by the processing method which was used to produce the sample. The flow field which the material undergoes is the combination of a shear flow and an elongational flow. The elongational component leads to some chain orientation in addition to microdomain orientation, resulting in residual stresses in the material and an overall distortion of the microstructure. Because of the symmetry of the roll-casting process, the lattice parameter obtained from the measurement of the d-spacings of the {110} planes in the patterns recorded in the $\hat{x}$ and $\hat{z}$ directions are very similar (355Å versus 348Å), whereas the parameter obtained from the pattern recorded in the $\hat{y}$ direction is significantly larger (393Å). This distortion was not taken into account to fit the experimental data with the theoretical position of the peaks in Figure 11 (the same value of a=364Å was used for all three lattice parameters), which explains the slight misfit for some of the reflections.

In the $\hat{y}$ and $\hat{z}$ SAXS patterns (Figures 11b and 11c, respectively), the [110] reflections are linked together by a continuous ring, which can be attributed to the presence of small, misoriented grains.

The pattern taken in the $\hat{y}$ direction (Figure 11b) exhibits a very clear zero of the form factor arising from the polystyrene spheres, as seen from the circular halo of minimum scattered intensity which surrounds the first reflections. One can show that the scattered intensity distribution from a spherical particle of radius R is given by the equation:

$$I(\bar{q}) = I_e(\bar{q})\, V^2(\rho_{PS} - \rho_{PI})^2 \frac{9\pi}{2}\left[\frac{J_{3/2}(qR)}{(qR)^{3/2}}\right]^2 \qquad (1)$$

where $I_e(\bar{q})$ is the lattice factor resulting from Bragg diffraction, V the volume of the particle, $(\rho_{PS} - \rho_{PI})$ it the electron density contrast factor, and $J_{3/2}$ a spherical Bessel function of order 3/2. The first zero of the function $\left[\frac{J_{3/2}(qR)}{(qR)^{3/2}}\right]$ occurs at qR= 4.482. The value of q corresponding to the minimum in scattered intensity is thus inversely proportional to the radius of the spheres. Since the first minimum in intensity occurs at $q=0.043\text{Å}^{-1}$, the radius of the polystyrene spheres is R=104Å. Assuming that the volume of a unit cell is the product of the three measured values for a, we can deduce the volume fraction of spheres: 19.6%. This value is consistent with the estimated value of the overall styrene weight fraction (18wt%) for this sample. Assuming that mineral oil does not go into the polystyrene, and neglecting the differences in densities of PS, PI and mineral oil, we estimate that the crosslinking functionality of the spheres (number of polystyrene chains per sphere) is approximately 200.

The first zero of the form factor is made clearly visible in Figure 11b due to the presence of important background scattering. This diffuse scattering arises from irregularities in the paracrystalline-lattice[46], which are also observable in the TEM micrograph in Figure 10.

By roll-casting a solution of triblock copolymer, mineral oil and toluene, we have succeeded in producing a very ordered and oriented sample of thermoplastic rubber, where the spheres, which act as physical crosslinks of known crosslinking functionality, are situated on a body-centered cubic lattice with the [111] direction aligned with the roll-casting flow direction, and with partial fiber symmetry around this [111] direction. This well-defined system constitutes a very good sample to study the deformation mechanism in sphere-forming block copolymer systems. The changes in the microstructure of this sample during uniaxial tensile deformation are studied in chapter 4.

Samples produced under low shear flow - annealed

The morphology of roll-cast samples of 40wt% initial mineral oil content is slightly modified upon annealing under vacuum. Figure 12 shows a two-dimensional SAXS pattern of a sample annealed for 6 days at 120°C, recorded with the incident x-rays in the $\hat{y}$ direction. The diffraction spots are very similar to the ones observed for the corresponding unannealed sample (Figure 11b), except for the presence of additional reflections on the $\hat{z}$-axis. Figure 13 shows a TEM micrograph of the same sample, viewed in the $\hat{y}$ direction. In addition to the glassy spheres visible in the unannealed sample, we now observe the presence of glassy cylinders. This effect can be explained by the loss of a fraction of mineral oil during the annealing process, which results in a decrease in mineral oil content in the sample. Assuming that the mineral oil only swells the rubber phase, the loss of mineral oil results in an increase of the effective polystyrene content of the sample (which is 18wt% for a mineral oil content of 40wt%). Since the transition from a spherical to a cylindrical morphology occurs between 15 and 20 vol% for triblock copolymers, the appearance of a phase of cylindrical morphology can be explained by the mineral oil loss during annealing.

The TEM micrograph in Figure 13 shows that although the cylinders have various orientations, the overall orientation of cylindrical grains in the sample is not completely

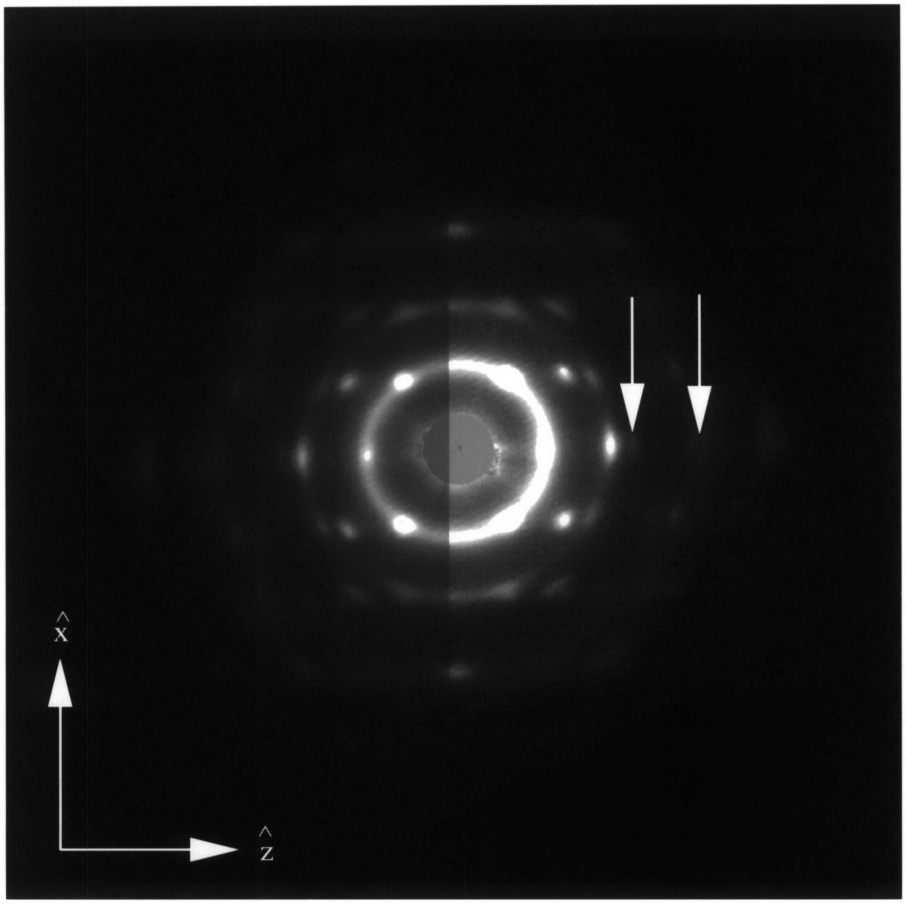

Figure 12. Two–dimensional SAXS diffraction pattern of a sample roll–cast under low shear and annealed for 6 days at 120C. Data was recorded with the incident x–rays in the $\hat{y}$ direction. In addition to the reflections present in Figure 11b, some additional reflections (indicated by the arrows) are visible on the $\hat{z}$–axis, which correspond to the cylinders aligned in the $\hat{x}$ direction.(Initial mineral oil content: 40wt%).

Figure 13. TEM micrograph of a sample roll–cast under low shear and annealed for 6 days at 120C. The sample is viewed in the $\hat{y}$ direction. (Initial mineral oil content : 40wt%). Both spherical and cylindrical microdomains are evident, and most cylinders are aligned in the flow direction.

random. In most grains the cylinders are oriented in a preferred direction. This observation is confirmed by the SAXS diffraction pattern shown in Figure 12, which shows that the cylinders have a preferred orientation in the $\hat{x}$ direction, since the additional peaks corresponding to the cylinders are situated on the $\hat{z}$-axis. This indicates that the [111] direction of the bcc lattice formed by the spheres corresponds to the [0001] direction of the hexagonal lattice formed by the cylinders. The correspondence between the two crystalline directions was also reported by Sakurai *et al.*[10,11] in their study of a thermally induced sphere to cylinder transition.

Samples produced under high shear flow

Samples which were submitted to high shear during roll-casting were found to exhibit very different physical properties and morphology from samples submitted to lower shear rates. Whereas roll-cast films produced under low shear rate are not birefringent and are mechanically isotropic in first approximation, films produced under high shear are optically birefringent and exhibit a clear mechanical anisotropy.

The TEM micrographs of an unannealed sample produced by high shear rates, shown in Figure 14, reveal a two-phase structure comprised of regions of cylindrical and spherical morphology. The cylinders are visible when the sample is viewed orthogonal to the shear flow ($\hat{y}$ direction) and are all well aligned in the flow direction. The cylindrical zones are of oblong shape and their typical dimensions are about 1μm in length and 300nm in width. Micrographs taken in the $\hat{x}$ direction show spheres and end-on cylinders.

The micrograph in Figure 14b also shows that at the interface between the spherical and the cylindrical regions the spheres coalesce and aggregate into cylinders. The two-dimensional SAXS pattern for this sample, which is similar to the pattern shown in Figure 12, indicates that the [111] direction of the cubic lattice formed by the spheres corresponds to the [0001] direction of the hexagonal lattice formed by the cylinders, since the reflections corresponding to the cylinders are located at 90° with respect to the [222] reflection of the

(a)

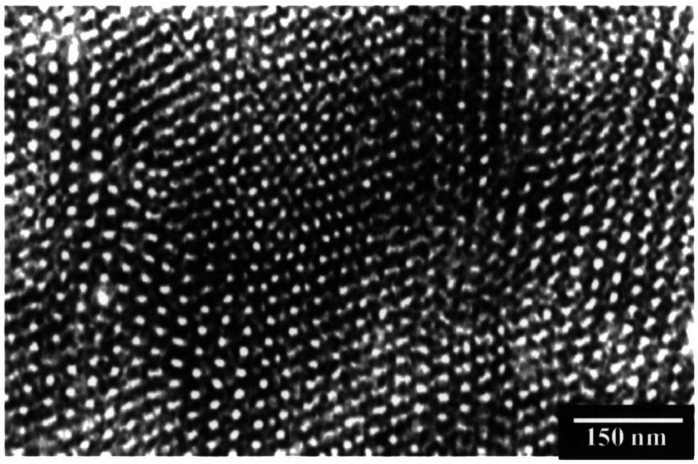

Figure 14 (a). TEM micrograph of an unannealed roll–cast sample produced by high shear flow, viewed in the $\hat{x}$ direction. (Mineral oil content:40wt%). The white polystyrene domains are of two types: some correpond to glassy spheres, while others are end–on cylinders.

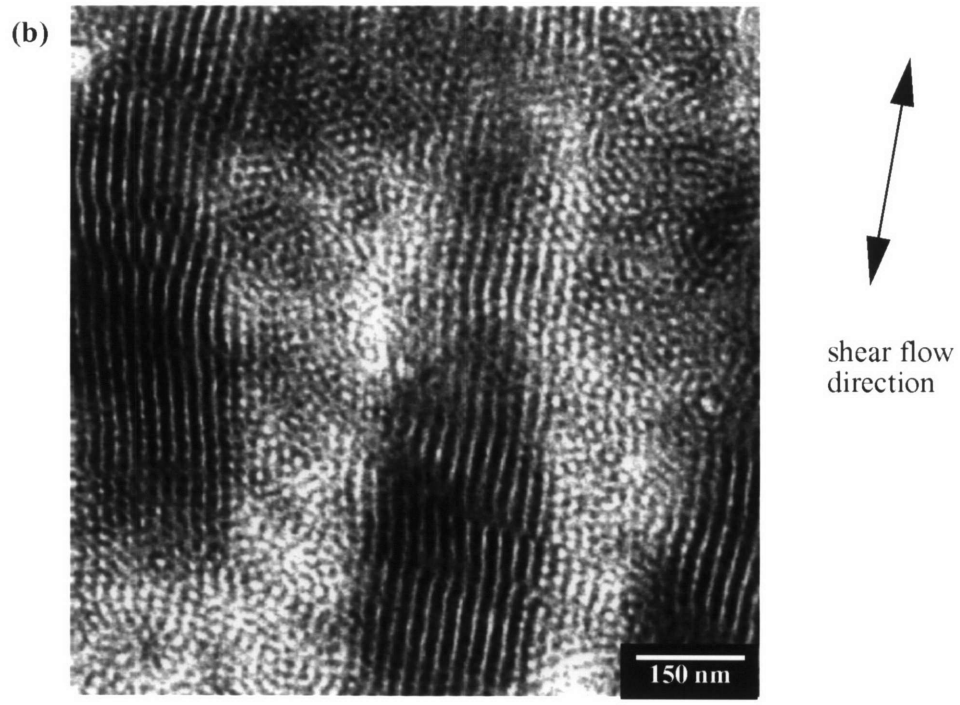

Figure 14 (b). TEM micrograph of an unannealed roll–cast sample produced by high shear flow, viewed in the $\hat{y}$ direction. (Mineral oil content: 40wt%). The white lines correspond to the glassy cylinders, and the circles correspond to the glassy spheres. The cylinders are aligned in the flow direction, and at the interface between both phases the cylinders progressively break up into spheres.

cubic lattice. Sakurai *et al.*[11] observed the same relationship between the two lattices in their study of a thermoreversible transition between spheres and cylinders. The mechanism that they propose for the morphology transition from spheres to cylinders involves a change in interfacial curvature from a sphere to a spheroid, followed by a coalescence of the spheroids to form cylinders with their long axis oriented in the [111] direction. Since in our sample spheres and cylinders coexist, it is useful in veryfying the proposed transition mechanism. The TEM micrograph in Figure 14b provides a confirmation for their hypothesis since some parts of the micrograph show the coalescence of spheres into cylinders along the shear flow direction (which is the [111] direction of the cubic lattice).

It is important to notice that the mixed morphology in the sample oriented by high shear flow is somewhat different from the morphology observed after annealing in the sample produced under low shear flow. In both samples grains of glassy spheres and grains of glassy cylinders coexist, but in the sample produced by high shear flow the size of the cylindrical microdomain grains is larger and all the cylinders without exception are oriented in the shear flow direction since the formation of cylinders was induced by a shear flow instead of a change in composition (loss of mineral oil).

This result shows that by applying a high shear rate to a blend of triblock copolymer and mineral oil which forms a spherical microstructure under normal conditions, it is possible to induce a sphere-to-cylinder transition and the coexistence of a spherical phase with a cylindrical phase. This transition, however, is probably not a thermodynamically stable state and should be reversible after annealing.

Upon annealing under vacuum (which induces a loss of mineral oil) the morphology does not change significantly. Figure 15 shows TEM micrographs of an annealed sample. The micrograph taken in the $\hat{y}$ direction ($\overline{xz}$ projection) shows coexistence of cylinders aligned in the flow direction with a spherical phase. The grains of both phases are larger and better ordered than in the unannealed sample. If the shear-induced sphere to cylinder transition was metastable, the morphology should completely revert back to

(a)

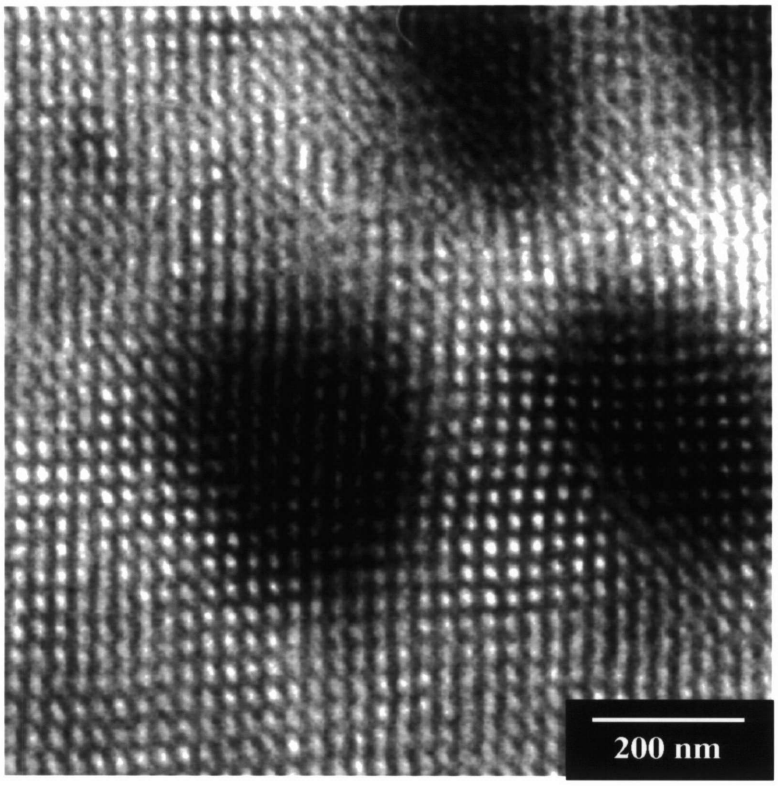

Figure 15. (a) TEM micrograph of an annealed roll –cast sample produced by high shear flow, viewed in the $\hat{x}$ direction.. (Initial mineral oil content: 40wt%). The image shows light zones and dark zones, corresponding to regions of different mineral oil concentration in the matrix.

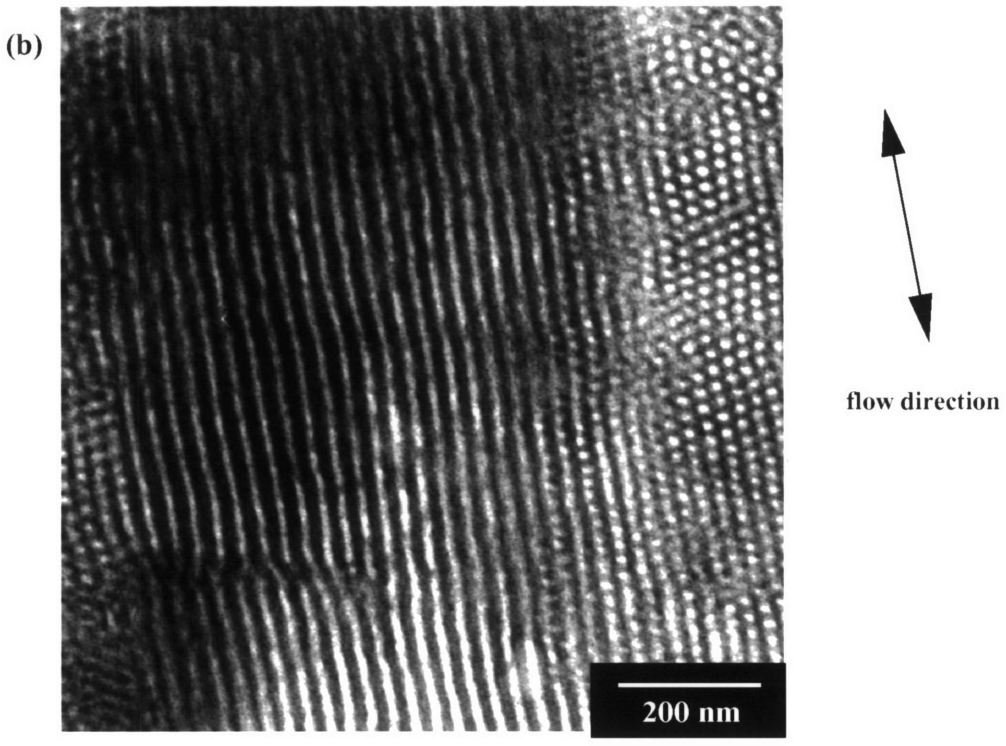

Figure 15(b). TEM micrograph of an annealed roll –cast sample produced by high shear flow, viewed in the $\hat{y}$ direction. (Initial mineral oil content: 40wt%).

spheres upon annealing. In our experiments, annealing induces a change in composition of the sample (the effective polystyrene content increases), which can explain why some of the cylinders do not revert to spheres. The coexistence of spheres and cylinders caused by the shear-induced transition can also be an equilibrium state. Since the system consists of two components (block copolymer and mineral oil), Gibbs' phase rule requires the presence of a bi-phasic microstructure at equilibrium at the transition between spherical and cylindrical microstructure. The cylindrical phase, containing a given proportion of mineral oil, can be in equilibrium with a spherical phase containing a higher proportion of mineral oil. In order to verify the assumption that the observed sphere to cylinder transition is an equilibrium state, it would be necessary to anneal the sample in such a way to prevent the loss of mineral oil. If the morphology is metastable, it should revert back to spheres after annealing.

The TEM micrograph taken in the $\hat{x}$ direction shows spheres and end-on cylinders, but it also shows a feature which is absent in the unannealed sample: the presence of dark and light zones approximately 0.5 microns in size. These zones have only been observed in annealed samples viewed in the shear flow direction. In the dark zones, the glassy microdomains are smaller on average than in the light zones and their d-spacings are smaller. The glassy domains in the dark zones are also less ordered than in the light regions. A possible explanation for this phenomenon could be that annealing causes the lighter fraction of the mineral oil to evaporate, which could reduce the compatibility between the block copolymer and the mineral oil that is left in the sample and that has a different composition from the original mineral oil. The mineral oil thus tends to phase separate from the polymer, which would also explain the higher 'stickiness' of annealed samples versus unannealed samples that is observed when handling the samples. This induces a new type of phase separation in the sample: segregation between oil-rich domains and oil-poor domains, the size of which is much bigger than the size of the domains resulting from the microphase separation between styrene-rich and isoprene-rich domains.

In the oil-rich domains the rubber contains a significantly higher proportion of mineral oil, and is thus less stained by OsO_4 (the mineral oil contains no double bonds). The matrix in the oil-rich domains thus appears lighter.

It is possible that the oil-rich phase corresponds to the regions of spherical morphology, and the oil-poor zones to the regions of cylindrical morphology. This assumption is hard to prove by TEM since the difference in contrast between oil-rich and oil-poor regions is not as visible when the sample is viewed in the directions perpendicular to the shear flow. Based on given values of the d-spacings of the cylinders (300Å) and the a parameter of the cubic lattice (370Å), one can calculate the radius of the spheres and the cylinders for given mineral oil concentrations in each phase (neglecting the differences in densities between styrene, isoprene, and mineral oil). The result of this calculation indicates that the difference in the radius of the spheres and the cylinders is highest when the oil concentration is uniform, and that this difference vanishes when the difference in oil concentration between the two phases increases. The assumption that the oil-rich phase corresponds to the spherical zones and the oil-poor phase to the cylindrical regions is thus incompatible with our observation that the glassy domains are larger in the oil-rich phase.

2.3.3 Summary

A summary of all the above-described morphologies observed in simple-cast and roll-cast blends of triblock copolymer and mineral oil is presented in Table 3. The last column indicates the figure(s) corresponding to each morphology. The results which have been discussed in chapter 2.2 can be summarized in four main conclusions:

- When blended with a sufficient amount of mineral oil containing no aromatics, the morphology of a cylinder-forming styrene - isoprene - styrene triblock copolymer changes to a spherical morphlogy, the spheres being arranged on a body-centered cubic lattice. The mineral oil mainly swells the rubber phase, thus acting as a preferential solvent for the isoprene. This change in morphology is not surprising, since adding

Table 3. Summary of the morphologies observed in simple-cast and roll-cast blends of styrene - isoprene - styrene triblock copolymer and mineral oil.

Mineral Oil Content	Processing Method	Annealing	Morphology	Figures
10wt% to 35wt%	Simple-Cast	Unannealed	cylinders randomly oriented grains	2
		Annealed	cylinders randomly oriented grains	3
	Roll-Cast	Unannealed	cylinders aligned in flow direction 'single-crystal'	4
		Annealed	cylinders aligned in flow direction 'single-crystal'	5, 6
40wt%	Simple-Cast	Unannealed	bcc spheres large grains, randomly oriented	8
		Annealed	bcc spheres large grains, randomly oriented	7, 8, 9
	Roll-Cast - low shear	Unannealed	bcc spheres [111] direction = flow direction partial fiber symmetry around [111]	11
		Annealed	grains of bcc spheres + grains of cylinders [111] direction of bcc lattice = flow direction partial fiber symmetry around [111] preferred orientation of cylinders in the flow direction	12, 13
	Roll-Cast - high shear	Unannealed	grains of bcc spheres + grains of cylinders [111] direction of bcc lattice = flow direction partial fiber symmetry around [111] cylinders oriented in flow direction	14
		Annealed	grains of bcc spheres + grains of cylinders [111] direction of bcc lattice = flow direction partial fiber symmetry around [111] cylinders oriented in flow direction dark and light zones in TEM micrographs	15

mineral oil preferentially to the isoprene phase is equivalent to decreasing the styrene volume fraction. Blending a block copolymer with mineral oil can thus be used to alter its morphology.

- Both cylinder-forming blends and sphere-forming blends can be oriented by solvent roll-casting. In the case of spheres, the grains are aligned with the [111] direction of the cubic lattice in the shear flow direction.
- When a sphere-forming blend is roll-cast from toluene under high shear flow (small gap between the rollers), the orientation of the body-centered cubic lattice is accompanied by a partial sphere-to-cylinders transition, leading to a mixed morphology of spheres and cylinders oriented by the shear flow. This morphology, could either be an equilibrium biphasic morphology due to the presence of two components in the system, or it could be metastable morphology which would return to a pure spherical morphology after annealing. Since in our study the annealing process induces a change in composition in the sample, we were unable to distinguish between these two possibilities.
- After annealing, the samples produced under high shear flow present a morphology of oil-rich regions and oil-poor regions. A possible interpretation of the TEM micrographs is that the oil-rich regions have a spherical morphology and the oil-poor regions a cylindrical morphology.

2.4 Mechanical Behavior of Roll-Cast Samples

Blending a triblock copolymer with mineral oil can be useful not only in order to modify its morphology, but also in achieving a wide range of different mechanical properties starting from a block copolymer of given composition and characteritics. In this section we study the mechanical properties of the unannealed roll-cast samples containing 10, 20 and 30wt% mineral oil, the cylindrical morphology of which was discussed in section 2.3.1.2. The sample preparation method is described in section 2.2.

Uniaxial tensile experiments were performed using an Instron 4501 apparatus. Samples typically 1mm thick, 5mm wide and 10 to 15mm long were deformed at a crosshead speed of 50mm/min. Displacement was measured with a strain gauge, and load was measured with a 5kN load cell. Samples were tested in the direction of the glassy cylinders ('parallel' stretching) and perpendicular to the cylinders ('perpendicular' stretching). On each sample 5 parallel tests and 5 perpendicular tests were performed in order to gather statistically significant results.

Figure 16 shows typical 'perpendicular' stress-strain curves for three samples containing 10, 20, and 30wt% mineral oil, respectively. Figure 17 shows typical 'parallel' stress-strain curves for another set of samples of the same mineral oil contents. In Table 4 the average values of the measured mechanical properties are reported. The measured modulus is the tangent modulus at the onset of stress-strain curve. When the samples are deformed in the parallel direction, the load is mainly supported by the glassy cylinders, which undergo plastic deformation at high stresses, resulting in yielding and necking of the sample. When the samples are deformed in the perpendicular direction, they do not exhibit necking, since the deformation is mainly supported by the rubber matrix, which keeps the stress in the glassy cylinders below the yield stress of the polystyrene.

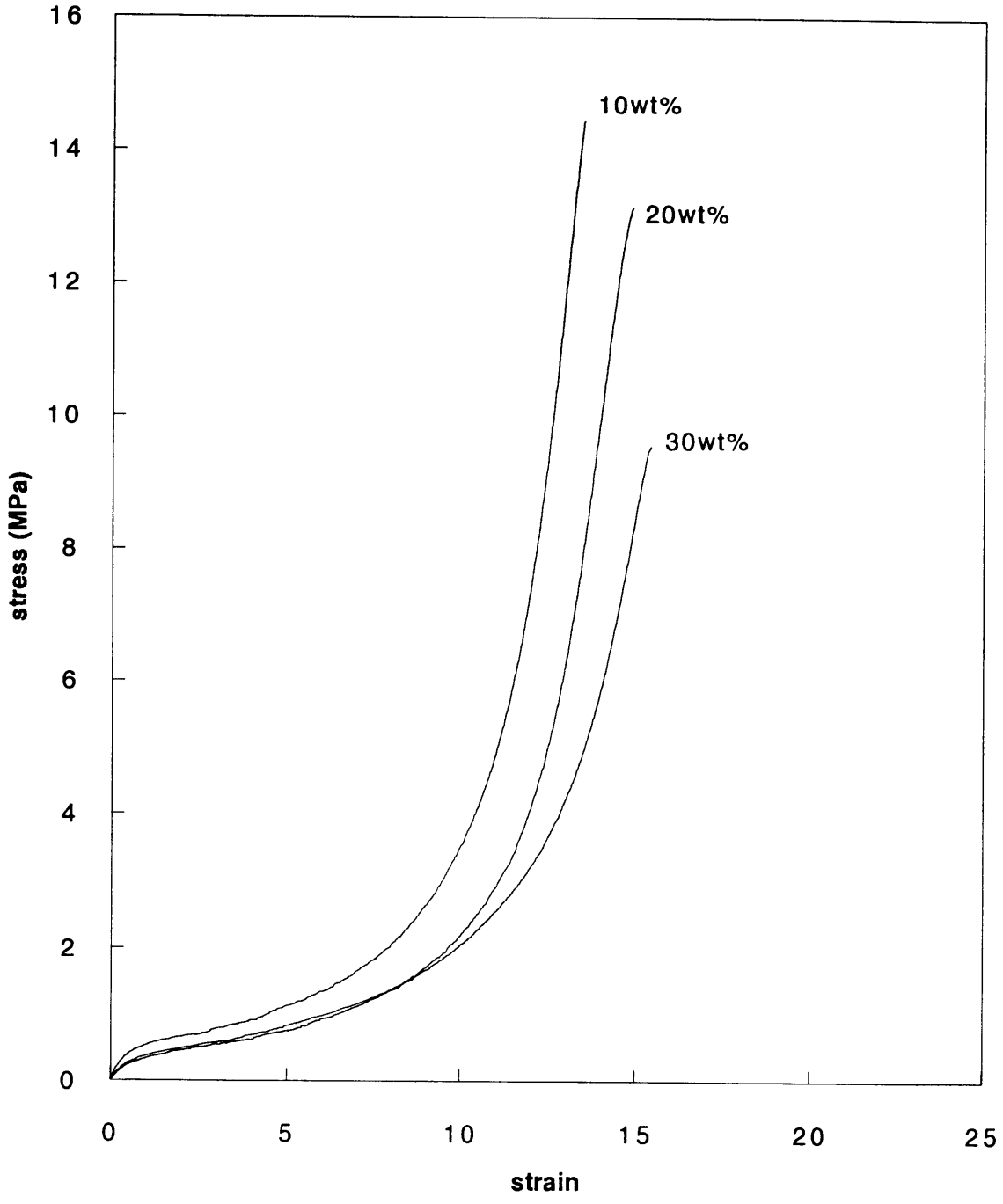

Figure 16. Stress-strain curves of roll-cast samples containing 10, 20, and 30wt% mineral oil, measured perpendicular to the glassy cylinders.

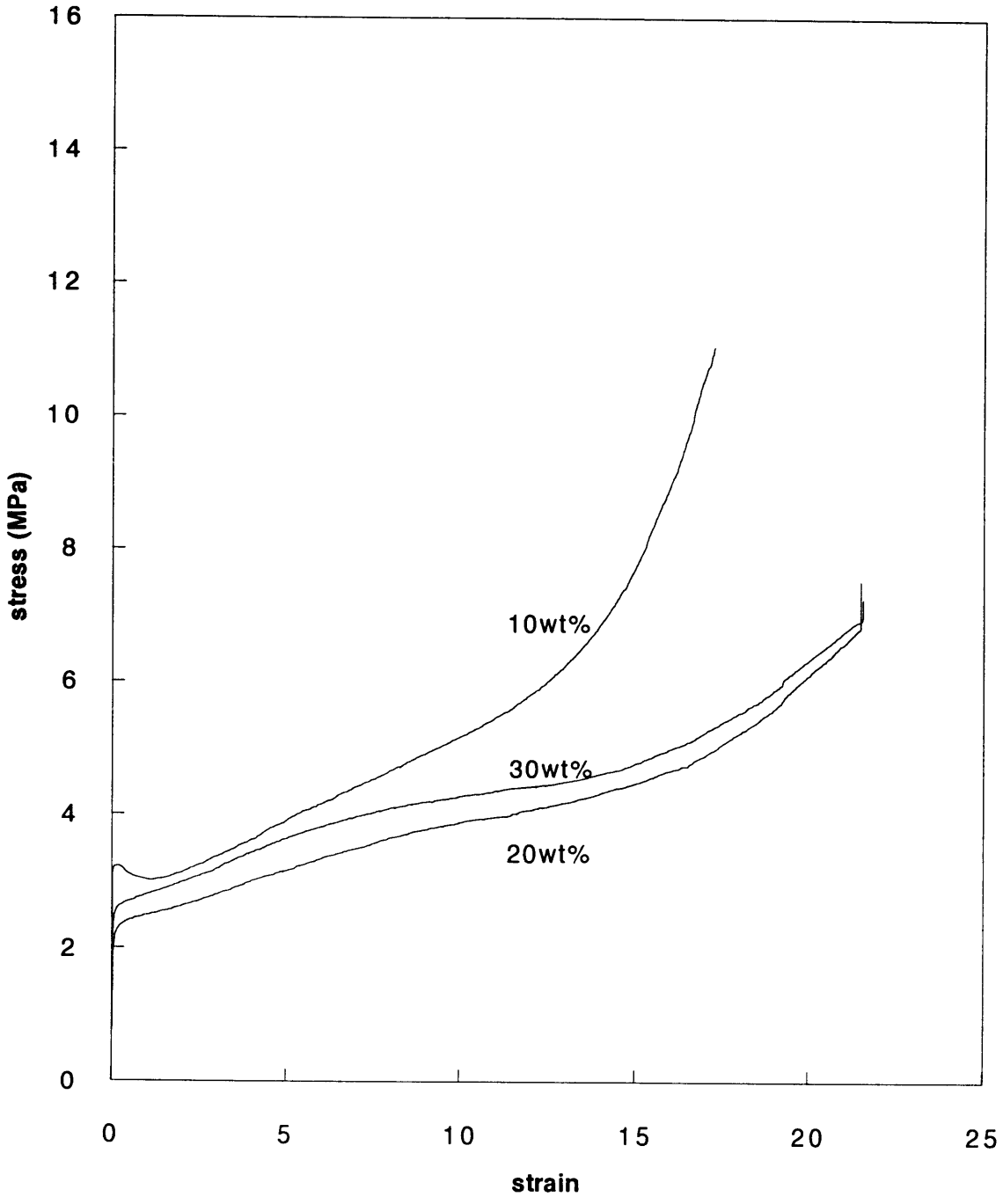

Figure 17. Stress-strain curves of roll-cast samples containing 10, 20, and 30wt% mineral oil, measured parallel to the glassy cylinders.

Mineral Oil Content	10 wt%		20 wt%		30 wt%	
	parallel	perpendicular	parallel	perpendicular	parallel	perpendicular
σ_{yield} (MPa)	3.14	---	2.41	---	2.54	---
σ_{break} (MPa)	11.0	14.5	7.74	8.01	5.94	9.21
ε_{break} (%)	1832	1595	2212	1480	2089	1548
E (MPa)	98.3	1.31	53.2	0.56	78.8	0.81
E_{par}/E_{perp}	75.2		94.5		122.0	

Table 4. Mechanical properties of roll-cast samples of triblock copolymer and mineral oil, measured parallel and perpendicular to the axial direction of the glassy cylinders. E is Young's modulus, σ_{yield} is the yield stress, σ_{break} and ε_{break} are the stress and strain at break, respectively. The ratio of the modulus parallel to the cylinders by the modulus in the perpendicular direction is also reported. The values in this table are the averages of the values measures in 5 experiments.

The yield stress (in the parallel direction) and the modulus (in both directions) decrease when the mineral oil content is increased from 10% to 20%, and then increase when the mineral oil is increased from 20% to 30%. The influence of mineral oil on stress and strain at break does not exhibit any clear trend. Since the measurement of the ultimate properties present a wide dispersion, and since most samples tend to break in the region surrounding the grips, this information is not significant. However, it is worth noting that the deformation at break lies in the range 1500 to 2000%, which is much higher than what is usually reported for pure triblock copolymers[1,2], but very similar to the properties reported for unoriented blends of triblock copolymer and mineral oil having a cylindrical

morphology[14].The ratio of the modulus parallel to the cylinders by the modulus in the perpendicular direction significantly increases with increasing mineral oil content. It increases from a value of 75 for samples containing 10wt% mineral oil, to 95 for samples containing 20wt% mineral oil, to 125 for samples containing 30wt% mineral oil.

In order to interpret these results, it is important to understand the various effects of mineral oil addition on a block copolymer, and more especially an oriented block copolymer sample presenting a cylindrical morphology. It is clear that properties such as parallel modulus and yield stress mainly depend on the properties of the glassy phase, whereas the value of the perpendicular modulus depends on the stiffness of the rubber phase.

The presence of the mineral oil in the system causes the modulus of the rubber phase (which is composed of isoprene and mineral oil) to decrease dramatically, but it also causes the isoprene chains to be somewhat stretched before any strain is applied to the sample, since the d-spacings between the glassy cylinders are increased over that for the neat triblock. This 'pre-stretching' of the isoprene chains can increase the modulus of the rubber phase. For small mineral oil fractions, the first effect is likely to dominate the mechanical response of the blend, resulting in a decrease of the perpendicular modulus with mineral oil content. At higher mineral oil contents the 'prestretching' effect might be dominant, which can explain the subsequent increase of the perpendicular modulus with mineral oil fraction.

The changes in values of the yield stress and the parallel modulus are most likely related to the influence of the mineral oil on the properties of the glassy cylinders. Here again, two opposite effects can be induced by the addition of a plasticizer. For low mineral oil fraction, the main effect is a decrease in the degree of phase separation between the polystyrene and the isoprene domains. This is detrimental to the mechanical properties of the sample stretched in the direction of the cylinders, since it reduces the effective radius of the glassy 'fibers' which are responsible for the high modulus and yield stress. At higher

mineral oil contents however, a small fraction of the mineral may penetrate into the glassy domains. Anderson *et al.*[23] have shown that blending small quantities of Penreco Drakeol 500 mineral oil into polystyrene causes its yield stress and its tensile modulus to increase significantly. This antiplasticization effect could explain our observation of an increase of the (parallel) yield stress and the parallalel modulus with mineral oil fraction.

The increased mechanical anisotropy (measured by the ratio of the parallel modulus by the perpendicular modulus) of our oriented blends with increased mineral oil content can be attributed to the improved ordering of the samples. The larger grain sizes in samples of high mineral oil content reduces the influence of grain boundaries on the mechanical behavior of the sample, therefore emphasizing the effect of orientation of the glassy cylinders and increasing the ratio of the parallel modulus to the perpendicular modulus.

Chapter 3

Thermal Roll-Casting of Block Copolymer - Mineral Oil Blends

3.1 Introduction

In Chapter 2 we have shown that roll-casting blends of a styrene - isoprene - styrene triblock copolymer and mineral oil processed from a toluene solution are a good means of producing films presenting excellent mechanical anisotropy due to the alignment of the glassy cylinders in the shear flow direction. The mechanical properties of such films can be tailored to specific needs by modifying the mineral oil content of the blend, allowing for the fabrication of films presenting different mechanical properties starting from a triblock copolymer of a given composition.

However, several factors limit the practical use of a solvent roll-casting process. Firstly, this processing method is fairly long, typically 45 minutes to produce a film of 1mm in thickness. Secondly, for environmental and safety reasons, the use of solvents should be limited as often as possible, especially in the case of large-scale production. It would therefore be useful to develop a similar process in which the role of the solvent is replaced by heating. By heating a block copolymer above its order - disorder transition and subsequently cooling it down while submitting it to roll-casting shear flow ('thermal roll-casting'), it could be possible to obtain anisotropic films similar to those produced by solvent processing. In the cases of triblock copolymers of high molecular weight such as the polymers we are considering the order - disorder transition is generally much higher than the degradation temperature, making thermal roll-casting of pure triblock copolymers virtually impossible.

Blending a triblock copolymer with mineral oil can solve this difficulty. It is to be expected that the presence of the mineral oil (which acts as a preferential solvent for the isoprene) will depress the order - disorder transition temperature, thereby making it possible to process the blend at a temperature which is lower than the degradation

temperature of the polymer. In the first part of this chapter (section 3.2) we determine the order - disorder transition temperature of blends of styrene - isoprene - styrene triblock copolymer and mineral oil. In sections 3.3 we describe the thermal roll-casting method that we used to make oriented blends and in section 3.4 we characterize the morphology of the films obtained by this method.

3.2 Determination of the Order-Disorder Transition of the Blends

Sample Preparation

The materials and the sample preparation method are the same as those described under section 2.2. The rubber block of the triblock copolymer was deliberately chosen to be isoprene rather than butadiene, since polyisoprene degrades less easily than polybutadiene. The choice of the Penreco Drakeol 500 mineral oil was also driven by considerations regarding resistance to high processing temperatures: this mineral oil has the highest oxidation temperature (150°C) and the highest volatilization point according to the manufacturer. Cylinder-forming blends were investigated, i.e. blends containing up to 35wt% of mineral oil.

Birefringence Measurements

Birefringence measurements were performed using a Zeiss optical microscope under crossed polarizers. The sample, about 1mm thick, was heated with a Linkam hot stage (HFS 91) and temperature controller (TP 91). The order-disorder transition of three different samples was measured by loss of birefringence: roll-cast, unannealed blends containing 20, 30, and 35wt% mineral oil. Samples were first heated at a rate of 90°C/min up to 150°C, then at 5°C/min up to 180°C, then at 1°C/min up to the order-disorder transition, which is characterized by extinction of light through the crossed polarizers.

The results are reported in Table 5. The measured ODTs decrease whith increasing mineral oil content, confirming the assumption that the addition of mineral oil depresses the

order-disorder transition temperature. However, these results should be interpreted very carefully due to the influence of several factors:

- The observed transition is very broad, and occurs over a temperature range of approximately 10-15°C, resulting in a fairly wide dispersion of successive measurements on a same sample. This apparent broadness of the transition might result from the presence of an order-order transition from cylinders to spheres, followed by the order-disorder transition from a spherical, phase-segregated morphology to a homogeneous melt. Since both the spherical morphology and the disordered homogeneous state are non-birefringent, the observed transition can be the order-order transition from cylinders to spheres.
- The observed transitions occur above the degradation temperatures of the polymer and the mineral oil, and above the volatilization temperature of the mineral oil. These phenomena might affect the blend during the heating process, thereby perturbing the measurement due to a change of composition and/or of chemistry during the experiment. At the end of each experiment, signs of these phenomena were observed, such as slight change in color of the sample and condensation of mineral oil on the window of the hot stage.

Mineral Oil Content	ODT (°C)
20wt%	250
30wt%	220
35wt%	210

Table 5. Order-disorder transition temperature measured by birefringence for blends of styrene - isoprene -styrene and mineral oil of various compositions.

The same experiment was performed on a roll-cast sample containing no mineral oil. Although the observed change in color of the polymer shows that oxidation was very

important during this experiment, the result seems to indicate that the ODT of the pure triblock copolymer lies around 300°C.

Small-Angle X-ray Scattering

In order to check the validity of the birefringence ODT measurements, the order-disorder transition was also measured using small-angle x-ray scattering. Synchrotron SAXS experiments were performed on the X12B beamline at Brookhaven National Laboratories, using $\lambda = 1.54$Å wavelength x-rays. Scattering patterns were recorded on a two-dimensional position-sensitive gas-proportional detector. The sample to detector distance was 173.5 cm and exposure time was varied for each pattern in order to compensate for the decreased signal to noise ratio with increasing temperature. SAXS data are azimuthally averaged and reported in arbitrary intensity units. The sample, about 2mm in thickness, was heated between two Kapton® polyimide films in a hot stage mounted on the x-ray rail. The hot stage was kindly provided by Dr. B. Hsiao at DuPont de Nemours.

In the first experiment, the sample was a simple-cast blend containing 30wt% mineral oil, which had previously been annealed for 6 days at 120°C. It was progressively heated from room temperature to 230°C in steps of 20°C, and SAXS patterns were recorded for durations varying from 2 minutes at room temperature to 12 minutes at 230°C. The imposed temperature profile is represented in Figure 18. After this experiment the sample was cooled down to room temperature, and an additional SAXS pattern was taken. Figure 19 shows the azimuthally averaged SAXS intensities recorded at the various temperatures. Several observations can be made regarding this plot:

- As temperature increases, the three higher order peaks fade away, whereas the first three peaks remain clearly distinct, even at the maximum temperature. This suggests that the order-disorder transition occurs above 230°C.

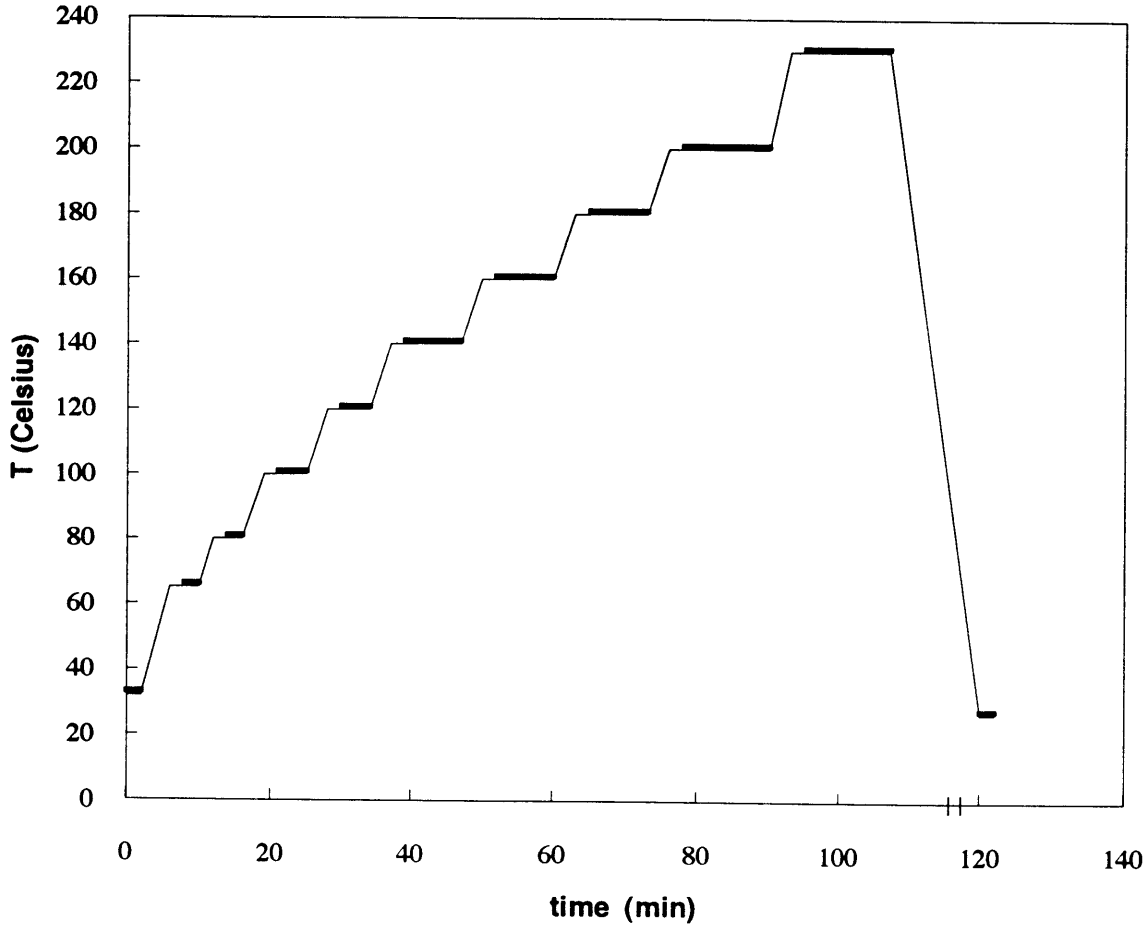

Figure 18. Imposed temperature profile in the first thermal SAXS experiment. The bold lines represent times when SAXS data was recorded.

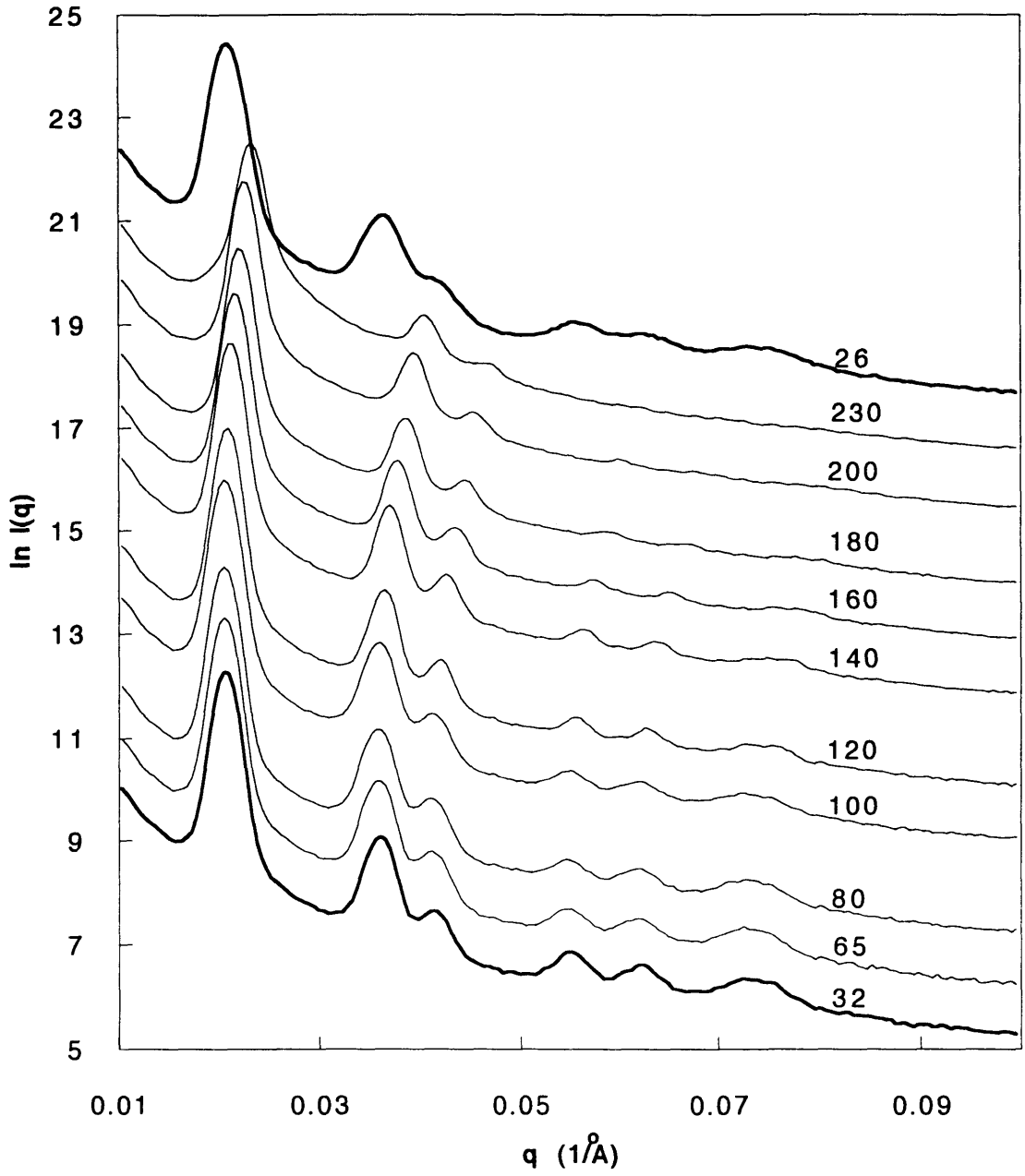

Figure 19. Azimuthally averaged SAXS intensities recorded at the various temperatures on an annealed, simple-cast sample containing 30wt% mineral oil. The different curves were vertically shifted by an arbitrary constant. The number on each curve refers to the temperature in ^{o}C at which data was taken.

- In addition, the position of the peaks moves to higher q-values when temperature increases, indicating that the d-spacings of the hexagonally packed cylinders decrease. This observation, which is especially strong above 150°C can be explained by the shrinkage of the rubber phase caused by the increase in temperature, due to the tendency of the isoprene chains to adopt configurations of higher entropy. Volatilization of some fraction of the mineral oil may also contribute to the decrease in d-spacings. It is interesting to notice that the value of the d-spacings return to their initial values after the sample is cooled down, indicating that the entropic effect is dominant and that volatilization of mineral oil is negligible.

In the second experiment, an unannealed sample of the same composition was heated to 200°C in steps of 50°C, then to 260°C in steps of 10°C. The imposed temperature profile is shown in Figure 20, and the diffracted SAXS intensities recorded at each temperature are reported in Figure 21. Exposure times were 12 minutes at high temperature. In this plot, the second and third reflections remain visible up to 220°C. Between 220°C and 230°C, those peaks disappear, and the first reflection suddenly flattens considerably, strongly suggesting that the polystyrene blocks, the polyisoprene blocks and the mineral oil form a homogeneous melt. This strong broadening of the first peak argues against the presence of a transition to a spherical phase before the actual order-disorder transition (although the temperature range in which a spherical phase exists could be too narrow to be observed in this study). The data thus indicates that the order-disorder transition temperature of the blend containing 30wt% mineral oil lies somewhere between 220°C and 230°C. At temperatures higher than 230°C, the position of the peak moves to smaller q values. This effect can be related to the change in average density fluctuations in the homogeneous melt, but its interpretation lies beyond the scope of this work.

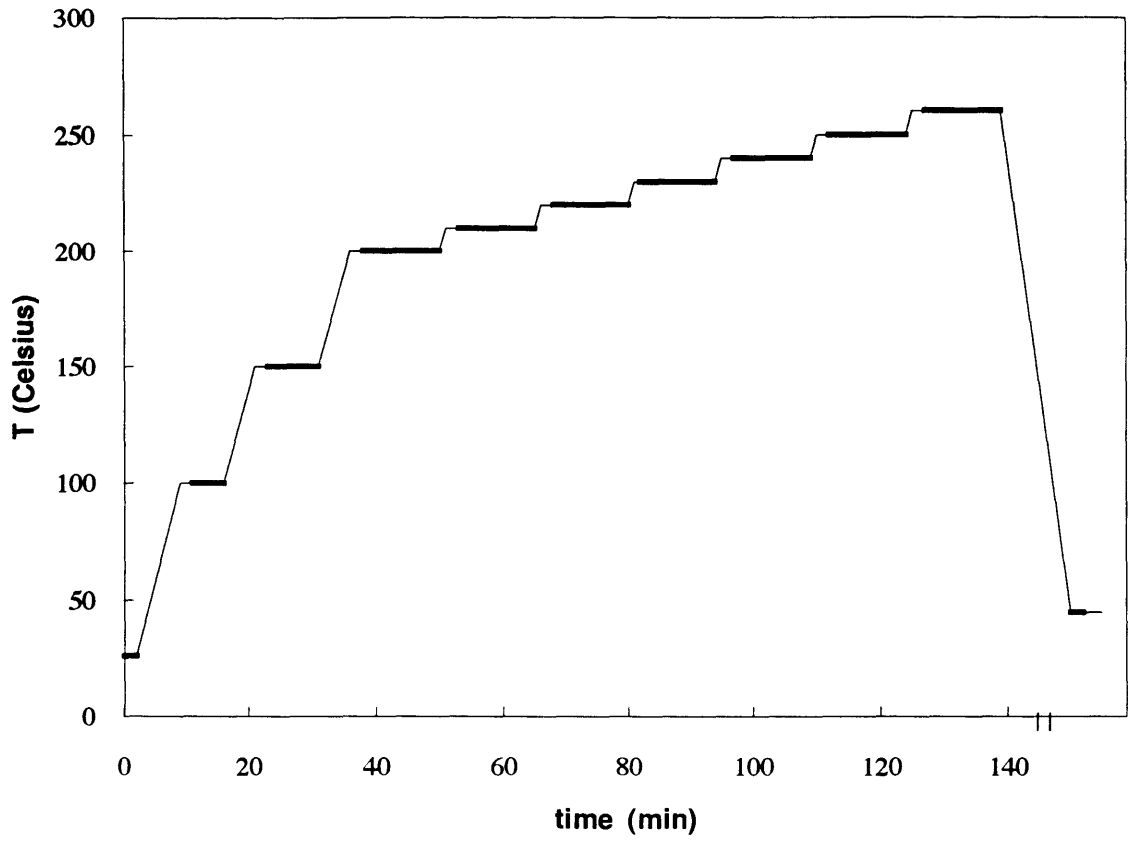

Figure 20. Imposed temperature profile in the second thermal SAXS experiment. The bold lines represent times when SAXS data was recorded.

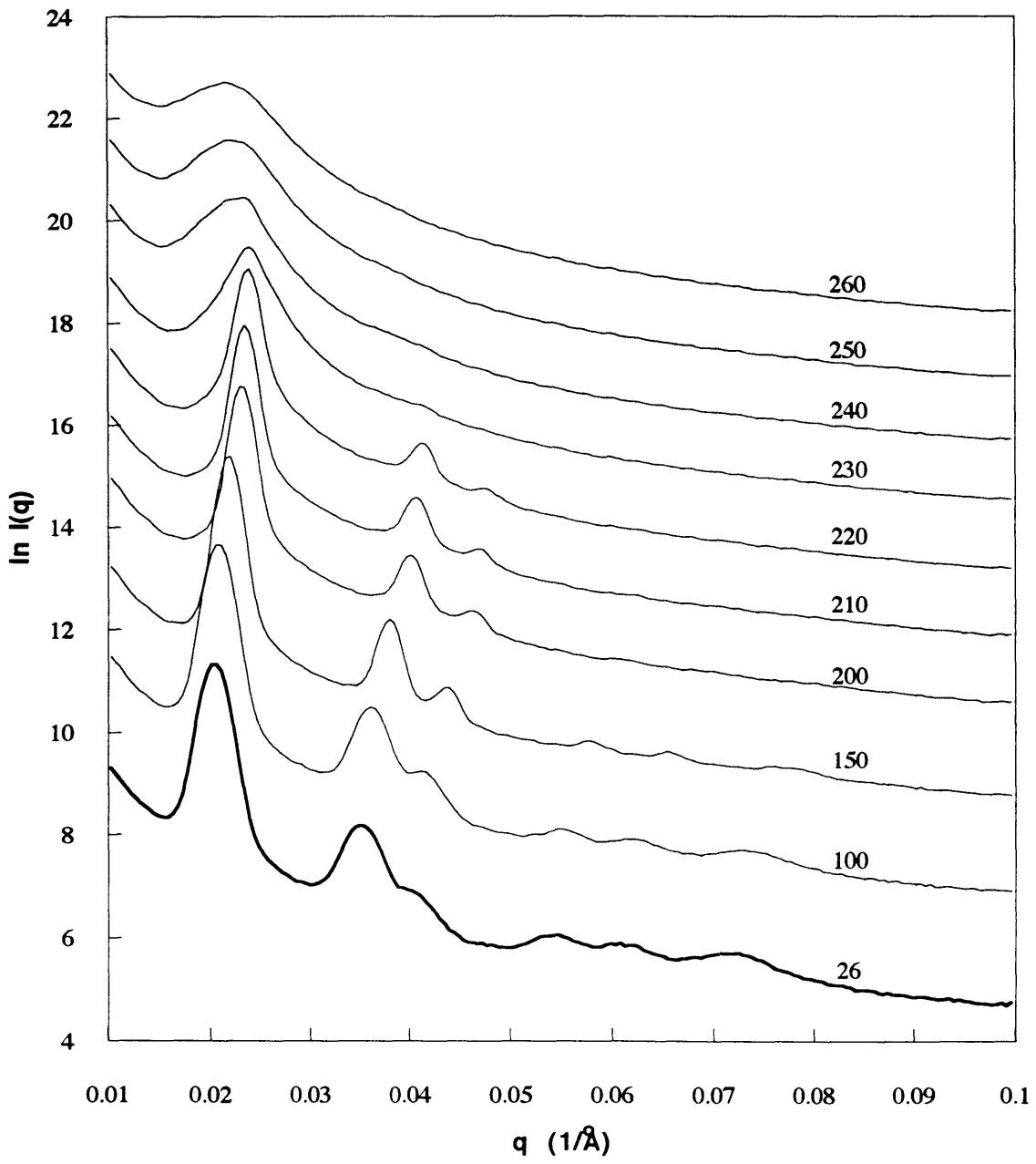

Figure 21. Azimuthally averaged SAXS intensities recorded at the various temperatures on an unannealed, simple-cast sample containing 30wt% mineral oil. The different curves were vertically shifted by an arbitrary constant. The number on each curve refers to the temperature in ^{o}C at which data was taken.

For the same reasons as we mentioned for the birefringence experiments, the result of these experiments should be used with caution. However, both type of experiments seem to indicate that the order-disorder transition of blends containing 30wt% mineral oil lies in the range 220°C - 230°C.

3.3 Processing and Morphology

Considering the above-mentioned results, one could easily conclude that the order-disorder transition temperature of the triblock copolymer - mineral oil blends, although depressed due to the presence of the mineral oil, is still too high to allow for processing above this temperature. Volatilization of the mineral oil as well as degradation of the polymer and the mineral oil during thermal processing above the ODT would still be detrimental to the mechanical properties of the final film. However, we were able to thermally roll-cast the blend at a temperature much lower than the measured ODT while still obtaining very good anisotropic properties. In this section, we describe the thermal roll-casting method and we characterize the samples obtained by this method with TEM and SAXS.

Processing method

A solution made of styrene - isoprene - styrene triblock copolymer (Dexco Vector 4211), mineral oil and toluene was first slowly evaporated in order to obtain an homogeneous blend of 65wt% triblock copolymer and 35wt% mineral oil. This blend was then cut into small 'pellets' typically 3mm in size. The thermal roll-casting apparatus is very similar to the solvent roll-casting apparatus. It is made of two counter-rotating stainless steel rollers 2 inches in diameter which can be heated by heaters placed inside the rollers. The temperature at the surface of the rollers is measured by a thermocouple wire.

The rollers were first sprayed with a polytetrafluoroethylene lubricative coating, and preheated to 125°C. The heaters were turned off and the pellets were then feeded between

the two hot counter-rotating rollers. The rotation speed of both rollers was 30 rpm, and the gap between the cylinders was 1mm. The material formed a film on one of the rollers. After 5 to 10 minutes, the temperature decreased to 115°C. The rollers were then taken apart and their rotation was stopped. After further cooling down of the film, it was removed from the surface of the roller.

The films obtained by this method exhibit optical birefringence and mechanical anisotropy in a similar way as the samples obtained by solvent roll-casting. However, one of the surfaces exhibits important rugosity, which could be avoided by adjusting some of the experimental parameters or by improving lubrication. This rugosity makes mechanical characterization difficult because of irregular film thickness.

Morphological characterization

The thermally roll-cast films were analyzed by TEM and SAXS. Experimental procedures are described in section 2.2. For the SAXS data, sample to detector distance was 150cm and exposure time was 60s.

Figure 22 shows a TEM micrograph of the sample viewed in the $\hat{z}$ direction. As in the solvent roll-cast sample, the glassy cylinders are aligned in the flow direction. These cylinders exhibit a higher degree of 'waviness' than what is commonly observed in solvent roll-cast samples. These irregularities in the direction of the cylinders also causes the presence of many defects and grain boundaries in the morphology. Although these defects merit a separate investigation of their own, we will not study them in detail here.

Figure 23 shows a two-dimensional SAXS pattern of the same sample, recorded with the incident x-ray beam in the $\hat{y}$ direction, i.e. perpendicular to the plane of the film. The azimuthal broadness of the reflections corresponding to the hexagonally packed cylinders is similar to the broadness observed in annealed samples roll-cast from a toluene solution (see Figure 5b), indicating that both processes lead to an equivalent degree of

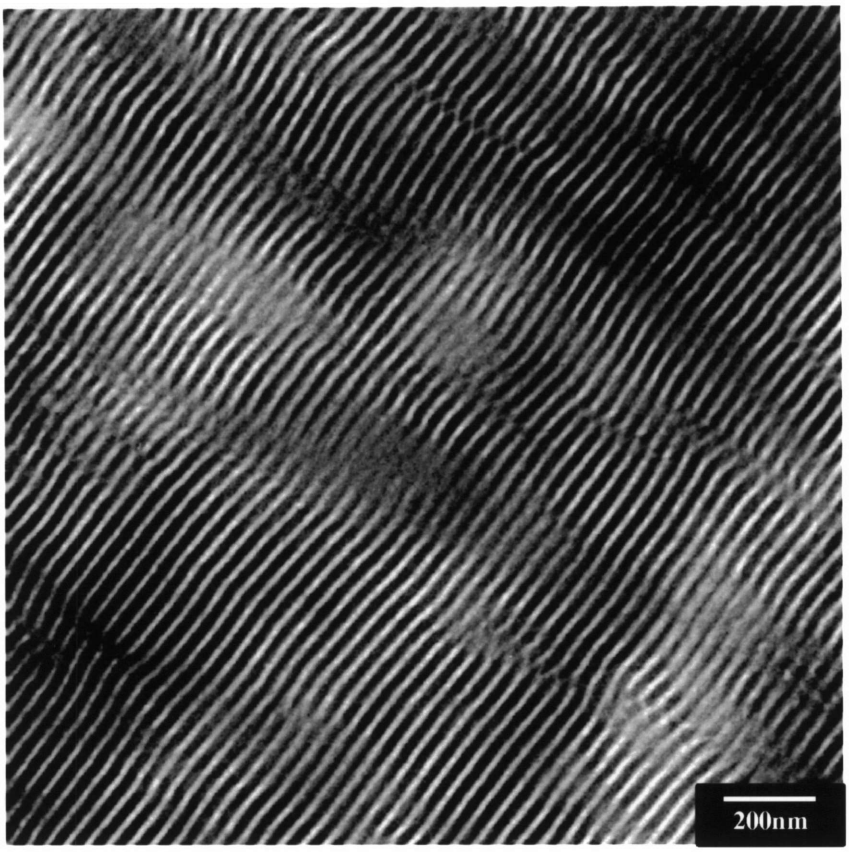

Figure 22. TEM micrograph of a thermally roll–cast sample containing 35wt% mineral oil, viewed in the $\hat{2}$ direction.

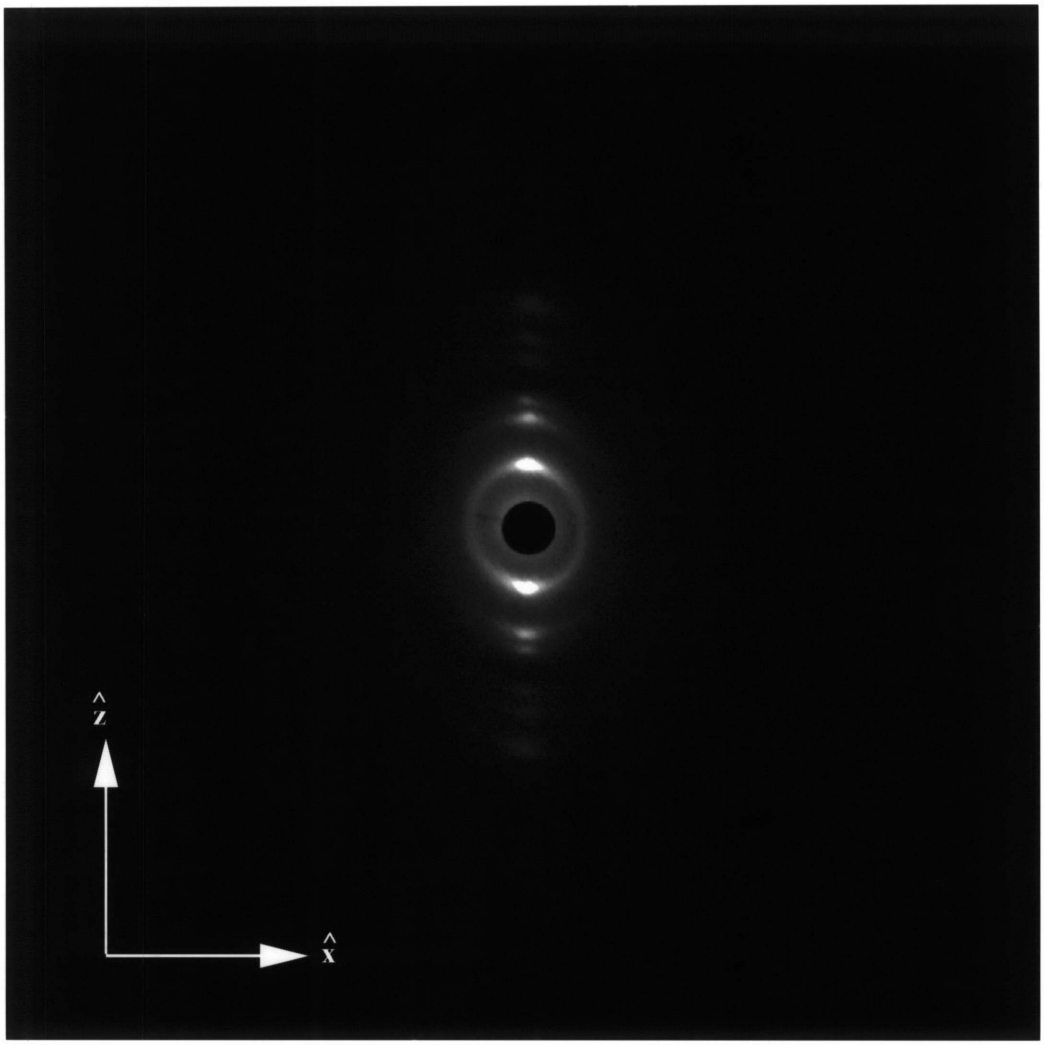

Figure 23. Two–dimensional SAXS pattern of a thermally roll–cast sample containing 35wt% mineral oil, recorded with the x–ray beam in the $\hat{y}$ direction, i.e. perpendicular to the plane of the film.

orientation of the glassy cylinders. However, the thermal roll-cast sample is less oriented than the unannealed samples prodcued by roll-casting (see Figure 5a).

These results thus suggest that although the blend was processed at a temperature of 125°C which lies well below its ODT, its morphology is very oriented, resulting in a high degree of anisotropy in the mechanical behavior of the sample. This good orientation can be explained by the effects of incorporating mineral oil into the sample:

- The mineral oil present in the rubber phase of the polymer acts as a plasticizer. It decreases the overall viscosity and modulus of the sample at a given temperature, resulting in higher values of the deformation when a given stress is applied to the material during processing. At 125°C, the polystyrene domains, although still phase separated from the rubber phase, are thus forced to align in the flow direction when submitted to the shear induced by roll-casting.
- A small fraction of the mineral oil is also likely to be present in the glassy domains, causing the glass transition temperature to decrease significantly[23]. At the processing temperature, the polystyrene is thus rubbery, which reduces even more the overall modulus and viscosity of the material.

3.4 Conclusion

By blending mineral oil into a styrene-isoprene-styrene triblock copolymer, it is possible to depress its order - disorder transition temperature. Birefringence and thermal SAXS experiments indicate that the ODT of blends containing 30 to 35wt% mineral oil lies in the 220°C - 230°C temperature range. Successful orientation of such blends was achieved by thermal roll-casting at a temperature of 125°C, which lies well below the ODT. This result can be interpreted in terms of the plasticization effect of the mineral oil, as well as the depression of the glass transition temperature of polystyrene due to the presence of small amounts of mineral oil in the glassy domains. The sample obtained by thermal roll-

casting presents a similar degree of orientation of the glassy cylinders as the annealed sample produced by roll-casting from a toluene solution.

Chapter 4

High-Strain Tensile Deformation of a Sphere-Forming Triblock Copolymer / Mineral Oil Blend

4.1 Introduction

In section 2.3.2, we have shown that by blending a cylinder-forming styrene - isoprene - styrene triblock copolymer with a sufficient amount of mineral oil, the morphology changes to a highly ordered body-centered cubic structure of glassy spheres embedded in a matrix of isoprene and mineral oil. By solvent roll-casting this blend, it is possible to orient the structure with the [111] direction of the cubic lattice aligned in the flow direction.

In this chapter, we study the changes in this morphology induced by high-strain uniaxial deformation. This investigation is achieved by a simultaneous SAXS - deformation experiment.

4.2 Experimental Procedure

The sample preparation method is described in section 2.2. The particular sample used in this study contains 60wt% triblock copolymer and 40wt% mineral oil. It was roll-cast and not annealed. Its morphology is described in detail in section 2.3.2.2 (under the title *Samples produced under low shear - unannealed*).

The sample was deformed using a small deformation apparatus in which two sets of grips holding the sample move apart at a constant stretching speed. Unlike samples with a cylindrical or lamellar morphology, samples presenting a spherical microstructure do not yield or neck when submitted to tensile deformation, because the glassy domains are discontinuous.

The sample dimensions were: gauge length 10.8mm, width 4.35mm, and thickness 0.88mm. Strain rate was $44s^{-1}$. The sample was deformed up to 300% deformation along the roll-casting flow direction ($\hat{x}$ axis in Figure 1). The SAXS data acquisitions were performed at constant values of the strain, and stress response was measured by a 50lb load cell. After maximum deformation, the sample was unloaded; an additional pattern was taken at zero load immediately after the experiment, and again after 36 hours. Exposure time was 5 minutes for each SAXS pattern in this deformation experiment and sample to detector distance was 260 cm.

4.3 Results and Discussion

In order to understand how the morphology changes with large-strain deformation, the sample was submitted simultaneously to a uniaxial tensile deformation experiment while in situ SAXS diffraction patterns were taken in the $\hat{y}$ direction (see Figure 1). The sample was stretched in the $\hat{x}$ direction, which corresponds to the [111] direction of the body-centered-cubic crystal and the shear flow direction. The applied strain function is described in Figure 24. The stress response is plotted as a function of deformation in Figure 25. This stress-strain curve resembles that of an ideal rubber. Stress relaxation during the pauses taken for data acquisition was negligible. For strains smaller than 60%, stress relaxation was less than 2%. For higher strains, stress relaxation was higher (up to 5.5% at 300% deformation), but since most of it occurred right after the strain step, thus before data acquisition, this effect hardly influenced the SAXS data. Figure 26 shows the two-dimensional SAXS patterns recorded at 30%, 60%, 100%, and 300% deformation. Data is represented with the $\hat{x}$-axis vertical.

As the strain increases, the meridional reflections, such as (222), move closer to the beam center (the corresponding d-spacings increase with strain), whereas the equatorial reflections, such as $(1\bar{1}0)$, move away from the beam center (the corresponding d-spacings

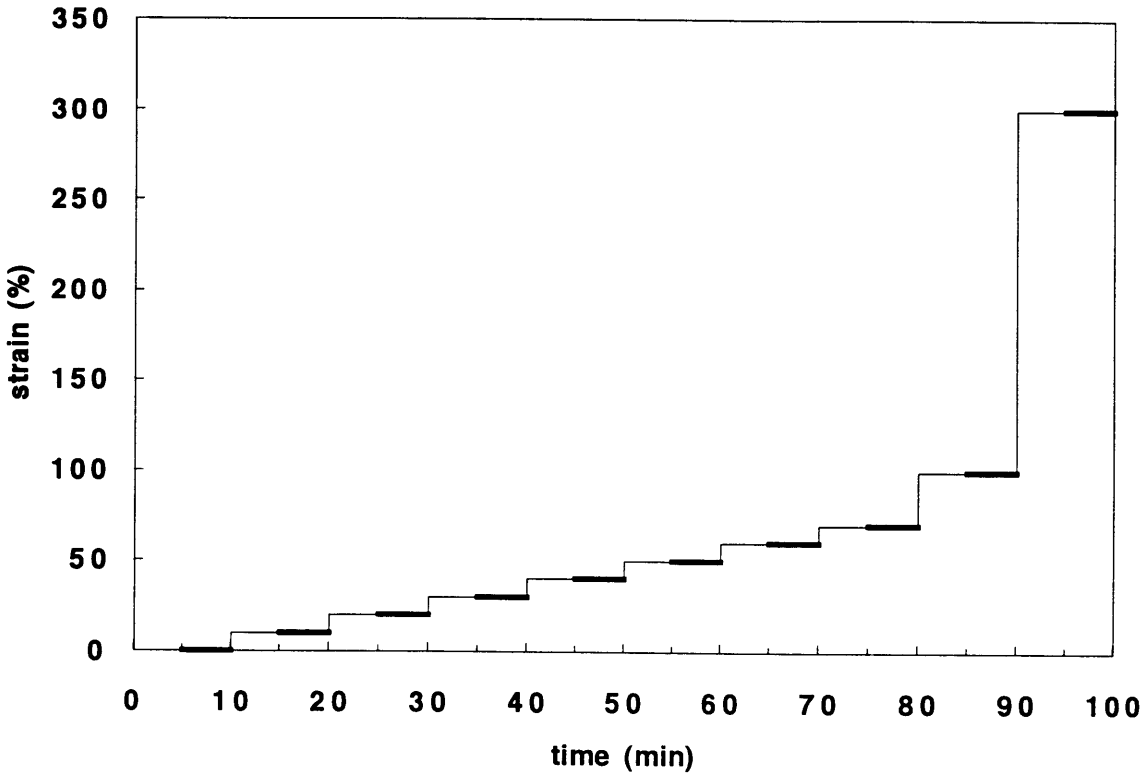

Figure 24. Applied strain function vs. time for the deformation experiment on the roll-cast sample. The bold lines represent the times of SAXS data acquisition.

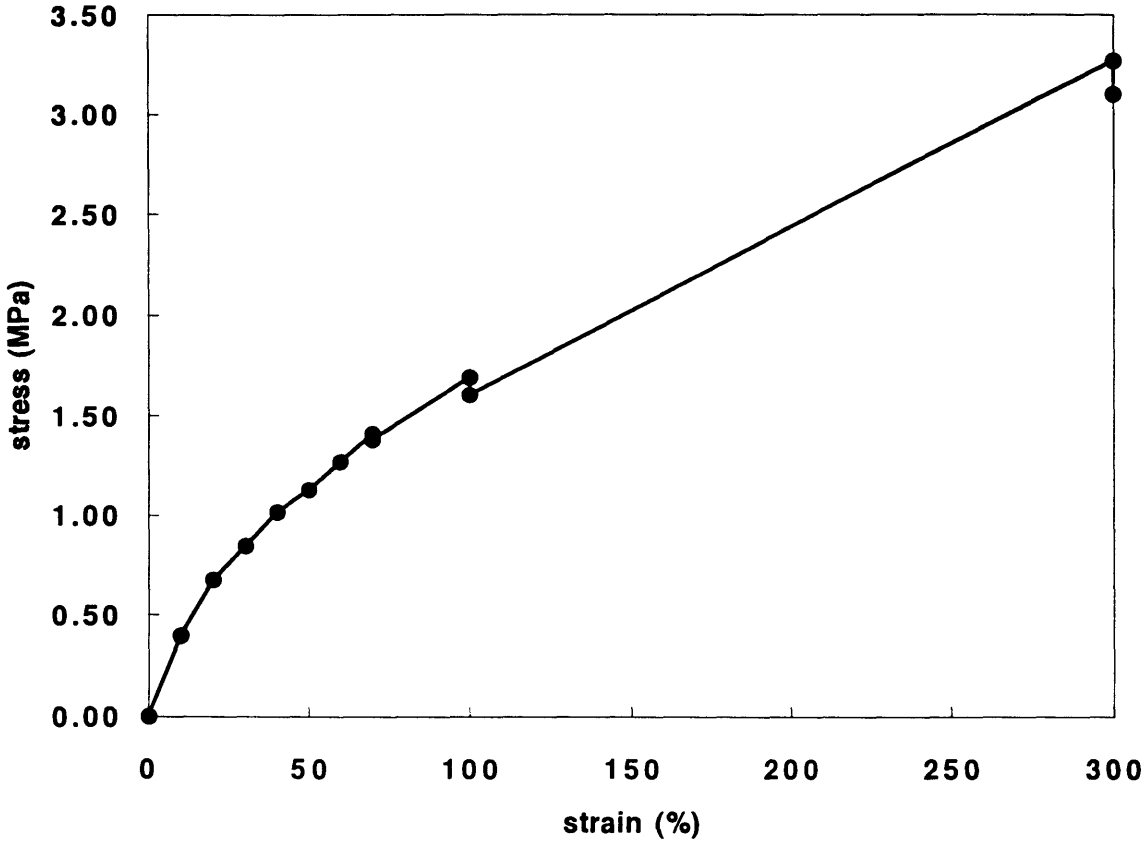

Figure 25. Stress - strain curve measured during the deformation experiment on the roll-cast sample. The dots correspond to the points where deformation was interrupted for SAXS data acquisition. Stress relaxation during data acquisition was negligible.

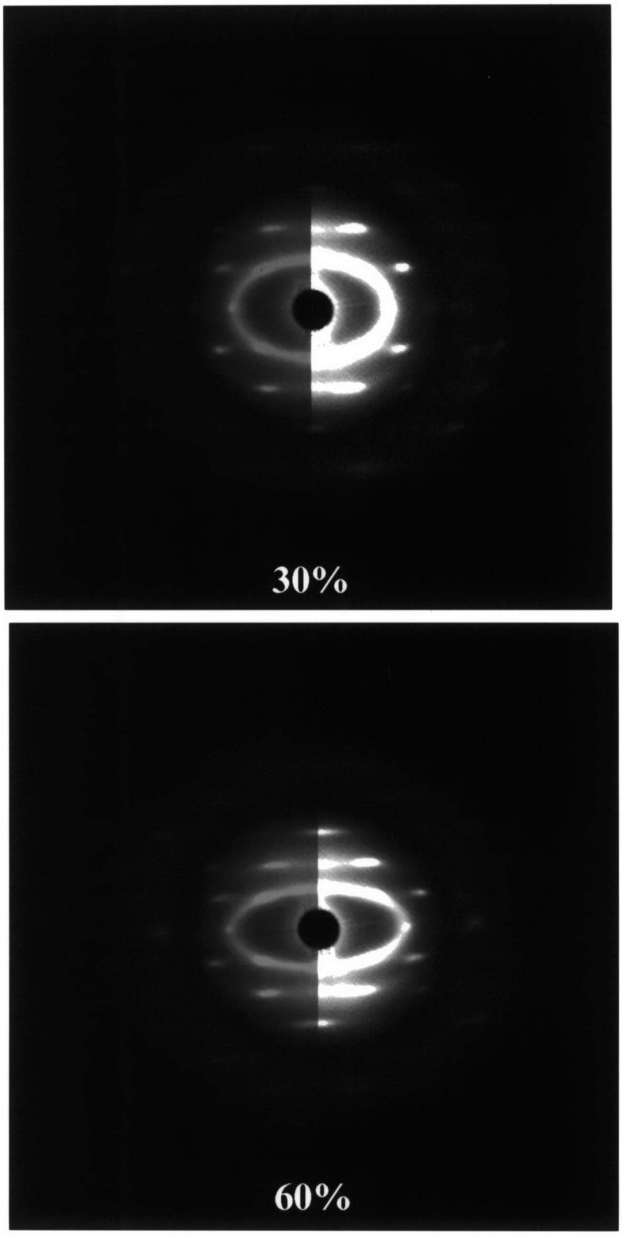

Figure 26. Two–dimensional SAXS patterns of the deformed roll–cast sample. The stretching direction ($\hat{x}$–axis) is vertical and the incident x–ray beam is in the $\hat{y}$ direction. The right–hand side of each image has been overexposed in order to reveal the high–q reflections.

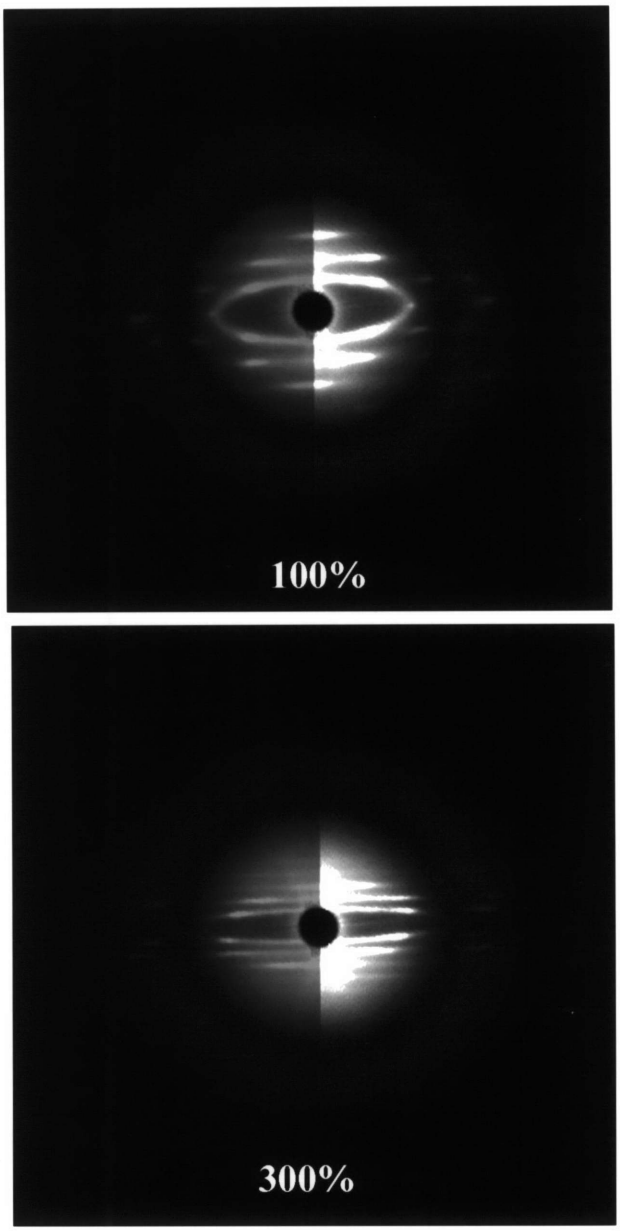

Figure 26. Two–dimensional SAXS patterns of the deformed roll–cast sample. The stretching direction ($\hat{x}$–axis) is vertical and the incident x–ray beam is in the $\hat{y}$ direction. The right–hand side of each image has been overexposed in order to reveal the high–q reflections.

decrease with strain). The cubic lattice, which was already slightly distorted before deformation, progressively changes into a rhombohedral lattice since it is stretched in the [111] direction. However we still index the reflections according to the original body-centered cubic structure. The values of the d-spacings for (222) and $(1\bar{1}0)$ are reported in Table 6. The variable strain ε_{xx} is defined as

$$\varepsilon_{xx} = \left(\frac{d_{222}}{(d_{222})_o} - 1 \right) \times 100 \qquad (2)$$

where $(d_{222})_o$ is the value of d_{222} before deformation. ε_{xx} relates to how the spheres on the body-centered-cubic lattice move when the macroscopic sample is submitted to uniaxial tensile deformation. Since the ε_{xx} values are equal to the macroscopically measured strain within experimental error, the deformation of the polystyrene sphere lattice is found to be affine with the deformation of the macroscopic sample. Values of ε_{xx} have been plotted versus the bulk deformation in Figure 27. When the sample is unloaded, the deformation of the lattice is not immediately recovered. However, the pattern taken 36 hours after the deformation experiment shows that after that time the sample has recovered completely.

We also calculated the [111] Poisson's ratio for the lattice:

$$\nu_{xz} = - \frac{\ln \frac{d_{110}}{(d_{110})_o}}{\ln \frac{d_{222}}{(d_{222})_o}} \qquad (3)$$

and found it to fluctuate between 0.45 and 0.5 for the whole range of strain values.

All SAXS patterns recorded during the deformation experiment exhibit a very clear zero of the form factor, as seen from the circular halo of minimum scattered intensity which surrounds the first reflections. As deformation increases, the shape of this halo

Table 6. Change in the d-spacings of the (222) and the $(1\bar{1}0)$ reflections with deformation. These values have been divided by the values of d_{222} and $d_{1\bar{1}0}$ before deformation (designated by $(d_{222})_o$ and $(d_{1\bar{1}0})_o$, respectively). The variable ε_{xx} represents the deformation of the cubic lattice in the [111] direction and is found to be equal to the strain within experimental error. The Poisson ratio for the lattice, ν_{xz}, has been derived for each value of the strain.

strain	d_{222}	$d_{222}/(d_{222})_o$	ε_{xx}	$d_{1\bar{1}0}$	$d_{1\bar{1}0}/(d_{1\bar{1}0})_o$	ν_{xz}
(%)	(Å)		%	(Å)		
0	120	1.00	0	278	1.00	---
10	132	1.10	10	266	0.96	0.46
20	---	---		255	0.92	---
30	159	1.33	33	245	0.88	0.45
40	171	1.43	43	236	0.85	0.46
50	185	1.54	54	228	0.82	0.46
60	198	1.65	65	221	0.79	0.46
70	212	1.77	77	213	0.77	0.47
100	251	2.09	109	200	0.72	0.45
300	487	4.06	306	---	---	---
(zero load)	144	1.20	20	255	0.92	0.47
(after 36 hours)	120	1.00	0	280	1.01	---

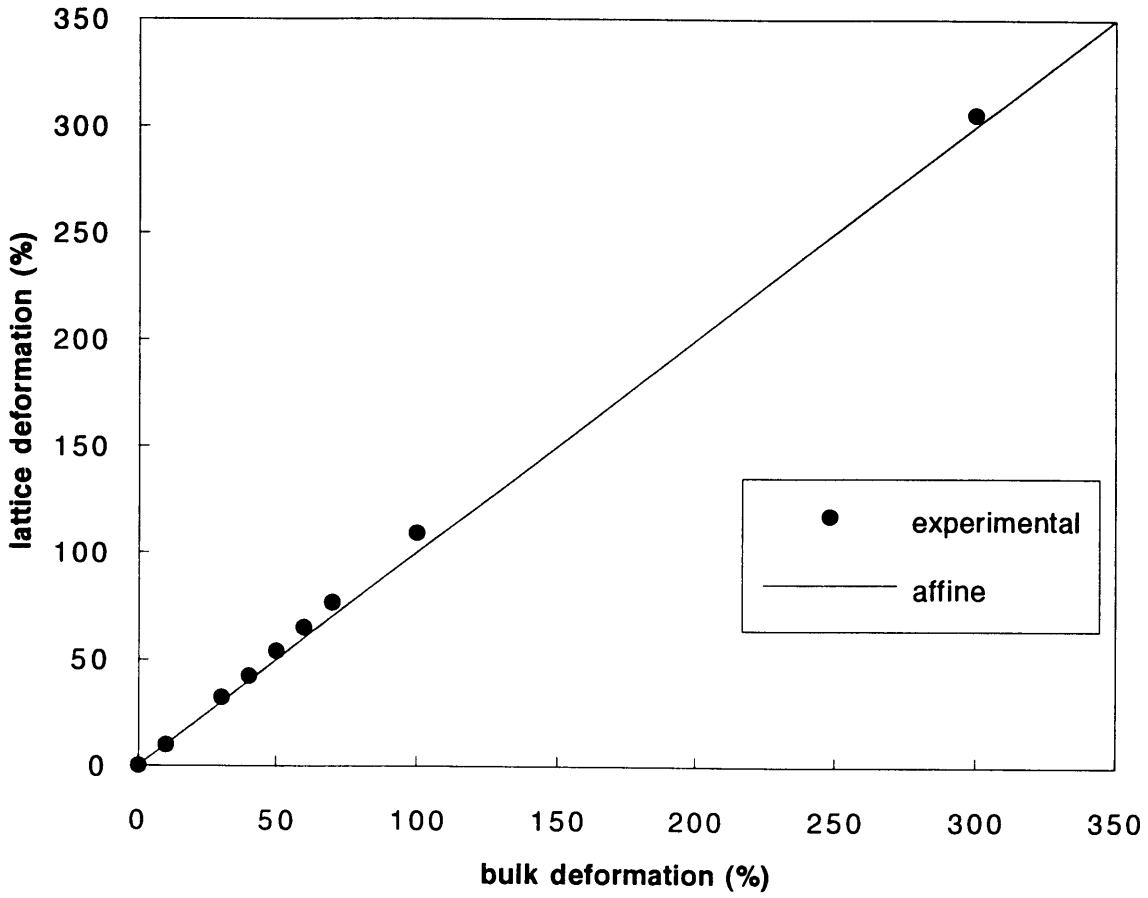

Figure 27. Plot of the extension ratio of the interdomain distance versus the bulk strain of the sample. The line passing through the origin with a slope of 45° represents the perfectly affine deformation.

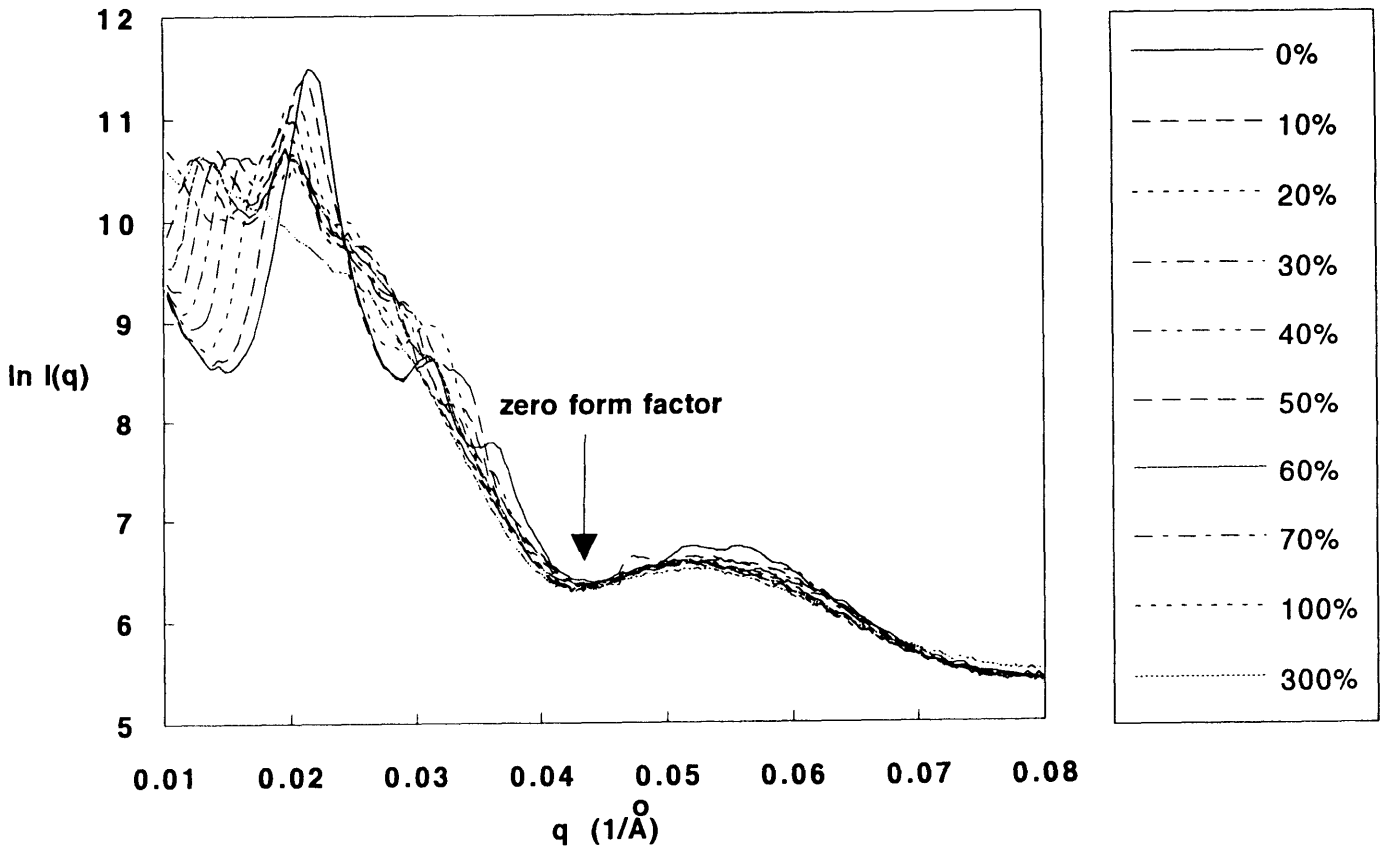

Figure 28. Circular average of scattered intensities of the various two-dimensional SAXS patterns recorded during deformation of the roll-cast sample.

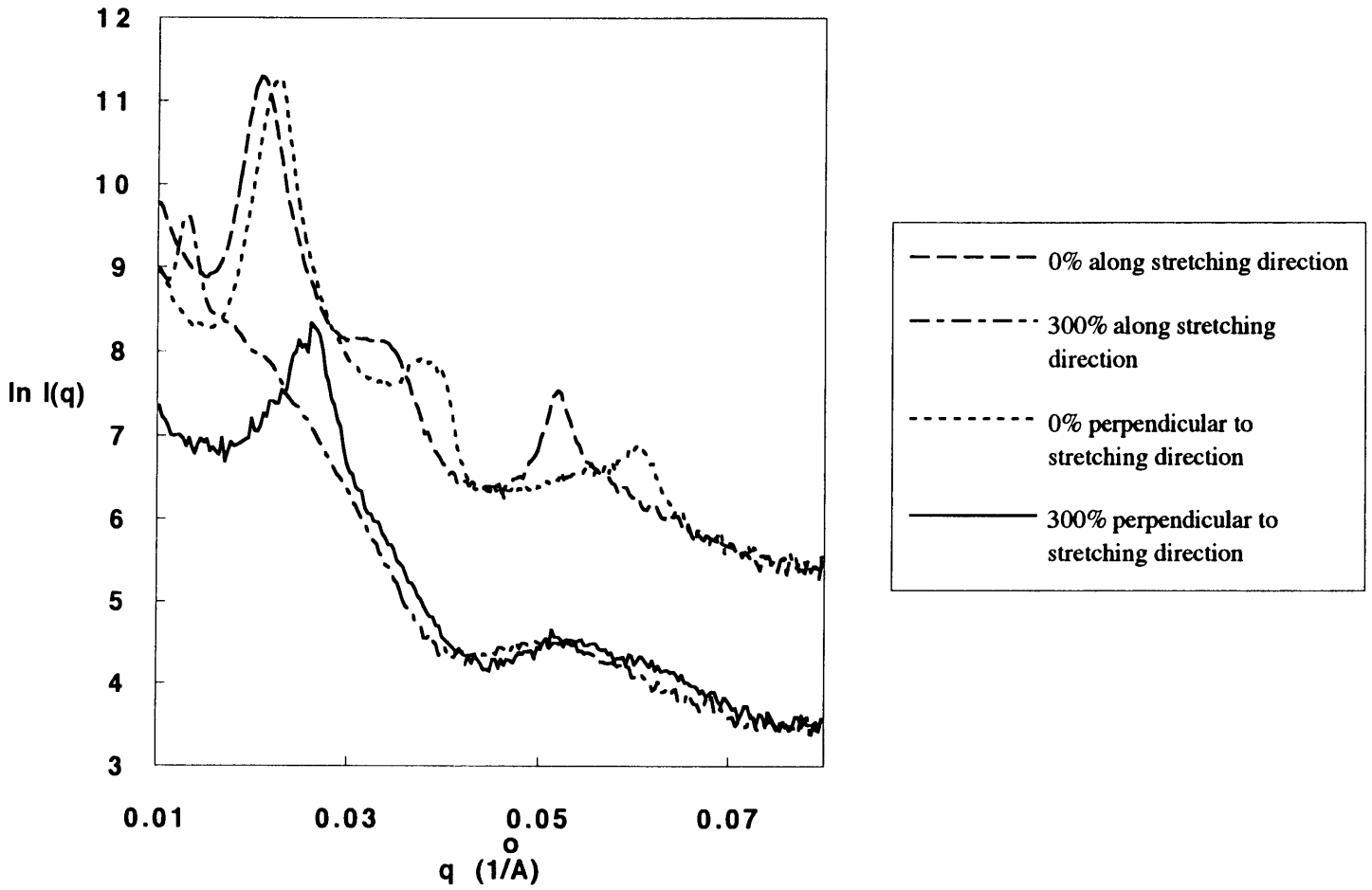

Figure 29. Comparison of the intensities along the deformation direction and perpendicularly to the deformation direction, at 0% and after 300% deformation.

All SAXS patterns recorded during the deformation experiment exhibit a very clear zero of the form factor, as seen from the circular halo of minimum scattered intensity which surrounds the first reflections. As deformation increases, the shape of this halo remains circular and its radius hardly changes. This observation is confirmed by the circular average of the scattered intensities plotted in Figure 28. Since the first minimum of the plots for all values of the strain occurs at the same value of q of $0.043Å^{-1}$, corresponding to a spheres radius of 104Å, this suggests that the glassy polystyrene spheres remain spherical during deformation, and that the strain is only accommodated by the rubbery matrix. A more careful measurement of the azimuthal average (over an azimuthal angle of 20^{o} only) of the reflected intensities along the deformation direction and perpendicularly to the deformation direction before stretching and after 300% deformation (Figure 29), suggests that after stretching, the spheres have become very slightly elliptical. However, the difference between the minima of intensities in the two directions is very small (in the order of 2%).

A simple calculation confirms that the stress in the polystyrene spheres is smaller than the yield stress of the glassy phase and thus too low to induce significant deformation of the spheres. The results of the mechanical tests performed on samples of cylindrical morphology (see section 2.4) show that the yield stress of the glassy spheres is approximately 2 to 3 MPa, whereas the modulus of the rubber phase can be estimated to approximately 0.5 MPa. At 300% deformation of a sample exhibiting a spherical morphology, the stress in the glassy phase is thus approximately 1.5 MPa, which lies below its estimated yield stress.

The third observation is the progressive horizontal 'streaking out' of the reflections as the strain increases. At high strains this effect is so pronounced that individual Bragg reflections are changed into almost continuous horizontal lines. It is known that the broadness of a peak in a given direction is inversely proportional to the number of coherent

scattering objects present in that direction, i.e. to the size of the diffracting collection of objects in that direction. The change in the horizontal dimensions of the peaks is thus related to a progressive decrease in the number of spheres per grain in the $\hat{z}$ direction as the sample is deformed in the $\hat{x}$ direction. For symmetry reasons, we expect the number of spheres per grain in the $\hat{y}$ dimensions to decrease similarly. Since the dimensions of the peaks in the $\hat{x}$ direction do not change with deformation, the number of coherent scattering spheres is not modified by the application of tensile strain in that direction.

We measured that the full width at half maximum of the (211) peaks in the $\hat{z}$ direction increases by a factor of 4 between the pattern of the undeformed sample and the pattern of the sample deformed at 100%. The width of the peaks in the pattern recorded at 300% deformation is more difficult to measure because it is partly erased by the form factor. Therefore, we suggest that a macroscopic tensile deformation of 100% in the $\hat{x}$ direction induces a progressive breakup of the original grains into subgrains whose $\hat{y}$ and $\hat{z}$ dimensions are approximately four times smaller than the initial grain dimensions. This breakup may be accomplished by small relative translations of the glassy spheres along the planes whose normals are orthogonal to the applied force. However, this sliding movement is strongly limited due to the high number of bridging chains between the spheres. We estimate that there are approximately 200 polystyrene blocks in each sphere. Given the relative dimensions of the lattice and the isoprene chains, we expect the proportion of chains extending from a given sphere to a second nearest neighbor sphere to be very small: most chains either reenter the same sphere, forming loops, or enter a nearest neighbor sphere, forming bridges. The proportion of chains forming bridges and loops was found to be the ratio of 60/40 by Watanabe *et al.*[21] for a solution of a triblock copolymer in a midblock selective solvent. An interesting observation is that after removal of the strain, the streaks completely disappear, meaning that the subgrains have reformed large grains.

This corroborates the assumption that the displacement of the spheres along the new axial boundaries must be of very limited amplitude, and is elastically recovered after unloading.

A two-dimensional model of the proposed deformation mechanism of a grain is represented in Figure 30. The breakup of large grains into subgrains of smaller dimensions can be explained by the geometric constraints inside a grain submitted to high tensile strain levels in one particular direction. The reasons for this breakup are explained in Figure 31. As mentioned earlier, a uniaxial tensile deformation in the [111] direction causes the d-spacings between the {222} planes to increase, and the d-spacings between {110} planes to decrease, causing the spheres located on {110} planes come closer together. The values reported in Table 6 indicate that $d_{\bar{1}10}$ changes from 278Å before deformation to 200Å at 100% deformation. Since the radius of the spheres is approximately 100Å, the gap between two adjacent spheres becomes very small (configuration B in Figure 31). This forces the isoprene chains located between such spheres to adopt very 'compressed' configurations. The elastic recovery of the isoprene chains tends to push the spheres apart. The spheres can slide parallel to the stretching direction in order to accomodate the relaxation of the isoprene chains. An additional contribution to this effect is caused by the presence of mineral oil in our system. The decrease in the gap between the spheres perpendicular to the deformation direction causes a fraction of the mineral oil to be expelled from this gap. The resulting gradients in oil concentrations cause an osmotic pressure to develop between regions of high oil content (regions where the rubber chains are elongated) and regions of low high content (where the rubber chains are compressed between adjacent spheres). Both this osmotic pressure and the relaxation of the isoprene chains can be accomodated by a sliding of the glassy spheres along {110} planes, the result of which is shown in configuration C. The progressive activation of this sliding mechanism at several places inside the grain is responsible for the breakup of the grain into smaller grains as shown in Figure 30.

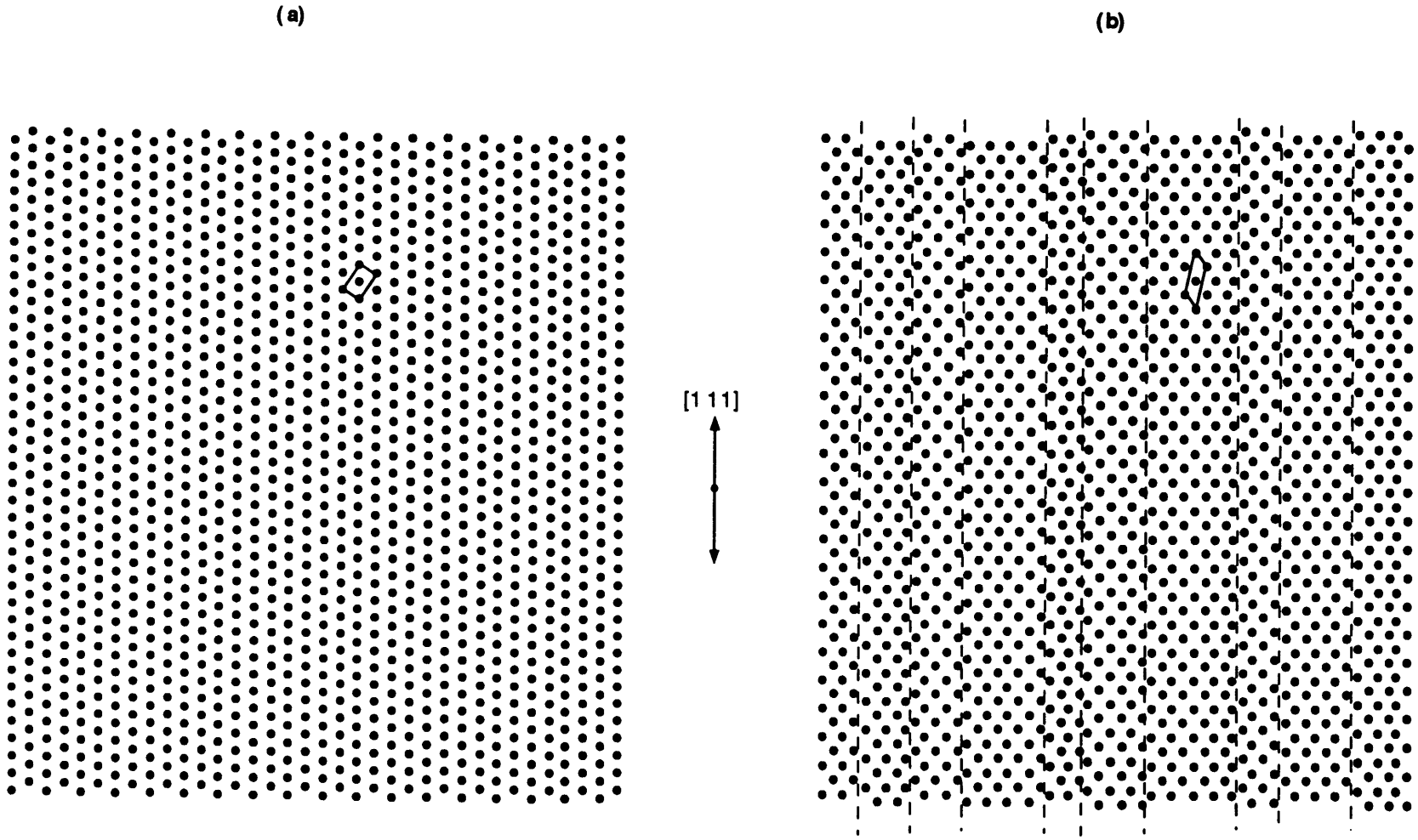

Figure 30. Model for the deformation mechanism inside a single grain. The (110) plane of a grain with the [111] direction vertical is represented (**a**) before deformation, (**b**) after deformation. After deformation, the grain progressively breaks up into smaller subgrains, due to sliding of the spheres along the new axial subgrain boundaries. A basis unit cell has been drawn in the deformed and in the undeformed lattice.

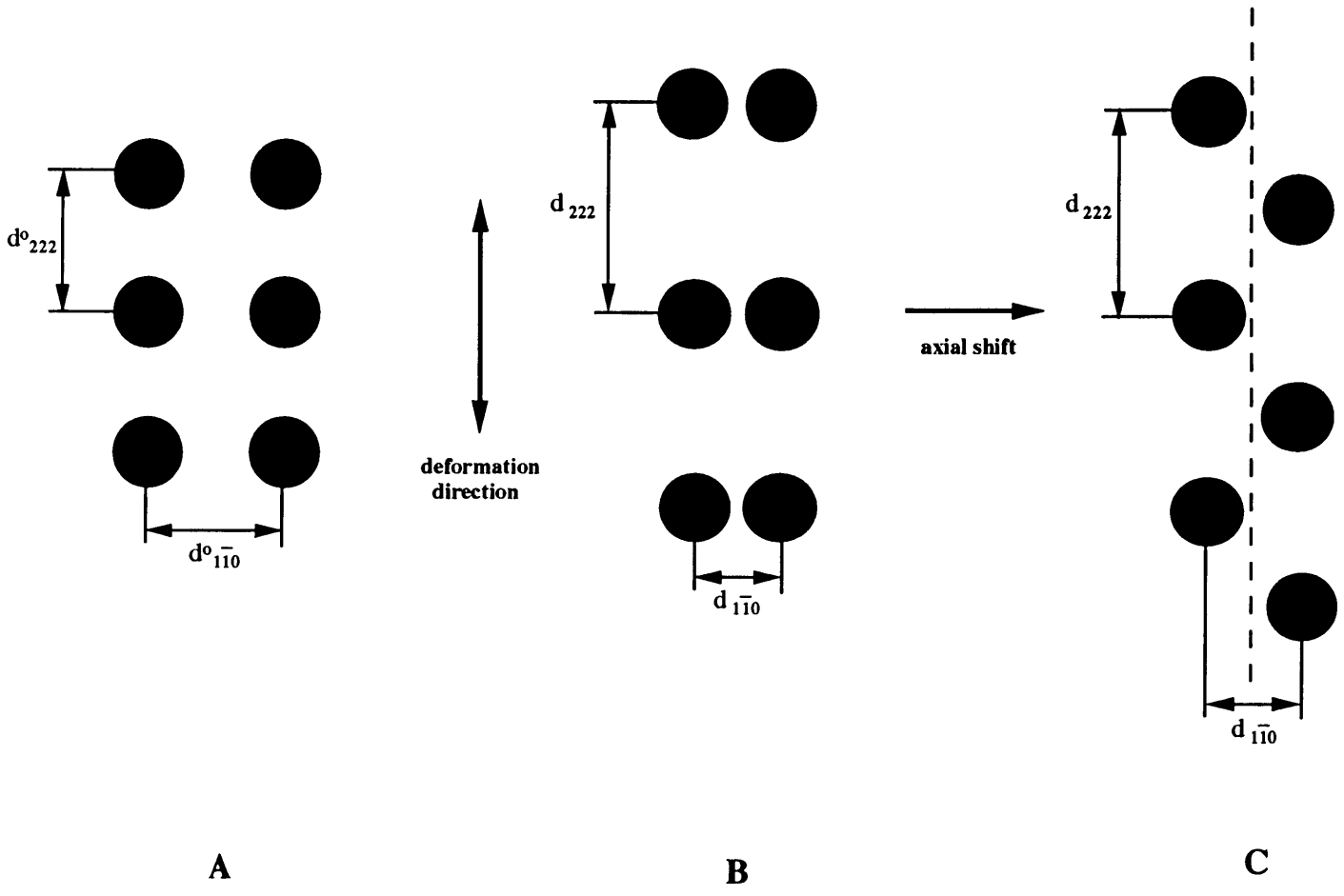

Figure 31. Schematic of the sliding mechanism along the {110} planes. A is the undeformed configuration. B is the deformed configuration in absence of sliding. The glassy spheres are very close to each other and the isoprene chains linking two spheres are 'compressed' in a very small gap. Configuration C, which is obtained by sliding along a (110) plane (dashed line), allows for more freedom in configuration of the isoprene chains and prevents the collision of two adjacent glassy spheres.

These conclusions are similar to the conclusions of Rharbi *et al.*[43] in their deformation study on cellular polymeric films. The system that they investigate is composed of a spherical dispersed phase in a continuous matrix. By adding a selective solvent either to the cell cores or to the matrix, they varied the relative strength. SANS patterns on deformed films composed of strong latex spheres in a weak (waterswollen) membrane matrix exhibit stripes perpendicular to the stretching direction, similar to our SAXS patterns shown in Figure 26. This feature is attributed in their samples to the formation of strings of water pockets which are regularly spaced in the deformation direction, but irregularly spaced perpendicular to the stretching direction. The appearance of water pockets is caused by random shifts between columns of cells along the stretching axis. In later works[44,45] on the same systems, AFM imaging showed that elongation progressively causes a geometrical rearrangement of the spherical particles in the form of zig-zags or chevrons.

4.4 Conclusion

Blending mineral oil into a cylinder-forming P(S-I-S) triblock copolymer causes the morphology to change to spheres as the mineral oil mainly enters the rubber phase of the polymer. Roll-casting of this blend from a toluene solution causes the [111] direction of the cubic crystal to orient in the shear direction, with a partial uniaxial symmetry around this [111] direction. This oriented specimen, whose structure is that of an ideal rubber of known crosslink functionality, was submitted to in situ SAXS experiments during high strain deformation. Data show that the polystyrene spheres remain spherical upon stretching even to very high strains, and that the cubic lattice deforms in an affine manner. Stress relaxation was negligible during the experiment. A model involving the progressive breakup of the grains in the directions perpendicular to the stretching direction is proposed to account for the observed streaking of the SAXS reflections.

Conclusions and Suggestions for Further Work

The results presented in this work raise a lot of interesting points, but also raise further questions which remain unanswered due to time constraints. The goal of this conclusion is to summarize the main results of this work, and to present ideas for further investigation.

We have shown that addition of mineral oil into a styrene - isoprene - styrene block copolymer can be used as a means to modify its morphology, its mechanical properties, and its processability. When a cylinder-forming triblock copolymer is blended with a midblock selective mineral oil (i.e. a mineral oil containing no aromatics), the oil swells the rubber, causing the d-spacings between the cylinders to increase. The overall ordering of the microstructure is observed to be improved, and the grain size is increased. Upon addition of a critical amount of mineral oil (40wt% in the material used in this study), the morphology changes from hexagonally packed cylinders to spheres arranged on a body centered cubic lattice.

Roll-casting cylinder-forming blends from a toluene solution causes the cylinders to orient with the [0001] direction of the hexagonal lattice in the flow direction. In a similar way, the sphere-forming blend can be oriented by solvent roll-casting. The [111] direction of the cubic lattice formed by the spheres was found to orient in the shear flow direction. The samples also present a partial fiber symmetry around this [111] axis, as evidenced from the SAXS diffraction patterns recorded in three perpendicular directions. This sample constitutes a well-ordered thermoplastic rubber. The size and density of the crosslinks, as well as their position on the cubic lattice are well-defined, which makes it an ideal rubber for the study of the deformation behavior of such materials.

In the case of high shear rates during the roll-casting process, the morphology of samples of containing 40wt% mineral oil is made of a juxtaposition of spheres situated on an oriented body centered cubic lattice and cylinders aligned in the flow direction. To our

knowledge this is the first evidence of a shear-induced sphere to cylinder transition in block copolymers. However our experiments do not allow us to determine whether this transition is a metastable or an equilibrium morphology (in a two-component system, a biphasic equilibrium morphology is required at the transition between two phases). In order to verify the stability of the shear-induced transition, it would be necessary to anneal the samples presenting a mixed spheres and cylinders morphology in such a way to prevent any mineral oil loss. If annealing causes the morphology to revert back to spheres only, this would mean that the observed shear-induced transition is not an equilibrium morphology.

The shear-induced sphere to cylinder transition is similar to the thermoreversible transition observed by other authors[10,11]. In the case of our study, the coexistence of spheres and cylinders in a same sample allows us to better understand the mechanism of the morphology transition. The mechanism proposed by Sakurai *et al.*[10,11] consists in the progressive coalescence of spheres along the [111] direction of the cubic lattice, and is in very good agreement with the microstructure that we observe at the interface between the cylindrical and spherical regions.

Sphere-forming simple-cast and roll-cast blends were found to exhibit a very ordered morphology. Clear grain boundaries are evident in our micrographs. A detailed investigation of all the types of grain boundaries present in our samples would constitute a very interesting project. To our knowledge, no systematic study of the grain boundaries in sphere-forming block copolymer systems has been reported so far.

The mechanical behavior of oriented cylinder-forming blends shows that the mechanical anisotropy of the samples increases with mineral oil content, leading to ratios of the parallel modulus to the perpendicular modulus on the order of 100. The strain at break was dramatically increased by the addition of mineral oil. The change in yield stress and modulus with mineral oil content are complicated to interpret, and can partly be attributed to the antiplasticization effect of the polystyrene in presence of small amounts of mineral oil in

the glassy cylinders. In order to better understand the effect of mineral oil blending on the mechanical behavior of the blends, the glass transition temperature of the polystyrene should be measured. If some mineral oil effectively penetrates the polystyrene microdomains, the addition of mineral oil should induce a depression of the glass transition temperature, and this effect could be measured by a simple DSC experiment. However, a minor complication arises from the fact that one needs to prevent the mineral oil from leaving the sample during the DSC experiment.

Addition of mineral oil can also be useful in improving the processability of block copolymers. Our birefringence and SAXS experiments show that the presence of mineral oil depresses the order-disorder transition of the material. A solvent-free thermal roll-casting processing method was developed and the samples prepared by this method were found to exhibit a degree of orientation similar to the samples obtained by roll-casting from a toluene solution. This thermal roll-casting method could be improved by adjusting the experimental parameters in order to avoid the roughness of the surface of the film and to increase the degree of orientation. The ideal processing temperature probably depends on the glass transition temperature of the polystyrene in the presence of mineral oil. One could also try to find a way to avoid the roughing of the film surface by improving lubrication.

Our deformation study on an oriented sphere-forming blend of triblock copolymer with mineral oil is the first deformation study of a well-defined ideal oriented rubber. Experimental data shows that the glassy spheres embedded in the rubbery matrix composed of isoprene and mineral oil remain spherical up to a deformation of 300%. The cubic lattice is found to deform in an affine way, contrarily to what was observed in other similar studies on less ordered samples[29-31]. The most interesting feature of the SAXS patterns of deformed samples is that the reflections broaden in the direction perpendicular to the stretching direction. This observation can be attributed to the progressive breakup of the grains by a sliding mechanism of planes which are parallel to the deformation direction. In order to confirm this hypothesis for the deformation mechanism, TEM micrographs of the

stretched state would definitely help in understanding the deformation mechanism of the microstructure and verifying our model involving the breakup of grains. Other possible projects include the study of the changes of morphology during relaxation, biaxial tensile deformation, or compression. Finally, similar samples of various sphere dimensions and d-spacings could be made by modifying one or more of the following parameters: mineral oil content, polystyrene content, and molecular weight of the isoprene block.

Bibliography

(1) Harpell, G.A. and Wilkes, C.E., Relationship of Morphology to Physical Properties of Styrene-Butadiene Block Copolymers, In: *Block Polymers*; Aggarwal, S.L., Plenum Press, New York, 1970; pp 31-41.

(2) Robinson, R.A. and White, E.F.T., Mechanical Properties of Styrene-Isoprene Block Copolymers, In: *Block Polymers*; Aggarwal, S.L., Plenum Press, New York, 1970; pp 123-135.

(3) Holden, G. and Legge, N.R., Thermoplastic Elastomers Based on Polystyrene-Polydiene Block Copolymers, In: *Thermoplastic Elastomers*; Legge, N.R., Holden, G. Schroeder, H.E., Eds Hanser, Munich, 1987; pp 47-65.

(4) Morton, M., Research on Anionic Triblock Copolymers, In: *Thermoplastic Elastomers*; Legge, N.R., Holden, G. Schroeder, H.E., Eds Hanser, Munich, 1987; pp 67-90.

(5) Wilder, C.R., Thermoplastic Styrene Block Copolymers, In: *Handbook of Elastomers*; Bhowmick, A.K. and Stephens, H.L., Marcel Dekker, New York, 1988, pp 313-339.

(6) Fetters, L.J. and Thomas, E.L., Model Polymers for Materials Science, In: *Materials Science and Technology*; Cahn, R.W.; Haasen, P.; Kramer, E.J., VCH, Weinheim, 1993; pp 1-31.

(7) Avgeropoulos, A.; Hadjichristidis, N.; Dair, B.J.; Thomas, E.L., The Tricontinuous Double Gyroid Cubic Phase in Triblock Copolymers of the ABA Type, submitted to *Macromolecules* .

(8) Bates, F.S.; Berney, C.V.; Cohen, R.E., Microphase structure of solvent-cast diblock copolymers and copolymer-homopolymer blends containing spherical microdomains, *Macromolecules*, **16**, 1101 (1983).

(9) Thomas, E.L.; Kinning, D.J.; Alward, D.B.; Henkee, C.S, Ordered packing arrangements of spherical micelles of diblock copolymers in two and three dimensions, *Macromolecules*, **20,** 2934 (1987).

(10) Sakurai, S.; Kawada, H.; Hashimoto, T.; Fetters, L.J., Thermoreversible morphology transition bewteen spherical and cylindrical microdomains of block copolymers, *Macromolecules*, **26**, 5796 (1993).

(11) Sakurai, S.; Hashimoto, T.; Fetters, L.J., Thermoreversible cylinder-sphere transition of polystyrene-block-polyisoprene diblock copolymers in dioctyl phthalate solutions, *Macromolecules*, **29**, 740 (1996).

(12) Sakurai, S.; Momii, T.; Taie, K.; Shibayame, M.; Nomura, S.; Hashimoto, T., Morphology transition from cylindrical to lamellar microdomains of block copolymers, *Macromolecules*, **26**, 485 (1993).

(13) Hadjuk, D.A.; Gruner, S.M.; Rangarajan, P.; Register, R.A.; Fetters, L.J.; Honeker, C.; Albalak, R.J.; Thomas, E.L., Observation of a Reversible Thermotropic Order-Order Transition in a Diblock Copolymer, *Macromolecules*, **27**, 490 (1994).

(14) Ceausescu, E.; Bordeianu, R.; Ghioca, P.; Buzdugan, E.; Stancu, R.; Cerchez, I., Dilute Block Copolymer Systems. Properties of Oil-Extended Butadiene-Styrene Block Copolymers, *Pure & Appl. Chem.*, **56**, 319 (1984).

(15) Ceausescu, E.; Bordeianu, R.; Ghioca, P.; Cerchez, I.; Buzdugan, E.; Stancu, R., Tensile Modulus of Oil-Extended Butadiene-Styrene Block Copolymers at Large Strains, *Revue Roumaine de Chimie.*, **28**, 299 (1983).

(16) Canevarolo, S.V.; Mattoso, L.H.C., Preferential Plasticization of SBS Triblock Copolymer, *Brit. Polym. J.*, **22**, 137 (1990).

(17) Polizzi, S.; Stribeck, N.; Zachmann, H.G.; Bordeianu, R., Morphological changes in SBS block copolymers caused by oil extension as determined by absolute small angle x-ray scattering, *Colloid Polym. Sci.*, **267**, 281 (1989).

(18) Florenzier, L.S.; Rohlfing, J.H.; Schwark, A.M.; Torkelson, J.M., The Effect of Blending Small Amounts of Homopolystyrene on the Mechanical Properties of a Low Styrene Content Styrene-Butadiene-Styrene Block Copolymer, *Polymer Engineering & Science*, **30**, 49 (1990).

(19) Florenzier, L.S.; Rohlfing, J.H.; Schwark, A.M.; Torkelson, J.M., The Effect of Blending Small Amounts of Homopolystyrene on the Mechanical Properties of a Low Styrene Content Styrene-Butadiene-Styrene Block Copolymer--Corrections, *Polymer Engineering & Science*, **30**, 1180 (1990).

(20) Florenzier, L.S. and Torkelson, J.M., Influence of Molecular Weight and Composition on the Morphology and Mechanical Properties of BSB-Polystyrene-Mineral Oil Blends, *Macromolecules*, **25**, 735 (1992).

(21) Mischenko, N.; Reynders, K.; Mortensen, K.; Scherrenberg, R.; Fontaine, F.; Graulus, R.; Reynaers, H., Structural Studies of Thermoplastic Triblock Copolymer Gels, *Macromolecules*, **27**, 2345 (1994).

(22) Laurer, J.H.; Bukovnik, R.; Spontak, R.J., Morphological Characteristics of SEBS Thermoplastic Elastomer Gels, *Macromolecules*, **29**, 5760 (1996).

(23) Anderson, S.L.; Grulke, E.A.; DeLassus, P.T.; Smith, P.B.; Kocher, C.W.; Landes, B.G., A model for Antiplasticization in Polystyrene, *Macromolecules*, **28**, 2944 (1995).

(24) Honeker, C.C. and Thomas, E.L., Impact of morphological orientation in determining mechanical properties in block copolymers systems, *Chem. Mater.*, **8**, 1702 (1996).

(25) Albalak, R.J. and Thomas, E.L., *J. Polym. Sc.: Part B: Polym. Phys.*, Microphase-Separation of Block Copolymer Solutions in a Flow Field, **31**, 37 (1993).

(26) Albalak, R.J., *Polymer*, The anisotropic thermal expansion of 'single-crystal' triblock copolymer films, **35**, 4115 (1994).

(27) Albalak, R.J. and Thomas, E.L., *J. Polym. Sc.: Part B: Polym. Phys.*, Roll-casting of block copolymers and of block copolymer-homopolymer blends, **32**, 341 (1994).

(28) McKelvey, J.M., *Polymer Processing*, Wiley, New York, 1962.

(29) Inoue, T.; Moritani, M.; Hashimoto, T.; Kawai, H., Deformation Mechanism of Elastomeric Block Copolymers Having Spherical Domains of Hard Segments under Uniaxial Tensile Stress, *Macromolecules*, **4**, 500 (1971).

(30) Richards, R.W. and Thomason, J.L., Small angle neutron scattering study of the structure of a triblock copolymer of styrene and isoprene during extension, *Polymer*, **24**, 275 (1983).

(31) Richards, R.W. and Welsh, G., Deformation of Matrix Macromolecules in a Uniaxially Extended Styrene-Isoprene-Styrene Linear Triblock Copolymer, *Eur. Polym. J.*, **31**, 1197 (1995).

(32) Almdal, K.; Koppi, K.A.; Bates, F.S., Dynamically Sheared Body-Centered Cubic Diblock Copolymer Melt, *Macromolecules*, **26**, 4058 (1993).

(33) Koppi, K.A.; Tirrell, M.; Bates, F.S.; Almdal, K.; Mortensen, K., Epitaxial growth and shearing of the body centered cubic phase in diblock copolymer melts,*J. Rheol.*, **38**, 999 (1994).

(34) Okamoto, S.; Saijo, S.; Hashimoto, T., Dynamic SAXS Studies of Sphere-Forming Block Copolymers under Large Oscillatory Shear Deformation, *Macromolecules*, **27**, 3753 (1994).

(35) Diat, O.; Porte, G.; Berret, J.-F., Orientation and twins separation in a micellar cubic crystal under oscillating shear, *Physical Review B*, **54**, 14869 (1996).

(36) Ackerson, B.J. and Clark, N.A., Shear-induced partial translational ordering of a colloidal solid, *Phys. Rev.*, **30**, 906 (1984).

(37) Ackerson, B.J.; Hayter, J.B.; Clark, N.A.; Cotter, L., Neutron scattering from charge stabilized suspensions undergoing shear, *J. Chem. Phys.*, **84**, 2344 (1986).

(38) Chen, L.B.; Zukoski, C.F.; Ackerson, B.J.; Hanley, H.J.M.; Straty, G.C.; Barker, J.; Glinka, C.J., Structural Changes and Orientational Order in a Sheared Colloidal Suspension, *Phys. Rev. Letters*, **69**, 688 (1992).

(39) Watanabe, H.; Kuwahara, S.; Kotaka, T., Rheology of Styrene-Butadiene-Styrene Triblock Copolymer in *n*-Tetradecane Systems, *J. Rheol.*, **28**, 393 (1984).

(40) Sato, T.; Watanabe, H.; Osaki, K., Rheological and Dielectric Behavior of a Styrene-Isoprene-Styrene Triblock Copolymer in *n*-Tetradecane. 1. Rubbery-Plastic-Viscous Transition, *Macromolecules*, **29**, 6231 (1996).

(41) Watanabe, H.; Sato, T.; Osaki, K., Rheological and Dielectric Behavior of a Styrene-Isoprene-Styrene Triblock Copolymer in Selective Solvents: 2. Contribution of Loop-type Middle Blocks to Elasticity and Plasticity, *submitted to Macromolecules.*

(42) Watanabe, H., *Feature Article submitted to Acta Polymerica.*

(43) Rharbi, Y.; Boué, F.; Joanicot, M.; Cabane, B., Deformation of Cellular Polymeric Films, *Macromolecules*, **29**, 4346 (1996).

(44) Lepizzera, S.; Scheer, M.; Fond, C.; Pith, T.; Lambla, M; Lang, J., Coalesced Core-Shell Latex Films under Elongation Imaged by Atomic Force Microscopy, *in preparation.*

(45) Lepizzera, S.; Pith, T.; Fond, C.; Lambla, M., Mechanical Behaviour at Finite Strain of Coalesced Core/Shell Latex Films, *submitted to Macromolecules.*

(46) Alexander, L.E., *X-Ray Diffraction Methods in Polymer Science*, Wiley Interscience, New York, 1969.